UNITED STATES DEPARTMENT OF THE INTERIOR
GEOLOGICAL SURVEY

Geochemistry and geology of gold in jasperoid, Elephant Head area, Lander County, Nevada

by

Ted G. Theodore[1/] and Gail M. Jones[2/]

1990

Open-File Report 90-13

This report is preliminary and has not been reviewed for conformity with U. S. Geological Survey editorial standards or with the North American Stratigraphic Code. Any use of trade, firm, or product names in this report is for descriptive purposes only and does not constitute endorsement by the U. S. Government

1/Menlo Park, CA 94025

2/Present Address: Western Geologic Resources, San Rafael, CA 94520

TABLE OF CONTENTS

ILLUSTRATIONS

GEOCHEMISTRY AND GEOLOGY OF GOLD IN JASPEROID, ELEPHANT HEAD AREA, LANDER COUNTY, NEVADA

by

Ted G. Theodore and Gail M. Jones

ABSTRACT

Numerous small masses of mineralized and unmineralized jasperoid crop out in the Elephant Head area in the northeastern part of the Battle Mountain Mining District, about 8 km west-southwest of the town of Battle Mountain. Distribution of most jasperoid is controlled structurally; most formed in the Upper Pennsylvanian and Lower Permian Antler Peak Limestone, probably synchronous with emplacement of 35 Ma granodiorite porphyry. Mesoscopic fabric of the jasperoids includes massive, bedded, and fractured forms. In many localities, brecciated jasperoid has been recemented by subsequent generations of silica. Color of the jasperoid is varied, and includes shades of brown, yellow, orange, and dusky red, together with some minor black, whitish purple, gray, and olive. Some multicolored jasperoid shows sweeping, well-developed, apparent flowage patterns, termed "variegated". Probably the most widespread microtextural type is jigsaw, and most of the jasperoid bodies resulted from introduction of multiple generations of silica, including colloform-banded chalcedonic quartz, cross-fiber-textured chalcedonic quartz, and banded opaline silica. Some very manganiferous-bearing and probably lead-oxide-bearing goethitic jasperoid shows open spaces filled by crystalline, sheaf-like aggregates of hemimorphite, and then filled subsequently by granular-textured jasperoidal silica.

Chemical analyses by various methods of 78 samples of jasperoid reveal a strong, positive association between base and precious metals. This suggests geochemical signatures may be indicative of polymetallic vein, polymetallic replacement, or distal disseminated silver-gold deposits. Brecciation of jasperoid apparently is not associated with increased concentrations of gold. Silver:gold ratios in jasperoid (approximately 150) differ significantly from silver:gold ratios (approximately 2.7) of jasperoid in sedimentary rock-hosted gold-silver deposits elsewhere in north-central Nevada. Statistical treatment of geochemical data

indicates that high arsenic, lead, zinc, and antimony abundances in jasperoid, the presence of nearby faults, and "variegated" jasperoid are good indicators of enhanced concentrations of gold at Elephant Head.

Lead:bismuth ratios in the jasperoids are typically in the range of hundreds-to-thousands to 1. However, one sample of jasperoid at Elephant Head shows a lead:bismuth ratio approximately equal to 1. This corresponds to the lead:bismuth ratio calculated for lead-bismuth phases associated with eutectoid-type intergrowths among native bismuth, galena, and gold in ore near the distal northern edge of the world-class Fortitude gold skarn deposit in the southern part of the Battle Mountain Mining District. Therefore, the one sample of jasperoid showing a lead:bismuth ratio approximately equal to 1 should be considered as having a signature favorable for metallization at depth comparable geochemically with that at the Fortitude deposit, provided that similar types of fluid were responsible for the metallization at both localities. Drilling by private industry prior to our studies had delineated the presence of a small copper-mineralized system in the immediate area of the jasperoid sample containing lead:bismuth concentrations approximately equal to 1.

INTRODUCTION

The Elephant Head area is located in the east-central part of the Battle Mountain Range, 8 km west-southwest of the town of Battle Mountain, Lander County, Nevada, and accessible by jeep trail from U. S. I-80 (Victory Highway) and State Highway 8A (fig. 1). The study area comprises about 10 km^2. Most of the study area, between the latitudes 40° 36' 35" N and 40° 38' 35" and the longitudes 116° 57' 30" and 117° 01' 25", lies within the boundaries of the Antler Peak 15-minute quadrangle and a small portion at the east edge of the area lies within the Battle Mountain 15-minute quadrangle. Elevation in the map area ranges from 4,550 feet to 5,936 feet at the top of Elephant Head. The study area is in the northeastern part of the Battle Mountain Mining District.

As summarized by Theodore and Hammarstrom (1989), mining in the Battle Mountain Mining District spans a period of more than 120 years, from 1866 to the present; currently (1989) lode-mining operations are focused on three mineralized areas, all of which include gold-bearing skarn: (1) the Fortitude deposit at Copper Canyon, (2) the Surprise deposit in the Copper Basin area, and (3) the Buffalo Valley gold deposit at the western edge of the district, about 19 km west-southwest from the Elephant Head area (fig. 2). The Copper Canyon Cu-Pb-Zn underground mine was operated sporadically between 1917 and 1955 (Roberts and Arnold, 1965). The first large-scale attempt to mine base and precious metals, mostly copper, by open-pit methods began in 1967 in the Copper Canyon and Copper Basin areas. Both large-scale mining operations were centered on porphyry-type metallization that has widely divergent ages: 38 Ma at Copper Canyon (Theodore and others, 1973), and 86 Ma at Copper Basin (Theodore and McKee, 1983; McKee, 1989). In addition, the Copper Basin metallization includes several secondarily-enriched copper ore bodies related to the Buckingham stockwork molybdenum system (Theodore and others, 1989). In both of these centers, porphyry-type metallization is surrounded in areas as much as 20 km^2 by a widespread halo of polymetallic veins whose metal contents systematically vary laterally with distance from the porphyry centers (Roberts and Arnold, 1965; Theodore and others, 1986). Porphyry-type mineralization in the district also is present in the general areas of Elder Creek, Trenton Canyon, and west-southwest of Rocky Canyon.

Placer gold was discovered in Copper Canyon in 1912, and intermittent small-scale placer operations were carried on into the early 1940s. From 1944 to 1955, a dredge was operated on the alluvial fan at the mouth of Copper Canyon and reportedly produced 100,000 oz. of Au (Johnson, 1973, p. 37-38). This fan will shortly be yielding gold again at a rate of approximately 18,000 oz. Au per year (Battle Mountain Gold Co., 1987, Annual Report to Stockholders, February 5, 1988).

Previous geologic studies in the district include the landmark studies by Roberts (1964) and Roberts and Arnold (1965), who described the stratigraphy, structure, and ore deposits of the Antler Peak quadrangle and the regional implications of geology therein. Theodore (1982) and Theodore and others (1989) mapped and described the Buckingham stockwork molybdenum system immediately to the west of the study area.

Silicification in north-central Nevada may have several origins. Structurally-controlled jasperoid at the Empire open-pit Au-Ag deposit, which is located approximately 0.5 km south of the study area and will be described below, apparently is related to the Buckingham stockwork molybdenum system (Theodore and others, 1989). Apparently similar jasperoid is present as float and also crops out in the drainage east-northeast of Elephant Head where, in places, it selectively replaces the Late Pennsylvanian and Early Permian Antler Peak Limestone (Roberts, 1964). Silicification of Antler Peak Limestone in the Elephant Head area might, on the one hand, be similar in character and overall genesis to silicification in other sedimentary rock-hosted disseminated Au-Ag deposits elsewhere in Nevada. This class of deposit is characterized by mineralized rocks showing elevated abundances of Au, Hg, As, and Sb (Ashton, 1989). On the other hand, numerous small bodies of jasperoid in the Elephant Head area (pl. 1) might be related to widespread porphyry-type metallization associated with either Cretaceous Buckingham stockwork molybdenum system, or Tertiary 35-40 Ma magmatism (Theodore and others, 1973; McKee, 1989). The latter magmatic event is widespread in the Battle Mountain Mining District, and it culminated in formation of the Fortitude gold skarn deposit in the southern part of the district (Wotruba and others, 1986; Myers and Meinert, 1988). Some economic concentrations of apparently Tertiary gold mineralization also are present just to the west of the Elephant Head area at the Labrador gold skarn deposit (Schmidt, 1988); gold mineralization at the Labrador deposit is associated with a small body of hornblende - clinopyroxene leucogranite, of which a much

larger body crops out to the northwest of the Labrador deposit (Theodore and Hammarstrom, 1989). Replacement of originally calcareous-rich rock by jasperoid elsewhere also is present as an alteration halo that mantles gold skarn systems (Wolfenden, 1965; Orris and others, 1987).

Geochemical analyses of jasperoid have been useful in identifying metal anomalies that surround and are related to economic sulfide ore deposits (Lovering and McCarthy, 1978; Lovering and Heyl, 1974). However, gold concentrations in jasperoid typically are very spotty. Studies along the Carlin trend of sedimentary rock-hosted Au-Ag deposits, about 50 km east of the area, have shown that chemical analysis of jasperoid from a known ore body can show insignificant gold concentration in one sample, whereas another sample only several meters away may show anomalously high gold concentrations (W. C. Bagby, oral commun., 1985). Recent studies of jasperoid from the northern Great Basin also have confirmed extreme variability in elemental concentrations in suites of samples obtained from a single deposit (Holland and others, 1988). In addition, many of the sedimentary rock-hosted Au-Ag deposits along the Carlin trend and the Preble-Pinson-Getchell gold trend, approximately 80 km northwest of the Elephant Head area, show a zonotion from distal carbonate veins, through mixed carbonate-jasperoid veins, to jasperoid-only mineralized veins proximal to the deposits (Madrid and Bagby, 1988). Anomalous concentrations of gold appear to be especially concentrated in the jasperoidal parts of the mixed carbonate-jasperoid veins.

In this report, we present (1) trace-element analyses of jasperoid and geologic relations of jasperoid of the Elephant Head area, (2) trace-element analyses of selected samples of jasperoid from the Empire Au-Ag deposit, and (3) comparisons of these data with suites of jasperoid analyzed from other areas. The primary objective of this report is to analyze relations at Elephant Head among gold contents, concentration of other trace-elements in jasperoid, and physical features of the jasperoid bodies such as color and the presence of brecciation. These parameters may be useful in identifying elsewhere specific locations favorable for gold mineralization, even if gold is not detected using sensitive analytical techniques. In addition, metal associations in jasperoid at Elephant Head may provide an indication of the type(s) of potential mineralized systems with which they may be allied.

DEFINITION OF JASPEROID

Jasperoid was originally defined as "a rock consisting essentially of cryptocrystalline, chalcedonic, or phenocrystalline silica, which has formed by the replacement of some other material, ordinarily calcite or dolomite" (Spurr, 1898). A detailed and useful discussion of physical properties and genesis of jasperoid was given by Lovering (1972); in addition, he also evaluated jasperoid as a potential guide to ore in porphyry copper and carbonate-hosted base-metal replacement districts in the western United States. Lovering (1972) followed Spurr's (1898) original definition, which expressly defines it in terms of petrography and genesis, to exclude syngenetic or diagenetic silica rocks, e.g. primary chert and novaculite. The silica of jasperoid is typically fine-grained to cryptocrystalline. Extremely fine-grained texture and ghost colloform banding commonly observed in finely crystalline quartz of jasperoid suggest that silica is generally deposited as a colloidal gel and later converted to quartz in such rocks (Lovering, 1972). Rock color in these rocks may be white, gray, red, brown or black depending primarily on the oxidation state of the included iron, and on the presence of various other hydrothermally introduced minerals (Spurr, 1898). The replaced host rock is most commonly limestone or dolomite. Shale, siltstone, pyroclastics, and siliceous hypabyssal and extrusive igneous rock are also susceptible to replacement by silica, but much less so than carbonate rocks and calcareous rocks (Lovering 1972). As Lovering noted, replacement of carbonate rock by silica may be accomplished by diffusion of reaction products through a gel layer behind a dissolution front, or by movement of silica-bearing fluid along fractures, or both. Lovering (1972) also observed that many jasperoid bodies are localized around structural planes of weakness such as faults, breccia zones, or perhaps bedding planes, which served as a conduit for silica-bearing fluids. The structure-controlled nature of the feeder zone(s) to such mineralized systems is emphasized strongly by Madrid and Bagby (1988). Many jasperoids are spatially related to granitic intrusions. Thus, enhanced silica contents in rocks resulting from their selective replacement by jasperoid may reflect initially SiO_2-saturated late-magmatic fluids emanating from a pluton or they may reflect initially SiO_2-unsaturated fluids that became SiO_2-saturated during reactions with wall rocks en route to their eventual deposition sites. Silica may originate from siliceous fractions of the host rock elsewhere from the site of deposition, or even may be due to paleoweathering cycles of overlying or adjacent rocks. In any case, a silica-

saturated, or nearly saturated solution is required to reach the site of deposition (Fournier, 1973).

SEDIMENTARY ROCK-HOSTED DISSEMINATED Au-Ag AND DISTAL Ag-Au DEPOSITS

Some discussion of sedimentary-rock hosted disseminated Au-Ag deposits and their associated jasperoid is warranted because many of these deposits include widespread concentrations of rock altered to jasperoid. A number of world-class sedimentary rock-hosted disseminated gold deposits are present in north-central Nevada (e.g. Carlin, Radtke (1985); Cortez, Wells and others (1969); and Getchell, Silberman and others (1974) to cite a few). Along a 104-km interval of the northwest-trending, Carlin mineralized belt, at least 21 sedimentary-rock hosted disseminated Au-Ag deposits contain a geologic resource of at least 55 million oz. gold (Mining Magazine, October, 1989, p. 263-267). Models for this deposit type have been published by Berger (1986), Romberg (1986), and Sawkins (1983).

Romberg (1986) considered sedimentary rock-hosted disseminated Au-Ag deposits as a subgroup of his epithermal class of precious-metal deposits. Grade and tonnage data for this deposit type underscore the importance of this deposit type. Geometric means of tonnage and grade of sedimentary rock-hosted disseminated gold deposits are 5.1 million tonnes ore and 2.5 grams per tonne Au (Bagby and others, 1986). Compared to other epithermal precious-metal deposit types, sedimentary rock-hosted Au-Ag deposits are lower grade and higher tonnage with overall contained gold generally much higher (Cox and Singer, 1986). This deposit type may be hosted by rock of any age, but typically in northern Nevada, Paleozoic carbonate rock forms the host, although age of mineralization probably is generally Tertiary (Romberg, 1986). Romberg lists four additional features shared by many deposits of this type: (1) occurrence of jasperoid; (2) close association between gold and pyrite; (3) low abundances of base metals; and (4) significant concentrations of arsenic, antimony, mercury, and thallium in the ores. In addition, most known sedimentary rock-hosted disseminated Au-Ag deposits are present along relatively narrowly defined mineralized belts that suggested to Madrid (1987) that they may have been localized along structurally-prepared hinge regions of broad anticlinial folds that formed some time during the Mesozoic. Favorable ore horizons in

replacement-controlled parts of mineralized systems are generally thinly-bedded or laminated, and argillaceous, silty or arenaceous limestone or dolomite. Mineralization is associated spatially with fractures in most sedimentary rock-hosted disseminated Au-Ag deposits (Madrid and Bagby, 1988). Generally, these fracture systems developed and experienced some normal displacement during the Tertiary in north-central Nevada.

Extensive petrographic investigations utilizing techniques that result in magnifications of many thousands generally have been required to establish the actual site and paragenetic setting of gold in the sedimentary rock-hosted disseminated Au-Ag deposits. Such investigations commonly have focused on many samples from ore zones of relatively high gold grades before critical relations of gold to other mineral phases have been found. In many of these deposits, sub-microscopic to microscopic gold typically is present as coatings on or fillings in fractures in pyrite grains, along with mercury, antimony and arsenic (Romberg, 1986) and in some documented instances, completely encapsulated in pyrite, quartz, and cinnabar and also associated with illite (Bakken and others, 1989). The latter study found that the particles of encapsulated gold are extremely small, on the order of about 50-1,000 angstroms. Madrid and Bagby (1988) found that small (approximately 0.5 micron), native gold particles in some of these deposits (Preble and Pinson) are spatially associated with, but not intergrown with, arsenic-bearing pyrite. Sulfides generally constitute less than 1 percent by volume of the rock in these deposits. Therefore, it is not surprising that the preliminary petrographic investigations of a limited number of jasperoids from Elephant Head, to be described below failed to fix the actual site of gold in the jasperoid there, even though some the samples studied contain highly anomalous concentrations.

The sedimentary rock-hosted disseminated Au-Ag deposits commonly show elevated abundances of other elements. Some of these deposits contain high concentrations of barium and fluorine (Percival and others, 1988); these two elements, however, are not generally considered to be among the most diagnostic geochemical signatures for these types of deposits. Gold, As, Hg, and Sb commonly show increased concentrations in the sedimentary rock-hosted Au-Ag deposits of north-central Nevada. Ashton (1989) notes that 460 rock-chip samples chemically analyzed from nine of these deposits in north-central Nevada show highly variable increases in concentrations of Au, As, Hg, and Sb; threshold values for the latter

three elements apparently are 100 ppm, 1 ppm, and 50 ppm, respectively. Although most of these types of deposits show relatively low base-metal abundances, some of them are nonetheless characterized by increased concentrations of lead and zinc. The concentration of lead is as much as 3,000 ppm along gold-mineralized fault zones in the Gold Quarry deposit; anomalous concentrations of zinc in the deposit seem to reflect distribution of pre-mineral carbonate rocks (Hausen and others, 1983; Rota, 1987).

Linear north-south arrays of a number of sedimentary rock-hosted Au-Ag deposits are present in the northernmost part of the Battle Mountain Mining District about 21 km northwest of the Elephant Head area. These deposits are on the projection to the south of north-south aligned ore zones at the Rabbit Creek Au-Ag deposit (Parratt and others, 1989). A tight cluster of at least four sedimentary rock-hosted Au-Ag deposits have currently (1989) been delineated by the Marigold Mining Co. (Graney and Wallace, 1988), and the 8-South deposit is in production. These deposits are present near the old Marigold Mine (Roberts and Arnold, 1965), and they formed mainly as replacement of Pennsylvanian and Permian Antler sequence rocks of Silberling and Roberts (1962); a minor amount of ore occurs in Ordovician Valmy Formation (fig. 2). Total reserves include 3.9 million tonnes oxidized, millable ore at 3.6 g/t Au and 6.9 million tonnes heap-leach ore at 0.9 g/t Au (London Mining Journal, March 3, 1989, p. 165). In addition, several other deposits, all hosted by the Valmy Formation, are being extensively drilled south of the deposits of Marigold Mining Co. North of the 8-South deposit and near the south end of Lone Tree Hill, economic grade mineralization has been encountered in 90 percent of the holes drilled in a 600 X 400 m area (The Northern Miner, Nov. 13, 1989, p.13). It is not clear how the mineralized jasperoids at Elephant Head might relate to these regional alignments. A broad, northwest-southeast trending fracture system may extend from the general area of these deposits near the Marigold Mine, parallel to the range front and including several clusters of Tertiary igneous stocks (fig. 2), and eventually to the Elephant Head area (see below).

Distal-disseminated Ag-Au deposits, a classification scheme of some distinctive sedimentary rock-hosted mineralized systems (Dennis P. Cox, written commun., 1989), include the Cove deposit, near the McCoy Mine; the Hilltop deposit in the Shoshone Range, about 30 km southeast of Elephant Head; and several other apparently porphyry-related or Au-skarn related systems. Many of

these deposits include significant concentrations of jasperoid as part of their suite of alteration assemblages. Examination of selected ore samples from the Cove deposit by scanning-electron microscope reveals that gold in mineralized jasperoid is present in several different textural associations (T.G. Theodore, unpub. data, 1989). Some of the largest concentrations of gold are as much as 30 microns wide and reside in limonite-rich domains of manganiferous jasperoid. These relations suggest that the gold may originally have been present in an iron-rich mineral, possibly pyrite. Other samples of jasperoid from the Cove deposit show numerous equant blebs, about 0.3 microns wide, of apparent auriferous argentite dispersed in relict grains of sedimentary calcite that has not been replaced by jasperoidal silica; Au:Ag ratios probably have a value of about 2 in the auriferous argentite. Similar blebs of auriferous argentite also are present in hydrothermal apatite. Reconaissance study of a limited number of additional ore samples of jasperoid from the Cove deposit also indicates that cerargyrite, a common silver mineral in these samples, is present in domains containing abundant carbonate minerals, some of which are quite manganiferous.

REGIONAL GEOLOGY

The present complex array of crustal and supracrustal rocks in north-central Nevada is a culmination of geologic events protracted over an extremely long span of time. Prior to the Antler orogeny, distribution of siliceous, transitional, and carbonate assemblage rocks in the Cordilleran belt was arrayed in a somewhat uniform fashion with siliceous rocks on the west and carbonate slope rocks on the east (Stewart and Poole, 1974).

Much of north-central Nevada is covered by siliceous and volcanic rocks in the upper plate of the Roberts Mountains thrust. At the latitude of the Battle Mountain Mining District, the width of allochthonous rocks from the apparent leading edge of the thrust on the east, to the westernmost known window in the East Range is approximately 150 km (Speed and others, 1988). The thrust carried oceanic volcanic rocks, chert, shale, and quartzite of early and middle Paleozoic age eastward over lower plate, continental shelf carbonate rocks of an equivalent age during Mississippian thrusting in the Antler orogeny (Roberts and others, 1958; Roberts, 1964; Speed and Sleep, 1982). The Antler orogeny seems to have been the first major tectonism to affect sedimentary patterns in the cordilleran miogeocline after rifting

during the Proterozoic of the continental crystalline crust (Stewart, 1980). The presence of alkalic basaltic lavas in the allochthonous Middle Cambrian Shwin Formation, which crops out in the Shoshone Range about 30 km southeast of Elephant Head, suggested to Turner and others (1989) that some extension took place in the depositional basin of these rocks. However, some rocks in the Cordilleran miogeocline also may have been affected by, and others owe their origins to, an early Paleozoic, pre-Antler, orogeny as proposed by Willden (1979). Many authors (Speed and Sleep, 1982; Nilsen and Stewart, 1980; Silberling, 1986) point out that the allochthons of the Roberts Mountains thrust comprise a number of internally deformed tectonic packets of rock that were emplaced owing to collision of east-facing island arcs with North America. As such, the allochthons represent forearc subduction-accretion wedges according to this model. Speed and Sleep (1982) maintain that a large accretionary prism was underthrust by the continental slope and outer shelf of the North American plate; the accretionary prism then became the Roberts Mountains allochton. The Roberts Mountains thrust, does not crop out in the Battle Mountain Mining District (fig. 3; Roberts, 1964). Deep drill holes into the Roberts Mountains plate indicate that this thrust probably underlies the district at depths greater than 1,300 m (Theodore and Roberts, 1971).

The region subsequently has been overridden by several structurally higher Paleozoic and Mesozoic thrusts. One of these thrusts, the post-late Early Permian to Early Triassic Golconda thrust, crops out prominently in the Battle Mountain Mining District. As noted by Speed (1977), the Golconda thrust marks a late Paleozoic (Pennsylvanian and Permian) boundary that juxtaposes rocks of two different terranes: an ocean basin terrane on the west and a continental borderland terrane on the east. Furthermore, the district apparently is entirely within a 350 by 150 km enclave of sparse Mesozoic deformation in central Nevada (Speed and Sleep, 1982, fig. 1). This enclave lies just to the east of the Luning-Fencemaker fold and thrust belt of Oldow (1983), wherein there has been regional-scale shortening in a northwest-southeast direction during the Middle Jurassic to Late Cretaceous.

Three major thrust plates of regional significance crop out in the Battle Mountain Mining District (fig. 2). Two are below an equally important autochthonous block (Roberts, 1964). The lowest plate exposed is made up of chert, shale, argillite, and greenstone of the Devonian Scott Canyon Formation; it also

includes quartzite and chert of the Ordovician Valmy Formation. Both formations, the Scott Canyon and the Valmy, make up the upper plate of the Roberts Mountains thrust (Roberts Mountains plate). These two formations are in fault contact at Galena Canyon, in the south central part of the mining district, along steeply dipping normal faults and along a shallow-dipping thrust fault. The Scott Canyon and Valmy were both, in turn, overthrust by sandstone and feldspathic sandstone of the Upper Cambrian Harmony Formation along the Dewitt thrust, which is a late middle or early late Paleozoic thrust that is about the same age as the Roberts Mountains thrust of the Antler orogeny (Roberts, 1964). The Harmony Formation makes up the middle (the Dewitt plate) of the three thrust plates. The Roberts Mountains and Dewitt plates are overlain unconformably by the Antler sequence, which includes the Pennsylvanian and Permian Antler Peak Limestone that crops out widely in the Elephant Head area (pl. 1).

The upper Paleozoic Antler sequence makes up a structural block that rests upon a major unconformity on the Harmony Formation and the Valmy Formation in the district. The rocks of the Antler sequence belong to the overlap assemblage of Roberts (1964). Three formations compose the Antler sequence in the district: (1) Middle Pennsylvanian Battle Formation, (2) Upper Pennsylvanian and Lower Permian Antler Peak Limestone, and (3) Upper Permian Edna Mountain Formation. Regional uplift, resulting in a rugged late Paleozoic highland between the 116° and 118° meridians, lasted into Middle Pennsylvanian time (Roberts, 1964). During Middle Pennsylvanian time coarse clastic rocks of the Battle Formation were deposited in basins and troughs within the highlands in angular unconformity to the underlying Harmony Formation and Valmy Formation. Although some of these rocks are terrestrial in nature, especially the basal member of the Battle Formation, the remaining rocks of the Antler sequence were deposited largely in a marine environment.

The Late Permian and Early Triassic Sonoma orogeny resulted in emplacement of the Golconda thrust, which crops out roughly 13 km to the west of the study area. A broad northeast-trending anticline, termed the Antler anticline by Roberts (1964), developed in rocks of the Harmony Formation. The hinge line of this anticline is located about 10 km west-southwest of the study area. Rocks of the Harmony Formation, Battle Formation, and Antler Peak Limestone in the area at

Elephant Head comprise an east-dipping limb of the anticline prior to eruption of unconformably overlying Oligocene Caetano Tuff of Gilluly and Masursky (1965).

Felsic intrusive rocks of varying sizes and much less abundant diabase and gabbro crop out in the Battle Mountain Mining District (Roberts, 1964). Some of the diabase and gabbro may be Ordovician and (or) Devonian in age. The felsic intrusive rocks are clustered mainly in four major loci in the mining district. The four major loci are centered at Copper Canyon in the southern part of the district, at Trenton Canyon where the largest intrusive body in the district crops out, at the Buckingham-Copper Basin area where widespread stockwork molybdenum mineralization is present, and at the Elder Creek area, which is about 8-10 km northwest of the Elephant Head area (fig. 2). The felsic intrusive rocks in the Buckingham-Copper Basin area range in age from Late Cretaceous to middle Tertiary, and they include several varieties of both probable Late Cretaceous monzogranite and latest Eocene or earliest Oligocene monzogranite, late Eocene or early Oligocene rhyolite and porphyritic leucogranite (including a porphyritic monzogranite and a porphyritic tonalite phase), and early Oligocene granodiorite porphyry (Theodore and others, 1989). Previous studies using the potassium-argon method established that felsic intrusive activity in the mining district initiated during the Late Cretaceous with emplacement at Trenton Canyon of a relatively large body of granodiorite (Theodore and others, 1973). Subsequently, there appears to have been a hiatus of approximately 46 m.y. during which there was no felsic magmatism in the mining district. At Elder Creek and at Copper Canyon, the felsic intrusive rocks are mostly altered granodiorite and monzogranite and they are late Eocene and (or) early Oligocene in age (38-40 Ma) (Theodore and others, 1973).

Two suites of volcanic rock crop in the Battle Mountain Mining District: (1) calc-alkaline rhyolitic welded tuffs are present as erosional outflow-facies-remnants of the previously much more extensive Oligocene Caetano Tuff (Gilluly and Masursky, 1965; Stewart and McKee, 1977), whose age is 34 Ma (McKee and Silberman, 1970), and (2) much younger Tertiary or Quaternary basalt (fig. 2). The Caetano Tuff crops out prominently in the Elephant Head area, and forms the conspicuous promontory near its south edge from which the area derives its name (pl. 1). A sample of basalt from the southern part of the mining district, near Copper Canyon, gives a K-Ar age of 3.2 Ma (Theodore and others, 1989).

REGIONAL METALLIZATION

Locations of many ore deposits in north-central Nevada are structurally controlled. This relation is documented by pronounced concentrations of metal-producing districts along the N. 45° W.-trending Eureka mineral belt (Roberts, 1966), the concentration of gold deposits along the Carlin trend (Roberts, 1966; Bloomstein, 1986; Bagby and Berger, 1985; Evans and Peterson, 1986), and by occurrence of the Getchell, Pinson, and Preble gold deposits, possibly together with the tungsten-bearing Golconda hot springs area, all along a north-northeast-striking fault system on the east flank of the Osgood Mountains. This fault system may extend into the Adelaide Mining District (Cookro and Theodore, 1989). Another structural control exerted on distribution of many ore deposits in north-central Nevada is the thrust zone of regionally extensive tectonic plates. The Roberts Mountains thrust, which crops out mainly east of Battle Mountain, has the Carlin, Bullion Monarch, Blue Star and several other disseminated, sedimentary rock-hosted Au-Ag deposits near its trace.

The Elephant Head area is located along the southeastern projection of an alignment of deposits, prospects, areally extensive mineralized systems, and small Tertiary stocks. These aligned mineralized areas extend from the area of the old Marigold Mine on the northwest, through the porphyry copper system and its satellitic polymetallic vein occurrences centered at Elder Creek, and the Bailey Day, Labrador and Surprise gold mines, just to the northwest of the Elephant Head area (fig. 2). In addition to the above-mentioned lode occurrences, the northwest-trending flank of the Battle Mountain Range also shows numerous placer gold occurrences along its trace (Roberts and Arnold, 1965; Theodore and others, 1989).

The Battle Mountain Mining District also resides within widespread gold, lead-zinc, mercury, silver, and tungsten metal provinces as outlined by Noble (1970) and near the eastern fringes of a broad, north-trending mercury belt (Joralemon, 1951). Within the Battle Mountain Mining District, the location of major copper-gold-silver and gold-silver deposits seems to have been controlled in large part by presence of sedimentary rocks favorable for development of replacement deposits below the Golconda thrust, and the cap-rock effect of impermeable rocks in the upper plate of the Golconda thrust (Nash and Theodore, 1971; Theodore and Blake,

1975). In the mining district, Late Cretaceous monzogranites in the Buckingham area and Late Cretaceous granodiorite in the Trenton Canyon area are associated genetically with quartz stockwork-related molybdenum mineralization, whereas, at Copper Canyon and at Buckingham, late Eocene and (or) early Oligocene altered granodiorite and monzogranite are associated with Cu-Au-Ag mineralization, respectively (Theodore and Blake, 1975,1978; Theodore and others, 1989). In addition, there are some Au-skarn orebodies at the Carissa Mine and at the Surprise Mine that appear to be related to Late Cretaceous felsic magmatism in the district (Schmidt and others, 1988). Moreover, in the Buckingham area, late Eocene and (or) early Oligocene rhyolite is mostly associated with minor silver mineralization; late Eocene and (or) early Oligocene porphyritic tonalite and porphyritic monzogranite with minor gold mineralization at the Overlook and Labrador properties; and, finally, Oligocene granodiorite porphyry with minor gold mineralization and some minor Pb-Zn mineralization (Theodore and others, 1989).

GEOLOGY OF THE ELEPHANT HEAD AREA

The Antler sequence, in particular the Antler Peak Limestone, crops out extensively in the Elephant Head area (pl. 1). The basal formation of the Antler sequence, the Battle Formation, is minimally exposed only in a small area near the southwest corner of the study area, where it crops out on the north and west flanks of Elephant Head (pl. 1). Roberts (1964) divided the Battle Formation into three members. The lower member (about 121 m thick) contains coarse conglomerate with fragments of quartzite, chert, limestone and greenstone. A middle member (about 23 m thick) contains interbedded pebble conglomerate, sandstone, shale limey shale and limestone. The upper member (about 79 m thick) consists of interbedded pebble conglomerate, sandstone, shale, and calcareous shale with shaley sequences predominant. However, the formation is poorly exposed in the Elephant Head area; abundant shale fragments and quartzite fragments suggest it may belong to the middle member of Roberts (1964). Light brown fine-grained sandstone with angular chert clasts, very pale orange sandy shale, and a probable quartzite with angular chert clasts about 1/2 cm in diameter are present in some outcrops. Several samples of jasperoid were also found in rocks of the Battle Formation in the area, suggesting former presence of a calcareous, pre-alteration component. Generally, the rocks of the Antler sequence in the area have northerly strikes, from about N.5°E. to about N.25°W., and dip gently to the east approximately 10-30° (pl. 1). As such, these

essentially homoclinal rocks are part of the eastern limb of a broad anticlinal arch through this part of the mining district that has been disrupted by mostly Tertiary normal faulting (Theodore and others, 1989).

Antler Peak Limestone in the Elephant Head area is composed of two major, interlayered facies (pl. 1) that correlate with uppermost units of the Antler Peak Limestone at its type locality, as described by Roberts (1964). A carbonate-dominant facies of the Antler Peak Limestone is composed chiefly of light to dark gray, massive micrite locally mottled by chert, and includes sandy to pebbly pelmicrite with black chert clasts, dolomite, and biomicrite. In this report we follow the classification scheme of Blatt and others (1972) for carbonate rocks. Bedding in micrite ranges from 0.3 m thick to massive and contains some sequences with shale interbeds. This unit is generally well exposed (fig. 4). Fossils in biomicrite include bryozoans, crinoids, and brachiopod fragments (Theodore and others, 1989). A siliceous facies of the Antler Peak Limestone is composed of pale grayish orange to pale brown thinly-bedded carbonate-rich siltite interlayered with pale yellow brown carbonate-rich sandy siltite, pale brown carbonate-rich sandstone and dark gray dolomite. Rocks of this facies are only locally well exposed and generally form smooth slopes strewn with abundant plate-like fragments that have weathered out.

Generally, it appears that Antler Peak Limestone in the northeastern part of the map area is stratigraphically higher than Antler Peak Limestone in the southern part of the area (pl. 1). The lower contact of Antler Peak Limestone with Battle Formation is not exposed in the study area. A section of 600 m for the Antler Peak Limestone in the Buckingham - Elephant Head area was measured by H.G. Ferguson (Roberts, 1964), but some sequences of the Antler Peak Limestone in the study area may have been repeated by faulting.

Several small bodies of extremely altered intrusive rock (unit Ti, pl. 1) subsequently intruded the Paleozoic rocks in the Elephant Head area. These small bodies of altered intrusive rock probably correlate with Oligocene granodiorite porphyry of the Buckingham area where dating by the K-Ar method of one of these bodies about 0.5 km west of the Elephant Head area yielded an age of 35.4 $\pm$ 1.1 Ma (Theodore and others, 1989). Granodiorite porphyry in the study area was affected by argillic alteration, thus exposures are poor; it probably represents dispersed cupolas of a very shallowly emplaced stock. According to Theodore and others (1989),

granodiorite porphyry adjacent to the west edge of the Elephant Head area probably was emplaced at a maximum depth of about 400 m below the projected erosion surface upon which Caetano Tuff at Elephant Head was extruded. Although the age of granodiorite porphyry closely corresponds to that of Caetano Tuff (34 Ma), Theodore and others (1989) conclude that granodiorite porphyry is not comagmatic with Caetano Tuff based on lack of coincidence of Ba/Zr and Nb/Zr enrichment trends between the two rock types. To the north of the promontory at Elephant Head, the tuff unconformably overlies altered granodiorite porphyry in two exposures. Therefore, altered granodiorite porphyry was partially exposed at the surface by the time that the Caetano Tuff was formed.

Caetano Tuff unconformably overlies the Oligocene granodiorite porphry and rocks of the Antler sequence in the Elephant Head area (pl. 1). The tuff is a crystal-rich welded tuff. Roberts (1964) originally described this unit as a quartz latite but it has since been correlated with the regionally extensive Oligocene low-silica or calc-alkaline rhyolite Caetano Tuff (Theodore and others, 1973). The tuff contains three lithologic units (Roberts, 1964): a lower slightly welded, grayish-orange to pale pink biotite-quartz crystal tuff (7 m thick); a dark gray to black welded crystal-rich hornblende-biotite-quartz vitrophyre (7 to 10 m thick); and an upper stoney, partly devitrified, pale red sanidine(?)-quartz welded tuff (40 m thick). The basal unit is soft and pumiceous, cropping out only in the immediate area of the promontory at Elephant Head (pl. 1). Hornblende-biotite-quartz vitrophyre of the middle unit is present in the northeastern part of the map area. Most of the Caetano Tuff in the southern part of the area belongs to the upper unit, which weathers to rounded, exfoliated forms. These lithologic units of the Caetano Tuff are not subdivided on the geologic map of the area, and the Caetano Tuff has been tilted slightly to the east and has been cut by northwest- and northeast-striking faults.

Numerous faults of varied ages crop out in the Elephant Head area. The somewhat sinuous north-trending fault near the western border of the map area is probably an extension of the Elvira thrust fault described by Theodore and others (1989). As described in that report, this fault probably broke in response to an antithetic accomodation in the toe region of east-directed listric normal faulting in the easternmost of a series of three major low-angle faults that dissect the Buckingham stockwork molybdenum system. The listric normal faulting probably occurred during late Oligocene and early Miocene time. High-angle faults that cut

the Antler Peak Limestone in the northern part of the Elephant Head area show strikes to northwest and east-west (pl. 1). In the southern part of the map area, northwest and east-west striking high-angle faults terminate against north- and northeast striking faults. Thus, northeast striking faults apparently are younger. These north-northeast-striking faults were active during post-Caetano Tuff time as indicated by mapped offsets (pl. 1). East-west tectonic extension in this part of the Great Basin most likely became widespread about 18 Ma (Theodore and others, 1989). The Elvira fault is terminated by a northwest-striking fault; therefore, the northwest-striking fault set that has been mapped in the northern part of the area is post-Oligocene or Early Miocene (pl. 1). Generally there is little evidence that in the Elephant Head area emplacement of most of the exposed intrusive rocks was strongly fault controlled at the currently exposed levels of erosion. However, an altered granodiorite porphyry body that crops out near the southwest corner of the map area may have been emplaced along an east-west striking fault mapped there. The east-west striking faults appear to be among the oldest high-angle fault set mapped and may be penecontemporaneous with emplacement of Oligocene granodiorite porphyry although this type rock has a predominant northerly trend where it is well-exposed to the west. The northwest striking fault set is post-Elvira fault displacement in age, that is, post-Oligocene or Early Miocene in age. The north and northeast-striking high-angle faults are the youngest faults, perhaps 18 Ma or younger, and are probably associated with regional extensional tectonics during the Miocene.

The Quaternary system of the study area comprises unconsolidated colluvium, older alluvium and alluvial fan deposits (pl. 1).

GEOLOGIC RELATIONS OF JASPEROID

Numerous relatively small masses of jasperoid, from approximately 1 m to as much as 80 m in length, crop out in the Elephant Head area (pl. 1). Fabric of jasperoid bodies at the outcrop scale includes massive, bedded, fractured without recementation by subsequent generations of silica, and brecciated with silica recementation (fig. 5). The color of jasperoid is varied, and includes chiefly shades of brown, yellow, orange, and dusky red, and some black, whitish purple, gray and olive. One interesting color feature observed is termed variegated, which consists of a mixture of several colors in a free-form, flow-like pattern. Other samples show

jasperoid of one color to be brecciated and recemented by silica of another shade. Table 1 lists the rock type and features of the various samples analyzed. East of hill 5299 in the northern part of the map area, jasperoid-forming fluids appear to have traveled mostly along bedding planes in Antler Peak Limestone (pl. 1). Jasperoid bodies south of hill 5299 generally show fault-controlled spatial relations with surrounding geology; the strike of these faults associated with jasperoid shows no predominent orientation.

Calcite and (or) quartz veins appear especially concentrated near jasperoid formed in micrite, pelmicrite, or sandy pelmicrite of the Antler Peak Limestone, which generally shows outcrops almost totally devoid of any veins in areas well away from outcrops of jasperoid. These veins in places delineate narrow alteration zones measuring a few meters wide around bodies of jasperoid. At some localities, iron-oxide and manganese-oxide stained quartz veins seem to be associated preferentially with thin sequences of highly resistant sandy pelmicrite located near faults. At these sites, the sandy pelmicrite may have fractured due to increased strain generated by dislocations along nearby faults. Development of jasperoid in massive sequences of micrite may be either parallel or oblique to bedding. Individual beds with parting planes spaced every several cm in otherwise massive sequences of micrite show selective silicification and, in places, form transition zones of several m between micrite and well-developed, continuous masses of jasperoid. Some quartz veins are banded; they show streaks of yellowish-gray to pale yellow-brown iron oxides in planes parallel to the walls of the veins. In addition, concentrations of fine-grained sulfides, in places galena and pyrite, are mixed with milky-white quartz in planar zones along the walls of the veins. Although moderately- to coarsely-crystalline quartz makes up the bulk of the vein material and fillings of pods in and near many of the jasperoid bodies, chalcedonic quartz also is present locally in some jasperoid as an open-space filling that post-dates brecciation. In contrast to well-developed, tabular quartz veins that cross-cut the fabric of jasperoid, other quartz veins are sinuous, irregular masses that appear to "flow" with the structural fabric of the enclosing jasperoid.

Jasperoid at Elephant Head is present in the hanging wall along some faults. The structural-controlled aspects and mineralogic zoning of much of the jasperoid in the Elephant Head area are well exemplified by geologic relations exposed in a prospect pit at locality 56-57 (pl. 1). At this locality, a N. 15° W.-striking fault dips

steeply to the southwest, and shows yellow-to-red clay-rich gouge along its trace. In the hanging wall, immediately adjacent to the fault gouge, a 10- to 30-cm-wide zone of brown, locally opaline jasperoid is present. In turn, this brown jasperoid is mantled by gray jasperoid that together locally extend as much as 1 m from the trace of the fault. The brown jasperoid contains 406 ppb gold, and a sample from the gray jasperoid contains 3,250 ppb gold (analysis nos. 56-57, table 2). Finally, the gray jasperoid is mantled by an approximately 30-cm-wide zone of medium dark gray sparite containing very abundant anastomosing veins of calcite. Individual crystals of calcite in the veins are as much as 2 mm wide; most, however, are 1 mm wide or less.

MICROTEXTURES OF JASPEROID

In all, 26 samples of jasperoid were examined by standard microscopic methods, and seven of the samples of jasperoid were also examined by scanning electron microscope (SEM) methods. Lovering (1972) recognized the following microtextural types of patterns in the groundmass of jasperoid be studied: (1) jigsaw, (2) xenomorphic, (3) granular, (4) reticulated, and (5) feathery. Probably the most widespread textural pattern in jasperoid at Elephant Head is jigsaw; approximately 80 percent of the examined samples of jasperoid show at least some of this type of textural pattern--that is, highly irregular interlocked grains. A granular textural pattern is perhaps the next most abundant in jasperoid, and reticulated and feathery patterns are rare, but nonetheless present (fig. 6).

Microscopic examination reveals multiple generations of silica introduction in most samples. There does not appear to be a consistent style to the paragenetic development of jasperoid textural patterns; some samples show an early granulose pattern grading into a late-stage, open-cavity filling jigsaw pattern, whereas others show early jigsaw followed by a cross-cutting late jigsaw textural pattern. Some jasperoid samples show the former presence of dolomite by relict outlines of rhombic-shaped crystals almost replaced entirely by fine-grained, jigsaw-textured jasperoid, and then subsequently cut by colloform-banded chalcedonic quartz (fig. 7A). In places, goethite-rich jasperoid may be fractured and then lined by opaline-rich silica before it is cross-cut finally by cross-fiber textured chalcedonic quartz (fig. 7B). In other places, apparently well-crystalline, veins of granulose-textured quartz are in turned veined by extremely fine-grained jasperoid (fig. 8B). Most quartz

microveins show the presence of cross-fiber-textured chalcedonic quartz, in places as the only mineral in the microveins, and in other places, as the final phase to crystallize in the veins after a preceding stage wherein opaline silica was deposited (fig. 7B).

The widespread presence of jigsaw-textured jasperoid at Elephant Head contrasts with textures of jasperoid at some sedimentary-rock hosted disseminated Au-Ag deposits. At the Jerritt Canyon, Nevada, deposit, most gold seems to be associated with jasperoid that predominantly has a xenomorphic to reticulate texture (Hofstra and Rowe, 1987). At this deposit, jigsaw-textured jasperoid is rare, but jigsaw-textured recrystallized chert is widespread in unmineralized and low-metamorphic grade rocks surrounding the deposit (Hofstra and Rowe, 1987). Nonetheless, many of the occurrences of jigsaw-textured jasperoid at Elephant Head are associated with introduction of notable concentrations of gold (see below).

HEMIMORPHITE IN JASPEROID

Some very manganiferous- and probably lead-oxide-bearing goethitic jasperoid shows open spaces filled by sheaf-like aggregates of hemimorphite (ideally $Zn_4Si_2O_7(OH)_2 \cdot H_2O$, Fleischer and others, 1984), and then filled subsequently by granular-textured jasperoidal silica (fig. 7C). The hemimorphite at Elephant Head probably deviates somewhat from the chemical formula reported by Fleischer and others (1984) because its birefringence is somewhat greater than the one assigned to the ideal formula (0.028 compared with 0.022). Clots of hemimorphite at Elephant Head are present in another textural mode; it apparently replaces large crystals of calcite, whose former presence is suggested by outlines of relict twin planes defined by concentrations of iron oxide. In one sample (analysis no. 85, table 2), massive red-brown goethite is filled interstitially by extremely fine-grained, jigsaw-textured quartz, and is mantled by a narrow zone of barite-rich jasperoid. Gold has a concentration of 95.2 ppb and arsenic has a concentration of 2,420 ppm (analysis no. 85, table 2). The white domains in some of the variegated jasperoids described above result from milky-white globular masses of opaline silica that contain very fine-grained, euhedral crystals of porphyroblastic quartz. These globular masses of opaline silica are as much as several cm wide, and they are set in multicolored jasperoid that shows sweeping, well-developed, apparent flowage patterns.

The microscopic textural relations attest to a very complex evolutionary history for the jasperoid despite their apparently simple appearance in outcrop. Some of the textural complexities may be attributed to time- and (or) depth-dependent phenomena of silica crystallization. In some active geothermal systems, opaline sinter has been shown to change with depth and time to cristobalite and chalcedony (White, 1955; D.E. White and Chris Heropoulos, unpub. data, 1989), possibly following thereby a decreased solubility of silica with time, at constant temperature, in the sequence amorphous silica-cristobalite-chalcedony-quartz as determined experimentally by Fournier (1973). Thus, the generally late-stage chalcedonic quartz that followed paragenetically some earlier formed jasperoid and (or) vein quartz may be indicative of a culmination of silica solubility at Elephant Head at the time(s) that the chalcedonic quartz was being deposited.

Hemimorphite is commonly associated with jasperoid and chalcedony at many localities in the western United States (Heyl, 1964), although it was not reported in the jasperoids studied by Lovering (1972). At Elephant Head, hemimorphite sheaf-like aggregates protrude from a base of early-formed jasperoid and they are, in turn, overgrown by an apparently compatible, subsequent stage of jasperoid. The hemimorphite here does not replace previously crystallized sphalerite. Qualitative constraints on the physical conditions of development of jasperoid at Elephant Head are permitted by relations in hemimorphite paragenetically the same age as jasperoid. Fluid inclusions and experimental data on hemimorphite stability indicate that the jasperoids may have formed at low temperature and low pressure. Apparently primary, two-phase (liquid + vapor) fluid inclusions in hemimorphite contain as much as 90-95 volume percent liquid at room temperature. Many fluid inclusions have highly irregular tubular- and triangular-shaped outlines that are elongated parallel to the 010 crystal faces of the host hemimorphite. Visual estimates of vapor:liquid proportions in these fluid inclusions suggest that they would homogenize to liquid at temperatures largely in the 100° - 200 °C range. Such temperatures might be fairly good estimates for development of some of the surrounding jasperoid. Experimental studies in the system ZnO-SiO_2-H_2O suggest that hemimorphite is stable at less than approximately 250 °C, at pressures no higher than approximately 1.4 kb for $P_{H2O} = P_{tot}$ (Roy and Mumpton, 1956). At pressure-temperature conditions in excess of the univariant breakdown curve for hemimorphite, willemite (Zn_2SiO_4)+H_2O are the stable phases. However, willemite has been found to be coexisting stably with

wulfenite and other minerals in the supergene environment (Plough, 1941; Williams, 1966).

GEOCHEMISTRY

SAMPLING AND ANALYTICAL PROCEDURES

Jasperoid crops out in many localities in the Elephant Head area. In all, 97 samples were collected for geochemical study; 78 of these samples are various types of jasperoid (tables 1 and 2). Eight samples of Antler Peak Limestone were analyzed. Several other rocks at Elephant Head also were analyzed chemically (table 2). These include one sample of conglomerate from the Battle Formation (analysis no. 9), one sample of the baked zone at the base of the Caetano Tuff (analysis no. 88), three samples of quartz vein containing highly variable amounts of visible sulfide (analysis nos. 89-91), five samples of highly argillic- and phyllic-altered granodiorite (analysis nos. 92-96), and 1 sample of gossan (analysis no. 97). The size of the samples collected typically was 1-2 kg, and the type of sample was either a single grab sample or a composite sample made up of several cm-wide rock chips. Sample sites are identified on plate 1.

All 97 samples were analyzed for 44 elements by a semi-quantitative inductively coupled plasma-atomic emission spectroscopy (ICP-AES) method in the laboratories of the U.S. Geological Survey (see Lichte and others (1987) for specifics of the analytical procedures). Seventy of these samples samples, including two known barren control samples, were sent to Geochemical Services, Inc. in Torrance, California, for quantitative analysis for Ag, As, Au, Cu, Hg, Mo, Pb, Sb, Tl, and Zn using ICP-AES techniques employing a 2.5 g aliquot for digestion. The variability in lower detection levels in the quantitative ICP-AES analyses for Hg and Tl (table 2) is a computer-generated, complex function of concentrations encountered for the remaining elements. The material submitted to Geochemical Services, Inc. consisted of fragments of rock broken off rock samples submitted for semiquantitative ICP-AES analysis. Therefore, the quantitative and semiquantitative ICP-AES analyses (table 2) do not represent replicate chemical analyses of respective aliquots obtained from a pulverized, homogenized sample. We draw attention to this because there may be some geochemical inhomogenity inherent in the rocks themselves, even at the scale of a hand sample, as indicated by

the mineralogical variability shown by our petrographic and SEM investigations. Samples found to be very high (above the upper detection limit) in arsenic and antimony were reanalyzed by D. Vivit of the U. S. Geological Survey using energy dispersive X-ray fluorescence spectrometry (ED-XRF). Quantitative ICP-AES values reported in table 2, but in excess of calibration standards, include one analysis for Ag, three for As, two for Cu, nine for Pb, four for Sb, and five for Zn . These values in excess of the high standard are widely divergent when compared with corresponding analyses by the semiquantitative ICP-AES method. However, because of the surprising general correspondence between quantitative and semi-quantitative ICP-AES values for many analyses of samples that show low elemental concentrations, the more representative value was taken to be that obtained by the semiquantitative ICP-AES method instead of the quantitative one for the analyses in excess of the high standard. In addition, an 0.2 mg aliquot from 40 of the samples pulverized for the semiquantitative ICP-AES analyses was analyzed for As, Au, Sb, T1, and Hg by the quantitative dc-arc emission spectrography method (Golightly and others, 1987). The combined results of these analyses are also given in table 2.

ANTLER PEAK LIMESTONE

Chemical analyses are available for eight samples of Antler Peak Limestone (analysis nos. 1-8, table 2). Three apparently unaltered samples of Antler Peak Limestone (analysis nos. 1, 7-8, table 2) were analyzed by semi-quantitative ICP-AES methods. Only one of these samples was analyzed by quantitative ICP-AES methods (no. 1); this analysis shows 0.12 ppm silver, 4.39 ppm arsenic, less than 1 ppb gold, 15 ppm copper, 0.558 ppm mercury, 13.1 ppm lead, 2.34 ppm antimony, and 54.5 ppm zinc. These latter values are probably a fairly good estimate of background concentrations in unaltered Antler Peak Limestone. The three semiquantitative ICP-AES analyses for barium, manganese, and strontium respectively show 190-340 ppm, 30-1,200 ppm, and 33-190 ppm ranges in unaltered Antler Peak Limestone. Five of these analyses (nos. 2-6) are of altered rock that shows minor, yet variable, amounts of introduced quartz and (or) partial replacement by narrow stringers of calcite. As such, these five analyses cannot be considered as part of a data base for geochemical background. The five samples of altered Antler Peak Limestone contain as much as 89.3 ppm silver, 94.7 ppm arsenic, 74.8 ppb gold, 462 ppm copper, 5.99 ppm mercury, 2,550 ppm lead, 429 ppm antimony, and about 5,600 ppm zinc (table 2).

MISCELLANEOUS ROCKS

The small nunber of samples of miscellaneous rocks analyzed from the Elephant Head area includes one sample of minimally altered, as determined from hand-specimen examination, conglomerate of the Battle Formation (analysis no. 9, table 2). This particular sample is a chert-pepple conglomerate that has some buff- to ochre-colored iron oxide staining on its weathered surfaces that results mostly from concentrations of iron oxide along hair-line microveins of iron oxide and chalcedonic quartz. The iron oxides along the microveins probably replace iron sulfide(s). SEM study of a polished thin section indicates that some relict pyrite is still preserved in some domains of the rock and that much of the pyrite is associated with rutile in anhedral clots as much as 30 microns wide. In addition, many of these clots show nearby blebs of hydrothermal barite. The sample contains 2,200 ppm Ti and 950 ppm Ba, as well as 12 ppb Au, about 78 ppm Cu , and 330 ppm Zn (table 2).

A sample analyzed from the baked zone at the base of the Caetano Tuff (analysis no. 88, table 2) shows concentrations of some elements that are elevated and others that are not elevated with respect to local background abundances in Antler Peak Limestone--the inferred lithologic equivalent of the baked zone. Prior to contact alteration by the Caetano Tuff, the sampled baked zone probably was a fine-grained sandy micrite. The sample includes 3,100 ppm Ti, about 3.3 ppm Ag, 5.6 ppb Au, and 240 ppm Zn.

The three mineralized quartz veins all contain high concentrations of Cu, Pb, and Zn (analysis nos.89-91, table 2). One of the quartz veins also contains 370 ppm Mo. Gold concentrations in the three quartz veins are in the range 2.6-27.6 ppb, and are not strikingly anomalous when compared to the gold contents of jasperoid to be described below.

Semi-quantitative ICP-AES analyses available for five samples of altered granodiorite from the Elephant Head area (analysis nos. 92-96, table 2) show generally low abundances of base and ferrous metals with the exception of two of the samples which have 450 and 640 ppm Zn. The low abundances of these metals probably are the result of leaching in the supergene environment.

VARIATION OF ELEMENTS IN JASPEROID

A composite data matrix for 11 elements (Ag, As, Au, Ba, Cu, Mo, Mn, Pb, Sb, Sr, and Zn) in 78 samples of jasperoid (analysis nos.10-87, table 2) is presented in table 3. Detectable concentrations of mercury ($\geq$0.5 ppm) were found only in 19 samples and of thallium ($\geq$1.0 ppm) only in 20 samples. Even though these elements are extremely important in many sedimentary rock-hosted disseminated Au-Ag occurrences, mercury and thallium were not considered in statistical evaluations in the present report. We consider these numbers of detectable concentrations of mercury and thallium to be an inadequate sampling of jasperoid for these two elements. All samples that show detectable mercury also show detectable gold in the 1.4-3,490 ppb (part per billion) range; one sample (analysis no. 60, table 2) has concentrations of 15 ppm mercury and 3,490 ppb gold. However, there is no direct correlation between concentrations of mercury and gold. For example, a jasperoid sample containing 121 ppm mercury only includes 15.7 ppb gold (analysis no. 14, table 2).

In order to fill the geochemical data matrix as much as reasonably possible with numerical values to enhance thereby strength-of-association calculations by Spearman rank-correlation and factor analysis techniques attempted below, a small number of qualified "less than" concentrations for Ag, As, Au, Mo, Pb, and Sb were replaced by numerical values. The substitute values in table 3 are 50 percent of the value at the lower detection level by the analytical technique showing the most sensitive "less than" determination for a given element if a sample was analyzed by more than one technique. Estimated values were not substituted for in other samples if a given element was not analyzed by a method that had a comparable sensitivity and that showed qualified "less than" concentrations of lower sensitivities. As a result, table 3 includes the following numbers, in parentheses, of substitute values for the six above-listed elements: Ag(1), As(1), Au(10), Mo(14), Pb(2), and Sb(1). Qualified "greater than" concentrations were taken as the value to be used in assembly of table 3. In addition, reported values listed in table 2 as being above the high standard are probably not accurate for quantitative ICP-AES analyses and were replaced by values obtained using the semiquantitative ICP-AES method. Summary statistics for the 11 elements in the 78 jasperoid samples at Elephant Head (table 3) are given in table 4.

Frequency distributions of the untransformed geochemical data obtained from jasperoid (table 3) are strongly skewed negatively; that is, the most frequently occurring values are in the lowermost ranges of the reported concentrations with long "tails" in distribution of elemental concentrations toward high values. They are thus strongly nonnormal in overall distribution. To perform standard statistical calculations, geochemical data of table 3 were transformed by logarithms to the base 10 to approximate thereby a closer fit to lognormality. Figure 9 shows frequency diagrams for the transformed data of the 11 elements. The long "tails" at the high-value range in frequency diagrams of the raw data largely are curtailed, thus providing a data set that is a somewhat better fit to normality than the raw data. Tests of kurtosis and skewness values (table 4), frequently used measures of goodness-of-fit for normality, at the 95% confidence level show that only Ba, Mo, Mn, and Sr distributions tend to fit lognormal distributions for both types of tests. However, visual inspection of the frequency distribution for molybdenum in these samples shows its distribution to be strongly multimodal.

Q-Q calculations also were used to test the normality of the sample population of the quantitative ICP-AES data. This test compares the sample population and its mean to standard normal quartiles of a normal curve (Johnson and Wichern, 1982). A correlation coefficient, Rq, estimates within certain confidence limits, in this case 90 percent confidence, whether or not data were obtained from a parent population whose frequency of log-transformed concentrations would approximate a normal curve. If the value of Rq exceeds a critical value at the chosen confidence level, then the data approximate normality well enough to use standard parametric tests of statistical association. The critical value was met for Ag, As, Au, Pb, Sb, and Zn according to this test in contrast to the more widely used tests employing kurtosis and skewness described above that show Ba, Mo, Mn, and Sr distributions to approach lognormality at the 95% confidence level. In light of questions that might be raised concerning correlation calculations employing statistical methods that require normal distributions in the sampled population, non-parametric Spearman correlations were calculated for the data of table 3 transformed by logarithms to the base 10.

A non-parametric correlation statistic for all trace-element pairs available for the 11-element data set of table 3 was calculated as Spearman's r (Davis, 1986), where

$r = 1 - [6\Sigma(RX - RY)^2 / [n(n^2 - 1]$. Each value is ranked and corrections made for tied observations. Results of the calculation for r are given in table 5, and scatter plots for gold compared with each of the other ten elements are given in figure 10. From values of Spearman rank-correlation coefficients, gold in jasperoid at Elephant Head shows apparently its strongest positive association, values higher than 0.5, with Sb, As, Pb, and Ag--listed in order of decreasing r. Plots of these four elements compared with gold are very similar to one another, and all plots emphasize truncation of gold distribution at values less than the lower limit of detection (1 ppb by the quantitative ICP-AES method) (fig. 10). Strong associations between gold and base metals are fairly common in the Battle Mountain Mining District (Roberts and Arnold, 1965; Theodore and Blake, 1975). Bismuth is also associated strongly with gold in many deposits and occurrences in the mining district (Theodore and Blake, 1975; Myers and Meinert, 1988; Theodore and others, 1989). Unfortunately, distribution and strength of association of bismuth for other elements in jasperoid could not be established by our study. Bismuth is present in concentrations greater than or equal to 10 ppm, the lower limit of determination by the semiquantitative ICP-AES method, in only five samples (table 2). The highest concentration of bismuth (130 ppm, analysis no. 87, table 2) is present in a sample with 20.3 ppb Au, 7,000 ppm As, 24,000 ppm Cu, and 1,800 ppm Zn.

Principal components factor analysis, another multivariate statistical approach (Klovan, 1968; Davis, 1986), was used in an attempt to detect additional, geologically significant elemental associations that may not have been resolved through the use of correlation coefficients . Our preliminary tests involved utilization of various other standard manipulations of the 11 element-by-78 sample data set (table 4). Of the options attempted, a relatively simple factor analysis using three factors provides a geologically reasonable discrimination of the variances among the geochemical data. This three-factor model accounts, on average, for 78 percent of the original variances of all 11 elements. The R-mode principal components analysis, using an orthogonal transformation solution (table 6), reveals the following high, positive loadings among elements in the three-factor model, listed in order of decreasing loadings:

Factor 1: Sb, Pb, As, Zn, Ag, Au, Cu
Factor 2: Ba, Sr, Mn
Factor 3 Mo, Sr, Cu

These loadings, or measures of the degree of intercorrelation among the grouped elements (Klovan, 1968), are considered to be firmly established statistically because total matrix sampling adequacy has a value of 0.855, and thus meets minimum mathematical expectations of partial correlations tending toward zero (Kaiser, 1970). For the three-factor model adopted, calculated communalities suggest that anywhere from approximately 50 percent (Mn) to approximately 94 percent (Sb) of any elemental variance in the 11-element-by-78 sample data set is predictable from the remaining ten other elements.

Elemental associations in the three-factor model suggest dominance in their loadings by three geologic processes or environments:

Factor 1: Base and precious-metal mineralization
Factor 2: Paleozoic carbonate rock
Factor 3: Copper-molybdenum mineralization

The strong association between base and precious metals in jasperoid at Elephant Head suggests a geochemical signature indicative of polymetallic vein or polymetallic replacement deposits as defined by Cox and Singer (1986) or distal disseminated Ag-Au deposits (Dennis P. Cox, written commun., 1989).

The absence of a strong loading for manganese in Factor 1 suggests that jasperoid at Elephant Head is not geochemically similar to jasperoid associated with the polymetal Ag-Au-Pb-Zn Cove replacement deposit located about 30 km south-southwest of Elephant Head. Jasperoid at Cove is associated with extremely high concentrations of manganese (Bruce Kuyper, oral commun., 1988), and preliminary description of the paragenetic relations of gold and silver in this deposit were described above. Median value for manganese in 78 jasperoid samples at Elephant Head is 970 ppm; maximum is 23,000 ppm (table 4).

The strong association between base and precious metals in jasperoid does not fit geochemical signatures associated with most sedimentary rock-hosted disseminated Au-Ag deposits (Romberg, 1986; Ashton, 1988). Sedimentary rock-hosted disseminated Au-Ag deposits near the old Marigold Mine area of the Battle Mountain Mining District also are strongly associated with multiple generations of

hydrothermal barite (Graney and Wallace, 1988). Barite is present as cm-sized tabular crystals in jasperoid along north-south faults near these deposits, and is present conspicuously in the 8 South deposit in approximately 10-20 m wide zones that have as much as 80-90 volume percent hydrothermal barite. In contrast, jasperoid at Elephant Head has a median concentration of 325 ppm Ba and, a maximum concentration of only 1,900 ppm Ba (table 4). In comparison, barium abundances in some other sedimentary rock-hosted disseminated Au-Ag deposits are as much as 3,800 ppm (Dean and others, 1987).

The Factor 1 loading described above could result from mineralization that is either Late Cretaceous (Buckingham stockwork molybdenum-related) or middle Tertiary at Elephant Head, although middle Tertiary is probably more reasonable, particularly if our correlation of intrusive rocks at Elephant Head with Oligocene granodiorite porphyry is correct. Arsenic and, to a lesser degree, antimony are both associated widely with mostly Tertiary, fault-controlled, vein-type mineralization across much of the Battle Mountain Mining District (Roberts and Arnold, 1965).

We interpret high loadings for barium, manganese, and strontium in Factor 2 to be indicative of, or relict from, premineral elemental associations in Antler Peak Limestone which hosts most jasperoid samples studied at Elephant Head (table 6). We do not, however, suggest that these three elements are present in Antler Peak Limestone in highly elevated concentrations. Instead we feel that barium, manganese, and strontium may covary in unaltered Antler Peak Limestone and that such covariation may have contributed to their high loadings found in Factor 2. In fact, analyses of three samples of unaltered Antler Peak Limestone show that concentrations for these three elements are not elevated (analysis nos. 1, 7-8, table 2). Barium concentrations are in the 240-340 ppm range; manganese concentrations in the 30-1,200 ppm range; and strontium concentrations in the 33-190 ppm range. These values seemingly are depleted when compared to commonly cited crustal averages for carbonate rock. For example, Turekian and Wedepohl (1961) ascribe 1,100 ppm as the crustal average for manganese in carbonate rocks. Plots of barium versus manganese and strontium in jasperoid at Elephant Head show low covariations between these pairs of elements (fig. 11).

The association of abundance of gold with other physical features such as brecciation, nearby faults, variegated coloring, and lithologic facies of Antler Peak

Limestone was tested. To test these possible associations of gold with other features of the jasperoids non-parametric statistics are used because only presence or absence of such features can be recorded. The Mann-Whitney is one test whereby differences between means of log-transformed gold concentration between two groups, such as jasperoid samples showing brecciation and those which do not, may be evaluated (Davis, 1986). Truth of the null hypothesis, Ho=E(X)-E(Y), is tested, where E(X) and E(Y) are means of transformed gold concentrations for each group. The alternative hypothesis is Ha=E(X)>E(Y). Each observation is ranked and denoted RX or RY. The test statistic has the form $T = \sum RX - [n(n+1)/2]$, where RX is the rank of observations in the group with the higher mean and n is number of samples in the same group. Critical values for T are given in Davis (1986, table 2.22). Results of the Mann-Whitney test are shown in table 7. The null hypothesis cannot be rejected for brecciated jasperoid. Therefore, brecciation of jasperoid is apparently not associated strongly with increased gold concentrations in these samples at Elephant Head. The null hypothesis is rejected for jasperoid associated with faults and those showing variegated coloring, thus these features are apparently associated with increases in overall gold concentration (table 7). As described above, variegated coloring in jasperoid seems to indicate protracted development of jasperoid through at least several paragenetic stages. The null hypothesis was also rejected for jasperoid derived from the carbonate-dominant facies of Antler Peak Limestone. The significance of this result is uncertain, but may simply reflect a more efficient development of jasperoid in the carbonate-dominant facies of Antler Peak Limestone because of increased permeability.

Relations among concentrations of elements in jasperoid at Elephant Head also were examined using standard "spider" graph-type plots for 11 elements after first grouping the 11 elements by geochemical association and normalizing to a selected sample (analysis no. 12, table 2) that contains low metal contents (Michael G. Sawlan, written commun., 1989). Spider graphs of jasperoid with strong gold enrichment over both silver and base metals (Au-to-Ag normalized ratios greater than 1) show a characteristic pattern that results from the strong correspondence between precious metals and base metals described above (fig. 12 A). The jasperoid sample containing the highest content of gold (analysis no. 21, table 2) is emphasized on this plot by dashed line. Such plots provide a graphical representation of elemental enrichments relative to a local geochemical threshold. Barium, strontium, and manganese, together with copper and molybdenum to a somewhat

lesser degree, typically show low-level and inconsistent enrichment patterns compared with the pattern for arsenic, antimony, silver, gold, lead, and zinc. As described above, some manganese is present in jasperoid as rhodonite, which contains trace amounts of barium, as small patches of hollandite in rhodenite, and as possibly some variety of a hydrous oxide of manganese. Other samples with high Au-to-Ag normalized ratios (sample nos. 15, 32, 44, 45, 60, 61, 64, 69, 83) were used to define a field which differs substantially from samples with high copper and high Ag-to-Au normalized ratios (fig. 12 B, C). The sample with high normalized content of copper (no. 87, fig. 12 B) contributed toward the high loadings for molybdenum, strontium, and copper determined in the three-factor model described above and is ascribed possibly as a reflection of one aspect of copper-molybdenum mineralization at Elephant Head. This particular sample of jasperoid (no. 87) also contains 130 ppm bismuth and shows a lead:bismuth ratio approximately equal to 1--a relation that may have important implications as an exploration guide to mineralization at depth (see below).

COMPARISONS WITH SEDIMENTARY ROCK-HOSTED AND POLYMETAL DEPOSITS

Jasperoid at Elephant Head has some geochemical characteristics which distinguish it from jasperoid that is present at numerous sedimentary rock-hosted disseminated Au-Ag deposits in the northern Great Basin. In general, these characteristics involve increased abundances of base metals, enhanced associations of base metals with precious metals, and markedly different precious-metal ratios.

ARSENIC AND ANTIMONY

Most jasperoid samples at Elephant Head show lower Sb, As, and Au overall abundances than jasperoids at productive sedimentary rock-hosted Au-Ag deposits. However, the field outlined by data from Elephant Head includes much of the domain outlined by data for 11 sedimentary rock-hosted deposits (fig. 13, A and B). The data for these 11 deposits (Alligator Ridge, Carlin, Gold Quarry, Jerritt Canyon, Maggie Creek, Northumberland, Pinson, Preble, Taylor, Tonkin Springs, and Windfall) were composited from 48 analyses of jasperoid in Hill and others (1986) and Holland and others (1988). The Taylor deposit has since been included with

distal disseminated Ag-Au models under some recently proposed classification schemes (Dennis P. Cox, written commun., 1989). Partial chemical analyses for gold, arsenic, and antimony of 60 samples of jasperoid from the "A" ore zone at the Pinson deposit (Powers, 1978) show concentrations of gold and antimony roughly comparable to their contents at 10 other sedimentary rock-hosted old deposits (Holland and others, 1988; Hill and others, 1986). Arsenic in jasperoid at the "A" ore zone (245-1,650 ppm range) apparently shows somewhat elevated abundances relative to the other deposits. On the basis of arsenic and antimony strengths of association with gold in jasperoid at Elephant Head (and presumably mercury and thallium if viable data were available), one might infer a somewhat stronger affinity for jasperoid here to sedimentary rock-hosted Au-Ag deposits than that resulting from consideration of base-metal relations. Median values for As, Hg, and Sb at Elephant Head are nevertheless less than threshold values assigned to many sedimentary rock-hosted Au-Ag deposits (Ashton, 1989).

BASE METALS

A zinc-compared with-gold plot for jasperoid at Elephant Head and for the 11 productive gold deposits cited above illustrates the strong contrast in base-metal relations between the two groups of data (fig. 13, C). With exception of only a few data points, the two defined fields are mutually exclusive of each other. The median zinc abundance in 48 analyzed samples of jasperoid from the 11 productive deposits is 35 ppm, whereas median value for zinc in jasperoid at Elephant Head is 172 ppm (table 4). As we described above, most zinc in jasperoid here probably is present in hemimorphite. Jasperoid in the 11 productive deposits shows zinc concentrations that show almost no variation with concentrations of gold ($r = +0.15$).

We do not mean to imply, however, that low concentrations of base metals are typical of all rocks in sedimentary rock-hosted Au-Ag deposits, although physicochemical conditions thought to have been prevailing during their genesis suggest sulfides of Ag, Pb, Cu, and Zn are minimally soluble (Rose and Keuhn, 1987; see also Rota, 1987). Dean and others (1987) find that organic carbon-rich samples from these deposits show zinc abundances, on average, to be five times that of the average shale of Turekian (1972); lead, however, is not enriched significantly over its concentrations in average shale. Some sedimentary rock-hosted Au-Ag deposits

show significant local concentrations of elevated base-metal abundances that are related to the Au-Ag mineralization. Lead at the Gold Quarry Mine is as much as 500-4,000 ppm along some of the structurally-controlled feeder zones to rock mineralized by disseminated Au-Ag alteration assemblages (Hausen and others, 1983; Rota, 1987). Over the entire Gold Quarry Mine, lead typically is present in concentrations less than 100 ppm in those parts of the deposit dominated by a disseminated type of Au-Ag mineralization (Rota, 1987).

The base-metal data suggest that there are major geochemical differences between jasperoid at Elephant Head and jasperoid genetically associated with many of the sedimentary rock-hosted disseminated Au-Ag deposits in north-central Nevada. Ashton (1989) concluded from a geochemical study of jasperoid in these types of deposits that many jasperoid samples do not show unique geochemical signatures strongly indicative of sedimentary rock-hosted Au-Ag systems. Instead, Ashton (1989) noted that most jasperoid samples seem to have geochemical signatures mostly indicative of their host rocks. However, the jasperoids sampled by Ashton (1989) show extreme variations in trace-metal contents.

Jasperoid at Elephant Head also shows generally elevated base-metal abundance and enhanced base-metal correlations with gold relative to jasperoid in some other areas. Soulliere and others (1988) include chemical analyses of 117 samples of jasperoid from reconnaissance geochemical surveys near Mackay, Idaho. According to them, probable Tertiary jasperoid at Mackay has many geochemical and geological similarities to jasperoid associated genetically with sedimentary rock-hosted Au-Ag deposits in north-central Nevada (Soulliere and others, 1988; Wilson and others, 1988). The geochemical data base at the Mackay area contains 100 samples for which unqualified determinations for both gold and zinc are available: gold and zinc show median concentrations of 0.004 and 14.1 ppm respectively. As such, overall abundance of these two metals seems to be less in jasperoid at Mackay than at Elephant Head (compare table 4). A graph of log(Au, in ppm) compared with log(Zn, in ppm) for jasperoid at Elephant Head and at Mackay emphasizes major dissimilarities in gold and zinc relations between the two areas (fig. 14). Gold in jasperoid shows an extremely low correlation with zinc at Mackay ($r<0.01$), whereas at Elephant Head there is a strong positive correlation as we discussed above. In addition, generally low abundances of zinc in jasperoid at Mackay are similar to base-metal relations reported in many sedimentary rock-hosted Au-Ag

deposits (Holland and others, 1988; Hill and others, 1986; Ashton, 1989; see above). However, the mode of genesis of jasperoids is still not completely established in the Mackay area; they may be due to silica-rich fluids percolating downward from Eocene Challis Volcanics that have since been removed by erosion, or fluids migrating along karsts (Wilson and others, 1988).

PRECIOUS METALS

Precious-metal ratios, namely silver:gold, differ significantly in jasperoid at Elephant Head from those reported for most sedimentary rock-hosted disseminated Au-Ag deposits (fig. 15; see also Bagby and Berger, 1985; Silberman and Berger, 1985; and Berger and Silberman, 1985). Thirty-four samples of jasperoid at Elephant Head, for which valid determinations of both silver and gold concentrations are available, show a median silver:gold ratio of approximately 150. In contrast, 48 samples of jasperoid at 11 sedimentary rock-hosted Au-Ag deposits (Holland and others, 1988; Hill and others, 1986) show a distribution of silver:gold ratios with a median value of about 2.7. Nonetheless, some of these gold deposits, Taylor for example, seem to include higher overall abundance of silver than others (Bagby and Berger, 1985).

The high silver:gold ratio in jasperoid at Elephant suggests a probable close relationship to polymetal types of deposits, including polymetal replacement, polymetal vein, distal disseminated Ag-Au of Dennis P. Cox (written commun., 1989), and possibly even skarn. The Cove polymetal replacement deposit has a silver:gold ratio of about 60 (Echo Bay Mines, Special Report to Stockholders, December 23, 1987). Alternatively, high abundances of base metals and the association of base metals with precious metals in jasperoid at Elephant Head may be attributed to development at depths below the paleosurface greater than that generally ascribed to sedimentary rock-hosted disseminated Au-Ag deposits in north-central Nevada (Silberman and Berger, 1985; Berger and Silberman, 1985). It is unlikely, however, that the high abundance of base metals and the association of base metals with precious metals are the result of formation at depths greater than those typical of sedimentary rock-hosted disseminated Au-Ag deposits in north-central Nevada. Although schematic geochemical cross-sections through many of these deposits show that base metals apparently increase with depth, fluid-inclusion studies in some deposits indicate that they may have formed as deep as 3 km, based

on several hundred bars partial pressure of CO_2 in fluid inclusions associated with mineralization (Rose and Kuehn, 1987).

Paleogeographic inferences indicate that the jasperoid at Elephant Head formed at relatively shallow depths. If jasperoid at Elephant Head is related temporally to emplacement of 35.4 Ma granodiorite porphyry (see above), then elevated base-metal abundances in jasperoid are not the result of formation significantly deeper than sedimentary rock-hosted Au-Ag deposits. The fact that the 34 Ma-old erosion surface at the base of the Caetano Tuff crops out at Elephant Head would require unreasonably high erosion rates between emplacement of 35.4 Ma granodiorite porphyry and deposition of Caetano Tuff to strip as much as 3 km in such a geologically-short interval of time.

LEAD:BISMUTH RATIOS IN JASPEROID AND SKARN

Spatial and genetic associations between jasperoid and gold-bearing skarn (Wolfenden, 1965; Orris and others, 1987), prompted us to consider whether any jasperoid at Elephant Head shows geochemical signatures similar to gold-bearing skarn elsewhere in the mining district. We were interested particularly in geochemical signatures, if any, that may have been undetected by standard microscopic and statistical evaluations. Samples from the Fortitude gold skarn deposit , which has been described by Wotruba and others (1986) and Myers and Meinert (1988), were chosen for petrochemical analysis and provide a selected geochemical base-line for a skarn environment in the mining district to which we then referred our observations in jasperoid at Elephant Head.

Some free gold and native bismuth are present in galena near the northern, distal edge of the Fortitude gold skarn deposit (fig. 16). These samples show prominent myrmekitic or eutectoid-type intergrowths between native bismuth and galena (fig. 16A), similar in many textural aspects to gold-sillenite relations described previously in placer nuggets at Paiute Gulch, approximately 3 km northwest of Elephant Head (Theodore and others, 1989). Some of these domains of mostly intergrown native bismuth and galena at the Fortitude deposit include small anhedral blebs of gold (fig. 16, B and C). Areal percentages of minerals composing domains of mostly intergrown native bismuth and galena were recalculated in terms of atomic proportions of lead and bismuth; these show an overall lead-to-

bismuth ratio of approximately 1 (actually 1.25; average of five determinations using image-analysis programs of the SEM). Other phases present in very minor amounts include bismuthinite, tellurobismutite, and possibly schirmerite (ideally $3(Ag_2, Pb)S \bullet 2\ Bi_2S_3$). Calculated lead:bismuth ratios are close to that of cosalite (ideally $CuPb_7Bi_8S_{20}$; Sugaki and others,1986). Cosalite was synthesized in the system CuS-PbS-Bi_2S_3 at 400 °C and was found to decompose to lillianite ($Pb_3Bi_2S_6$) at 490 °C by Sugaki and others (1986). Ramdohr (1969) furthermore reported that granular masses of cosalite in some deposits may decompose or dissociate into native bismuth and galena. He also described other textural relations wherein cosalite is present in an apparently stable myrmekitic intergrowth with galena. Experimental studies in the system Bi-Pb-S indicate that cosalite, galena, and native bismuth are a stable assemblage at 100 °C, and that the assemblage native bismuth-galena can be stable at temperatures of about 400 °C (Craig, 1967). Therefore, the galena-native bismuth-gold textural relation at the Fortitude deposit (fig. 16A) may result from (1) crystallization of galena and native bismuth on or very close to a galena-native bismuth join at elevated temperatures of about 400 °C; or (2) initial crystallization of cosalite, or some other lead-bismuth sulfide that contains approximately equal amounts of these two metals, during sulfide stages of skarn development followed by a decline in sulfur activity and temperature such that galena and native bismuth become stable. The latter interpretation is preferred. Lead:bismuth ratios of rocks close to the calc-silicate-marble interface and altered by fluids depositing gold-bearing cosalite also should show roughly comparable lead-bismuth ratios. Such ratios may occur in any penecontemporaneous jasperoid that may have formed.

At Elephant Head, only one jasperoid sample (analysis no. 87, table 2; pl. 1) shows an approximate 1:1 ratio for lead to bismuth (110 ppm Pb; 130 ppm Bi). This jasperoid crops out just south of the promontory at Elephant Head in a north-striking fault zone that cuts Caetano Tuff along its trace farther to the north from the sampled locality. However, absence of jasperoid cutting Caetano Tuff anywhere in the area indicates that this particular occurrence is best evaluated as pre-Caetano Tuff jasperoid fortuitously caught up along a post-Caetano Tuff fault. Skarn was not noted to be present in surrounding outcrops of Antler Peak Limestone. However, prior to our work, a small high Cu-low Au system had been delineated by Duval Corp. by their drilling on a copper occurrence in the immediate area of this jasperoid sample (Patrick R. Wotruba, oral commun., 1989). This relation seems to enhance the viability of district-wide application of appropriately determined base-metal

ratios in sulfide-bearing ore as a discriminant among jasperoids that show wide-ranging base-metal ratios. Although some might argue that the system on the south flank of Elephant Head may be related to 38-40 Ma magmatism as is the Fortitude deposit, lead:bismuth ratios of approximately 1 also are present in many samples of jasperoid at the apparently Late Cretaceous Empire Au-Ag deposit, just southwest of the Elephant Head area (see below).

JASPEROID FROM THE EMPIRE DEPOSIT

Suites of chemically-analyzed jasperoid available for comparative purposes include 22 samples from the Empire Ag-Au deposit, a small deposit approximately 1.6 km southwest of Elephant Head (table 8). The Empire open-pit Au-Ag deposit included about 50,000 tonnes ore developed and mined in 1982 by Battle Mountain Gold Co. from a north-northeast striking fault zone (P. R. Wotruba, oral commun., 1982). Both hanging wall and footwall of the mineralized fault zone are mostly metamorphosed clastic rocks (quartz arenite, subarkose, arkose, and calcerous shale) of the Harmony Formation. The orebody itself consisted of a pod-like mass of variegated-in-color jasperoid that probably represents a silicified sandy micrite also belonging to the Harmony Formation. Alternatively, but less likely, the orebody at the Empire open-pit mine may be a lensoid mass of Antler Peak Limestone faulted downwards into surrounding rocks of Harmony Formation. This deposit is considered to have formed in conjunction with emplacement of the Buckingham stockwork molybdenum system (Theodore and others, 1989) and probably should be included among distal disseminated Ag-Au deposits as defined recently by Dennis P. Cox (written commun., 1989).

Methods by which jasperoid from the Empire open-pit deposit were analyzed differ from methods used to analyze jasperoid at Elephant Head (see table 8 and above). As a result, sensitivities of detection also differ for some elements and this creates certain difficulties for us to link validly pertinent geochemical characteristics between the two sets of data. Values for gold from the Empire open-pit deposit are one of most troublesome aspects because of its relatively high detection levels (50 ppb). Only three of 22 samples show detectable gold in the 60-200 ppb range (table 8). These three samples have Ag:Au ratios of about 15:1, 80:1, and 110:1. Therefore, we were not able to prepare comparative plots using concentrations of gold; we instead used concentrations of silver. However, limits of determination for some other

elements (mercury and thallium, in particular) are such that quantitative determinations are available for the entire set of samples from the Empire open-pit deposit. Table 9 shows summary statistics of data obtained from jasperoid at the Empire open-pit deposit, and comparison of elemental medians with medians of elements in jasperoids at Elephant Head suggests that concentrations of Ag, As, Ba, Cu, Pb and Sr are generally higher in jasperoid at the Empire open-pit deposit. However, we may not have adequately characterized distributions of elements at the Empire open-pit deposit because of relatively small number of samples Manganese, antimony, and zinc seem to have higher concentrations in jasperoid at Elephant Head than at the Empire open-pit deposit. When we further consider sensitivities at the lower limit of determination by the various analytical methods and compare the two data sets (table 2 and 8), the Empire open-pit deposit has higher abundances of bismuth and lower abundances of molybdenum than jasperoid at Elephant Head. This latter relation is somewhat surprising because of inferred genetic ties between the Empire deposit and the Buckingham stockwork molybdenum system (Theodore and others, 1989). It is interesting to note that lead:bismuth ratios in many samples from the Empire deposit are approximately 3:1 to 1:1 or less. This suggests that, had fluids responsible for generation of the deposit not been so strongly confined and controlled by the fault system, then any surrounding calcareous rocks of the Harmony Formation at depth near the core of the system might have been highly favorable for development of a gold-bearing deposit of much greater tonnage (see above).

Graphs of silver compared with zinc, arsenic, and antimony concentrations in jasperoid at Elephant Head, sedimentary rock-hosted Au-Ag deposits, and at the Empire deposit show variable overlap among outlined domains (fig. 17). Silver compared with zinc (fig. 17A) shows data from the Empire deposit to define a somewhat restricted field that falls well within the domain outlined by samples from sedimentary rock-hosted Au-Ag deposits. The generally low concentrations of zinc at the Empire deposit result in jasperoid from there showing silver-compared-with-zinc concentrations to fall well off the main trend of data points from jasperoid at Elephant Head. A plot of silver-compared with-arsenic data shows a strong correspondence of overlap among data from the three areas (fig. 17B). However, a silver-compared with-antimony graph seems to show a fairly high degree of discrimination for the three sets of data (fig. 17C). As shown in this plot, most of the field defined by data points from the Empire open-pit deposit occurs well away from

most plotted data points of analyses of jasperoid from sedimentary rock-hosted Au-Ag deposits. This relation is an indication of generally much lower overall concentrations of antimony in jasperoid samples at the Empire deposit than at the sedimentary rock-hosted Au-Ag deposits. Geologic environment and possibly age of formation apparently differ significantly among analyzed rocks comprising the three data sets. Abundance of antimony (4.6 ppm median; 0.15 to 22 ppm range; table 9) at the Empire deposit is well below the 50 ppm threshold level that seemingly characterizes many sedimentary rock-hosted Au-Ag deposits (Ashton, 1989).

GOLD IN JASPEROID--WHICH VALUES ARE ANOMALOUS?

Treatment of our data by various correlation statistics indicates that high As, Pb, Zn, and Sb concentrations in jasperoid, together with presence of nearby faults and "variegated" jasperoid, seem to be fairly good indicators of enhanced gold concentration in a jasperoid-forming environment probably related to polymetal-types of deposits, including distal disseminated Ag-Au deposits of Dennis P. Cox (written commun., 1989). We first attempted to define an anomalously high concentration of an element as values greater than one standard deviation above the geometric mean; this is commonly taken as a reasonable approximation of an anomaly by many others. However, this procedure resulted in excluding from further consideration a large number of samples of jasperoid because of the exceptionally wide range in their trace concentrations. For example, arsenic in jasperoid at Elephant Head has a geometric mean of 45.4 ppm, but a standard deviation of 1,907 ppm because of the 0.45-15,000 ppm range in its values (table 4). Similarly, gold in jasperoid would show an anomalous threshold at 1.6 ppm (or 1,600 ppb) -- values that geologically are unreasonably high by any currently-used exploration methodologies.

A more reasonable approximation of an anomalous threshold value for gold in jasperoid appears to be a value of twice the median, or 20 ppb (table 4). By this standard, 20 of the 78 samples of jasperoid contain gold concentrations greater than local geochemical background at Elephant Head. The range in gold concentrations in these 20 samples is 20 - 11,000 ppb.

Most sampled bodies of jasperoid showing anomalous concentrations of gold as defined above are in the southern one-half of the area studied where density of

mapped faults is most pronounced (table 2; pl. 1). In addition, a large number of jasperoid bodies showing gold concentrations greater than 20 ppb appear to be associated spatially with intensely altered intrusive rock that we have tentatively correlated with Tertiary granodiorite porphyry. Some gold and jasperoid, however, must post-date final emplacement of these bodies because gold-bearing jasperoid is present along some well-developed northeast-striking faults that cut altered granodiorite porphyry (loc. no. 95, pl. 1). Jasperoid that shows the highest concentration of gold (analysis no. 21, table 2; pl. 1) crops out approximately 100 m from the largest mapped body of altered granodiorite porphyry, just to north-northwest of the promontory named Elephant Head. This body of jasperoid is present along the mapped trace of an east-west fault that also cuts altered granodiorite porphyry. These relations suggest that circulation of gold-bearing fluids associated with jasperoid development were channeled strongly by faults, and that such circulation of gold-bearing fluids at Elephant Head continued after final emplacement of granodiorite porphyry to the erosion levels currently exposed, and that this protracted event may have occurred during a very narrow interval of time: post-altered granodiorite porphyry (35.4 Ma) and pre-Caetano Tuff (34 Ma).

SUMMARY

Jasperoid at Elephant Head has some geochemical characteristics which distinguish it from jasperoid that is present at numerous sedimentary rock-hosted disseminated Au-Ag deposits in the northern Great Basin. In general, these characteristics involve increased abundances of base metals, enhanced associations of base metals with precious metals, and markedly different precious-metal ratios. From these geochemical characteristics, we suggest that the jasperoids are related to polymetal types of mineralization rather than to sedimentary rock-hosted disseminated Au-Ag mineralization. In addition, base-metal ratios determined near the fringes of known ore in a mining district may serve as a useful discriminant among jasperoids elsewhere that typically show wide-ranging base-metal ratios. Application of this technique to the jasperoids at Elephant Head would have focused attention on one sample of jasperoid that had been shown previously to be in the immediate area of some copper mineralization at depth.

REFERENCES

Ashton, L.W., 1989, Geochemical exploration guidelines to disseminated gold deposits: Mining Engineering, v. 41, no. 3, p. 169-174.

Bagby, W.C., and Berger, B.R., 1985, Geologic characteristics of sediment-hosted, disseminated precious-metal deposits in the western United States, in Berger, B.R., and Bethke, P.M., eds., Geology and geochemistry of epithermal systems: Society of Economic Geologists Reviews in Economic Geology, v. 2, p. 169-202.

Bagby, W.C., Menzie, W.D., Mosier, D.L., and Singer, D.A., 1986, Grade and tonnage model carbonate-hosted Au-Ag, in Cox, D.P. and Singer, D.A., eds., Mineral deposit models: U.S. Geological Survey Bulletin 1693, p. 175-177.

Bakken, B.M., Hochella, M.F., Jr., Marshall, A.F., and Turner, A.M., 1989, High-resolution microscopy of gold in unoxidized ore from the Carlin Mine, Nevada: Economic Geology, v. 84, no. 1, p. 171-179.

Berger, B.R., and Silberman, M.L., 1985, Relationships of trace-element patterns to geology in hot-spring type precious-metal deposits, in Berger, B.R., and Bethke, P.M., eds., Geology and geochemistry of epithermal systems: Society of Economic Geologists Reviews in Economic Geology, v. 2, p. 233-247.

Berger, B.R., 1986, Descriptive model of carbonate-hosted Au-Ag, in Cox, D.P. and Singer, D.A. eds., Mineral deposit models: U.S. Geological Survey Bulletin 1693, p. 175.

Blatt, Harvey, Middleton, Gerard, and Murray, Raymond, 1972, Origin of sedimentary rocks: Englewood Cliffs, New Jersey, Prentice-Hall, Inc., 634 p.

Bloomstein, E.I., 1986, Ammonia alteration is a geochemical link in gold deposits of the Carlin-Midas belt [abs.]: Journal of Geochemical Exploration, v. 25, no. 1-2, p. 239.

Cookro, T.M., and Theodore, T.G., 1989, Geology and geochemistry in the vicinity of the Adelaide Crown Mine, Humboldt County, Nevada [abs.], in Schindler, K.S., ed., USGS research on mineral resources-1989: Program and Abstracts: U.S. Geological Survey Circular 1035, p. 10.

Cox, D.P., and Singer, D.A., editors, 1986, Mineral deposit models: U.S. Geological Survey Bulletin 1693, 379 p.

Craig, J.R., 1967, Phase relations and mineral assemblages in the Ag-Bi-Pb-S system: Mineraliun Deposita, v. 1, p. 278-306.

Davis, J.C., 1986, Statistics and data analysis in geology: New York, John Wiley, 646 p.

Dean, W.E., Pratt, L.M., Briggs, P.H., Daws, T.A., Engleman, E.E., Jackson, L., Layman, L.R., Ryder, J.L., Stone, C.L., Threlkeld, C.N., and Vuletich, A.K., 1987, Data on the geochemistry of Carlin-type disseminated gold deposits and associated rocks, northcentral Nevada: U.S. Geological Survey Open-file Report 87-446, 19 p.

Evans, J.G., and Peterson, J.A., 1986, Distribution of minor elements in the Rodeo Creek NE and Welches Canyon quadrangles, Eureka County, Nevada: U.S. Geological Survey Bulletin 1657, 65 p.

Fleischer, Michael, Wilcox, R.E., and Matzko, J.J., 1984, Microscopic determination of the nonopaque minerals: U.S. Geological Survey Bulletin 1627, 453 p.

Fournier, R.O., 1973, Silica in thermal waters--laboratory and field investigations, in Ingerson, Earl, ed., Symposium on hydrogeochemistry and biogeochemistry, Tokyo, 1970, Proceedings, v. 1, Hydrogeochemistry: Washington, D.C., The Clark Company, p. 122-139.

Gilluly, James, and Masursky, Harold, 1965, Geology of the Cortez quadrangle, Nevada, with a section on Gravity and aeromagnetic surveys, by D.R. Mabey: U.S. Geological Survey Bulletin 1175, 117 p.

Golightly, D.W., Dorrzapf, A.F., Jr., Mays, R.E., Fries, T.L., and Conklin, N.M., 1987, Analysis of geologic materials by direct-current arc emission spectrography and spectrometry, in Baedecker, P.A., ed., Methods for geochemical analysis: U.S. Geological Survey Bulletin 1770, p. A1-A13.

Graney, J.R., and Wallace, A.B., 1988, Stratigraphic and structural controls of gold mineralization in the Marigold project area, Nevada [abs.]: Geological Society of America Abstracts with Programs, v. 20, no. 7, p. A141.

Hausen, D., Ekburg, C., and Kula, F., 1983, Geochemical and XRD-computer logging for lithologic ore type classification of Carlin-type gold ores, in Hagni, R.D., ed., Process Mineralogy II, Applications in Metallurgy, Ceramics, and Geology: Warrendale, PA, Metallurgical Society of American Institute of Mining, Metallurgical, and Petroleum Engineers, p. 421-450.

Heyl, A.V., 1964, Oxidized zinc deposits of the United States, Part 3. Colorado: U.S. Geological Survey Bulletin 1135-C, 97 p.

Hill, R.H., Adrian, B.M., Bagby, W.C., Bailey, E.A., Goldfarb, R.J., and Pickthorn, W.J., 1986, Geochemical data for rock samples collected from selected

sediment-hosted disseminated precious-metal deposits in Nevada: U.S. Geological Survey, Open-file Report 86-107, 30p.

Hofstra, A.H., and Rowe, W.A., 1987, Sediment-hosted disseminated gold mineralization at Jerritt Canyon, Nevada. II--Jasperoid paragenesis and occurrence of gold [abs.]: Geological Society of America Abstracts with Programs, v. 19, no. 7, p. 704.

Holland, P.T., Beaty, D.W., and Snow, G.G., 1988, Comparative elemental and oxygen isotope geochemistry of jasperoid in the northern Great Basin: Evidence for distinctive fluid evolution in gold-producing hydrothermal systems: Economic Geology, v. 83, no. 7, p. 1401-1423.

Johnson, M.G., 1973, Placer gold deposits of Nevada: U.S. Geological Survey Bulletin 1356, 118 p.

Johnson, R.A., and Wichern, D.W., 1982, Applied multivariate statistical analysis: Englewood Cliffs, New Jersey, Prentice-Hall, Inc., 594 p.

Joralemon, Peter, 1951, The occurrence of gold at the Getchell mine, Nevada: Economic Geology, v. 46, no. 3, p. 267-310.

Kaiser, H.F., 1970, A second generation little jiffy: Psychometrika, v. 35, p. 401-415.

Klovan, J.E., 1968, Selection of target areas by factor analysis: Proceedings, Symposium on decision-making in exploration, Vancouver, B.C., January 26, 1968, [9 p.]

Lichte, F.E., Golightly, D.W., and Lamothe, P.J., 1987, Inductively coupled plasma-atomic emission spectrometry, in Baedecker, P.A., ed., Methods for geochemical analysis: U.S. Geological Survey Bulletin 1770, p. B1-B10.

Lovering, T.G., 1972, Jasperoid in the United States--its characteristics, origin, and economic significance: U.S. Geological Survey Professional Paper 710, 164 p.

Lovering, T.G., and Heyl, A.V., 1974, Jasperoid as a guide to mineralization in the Taylor mining district and vicinity near Ely, Nevada: Economic Geology, v. 69, no. 1, p. 46-58.

Lovering, T.G., and McCarthy, J.H., Jr., 1978, Detroit mining district, in Lovering, T.G., and McCarthy, J.H., Jr., eds., Conceptual models in exploration geochemistry; the Basin and Range Province of the western United States and northern Mexico: Journal Geochemical Exploration, v. 9, no. 2-3, p. 168-174.

Madrid, R.J., 1987, Stratigraphy of the Roberts Mountains allochton in north-central Nevada: Stanford, Calif., Stanford University, Ph.D. Dissertation, 341 p.

Madrid, R.J., and Bagby, W.C., 1988, Gold occurrence and its relation to vein and mineral paragenesis in selected sedimentary-rock-hosted, Carlin-type deposits in Nevada, in Goode, A.D.T., and Bosma, L.I., compilers, Bicentennial Gold 88, Extended Abstracts Oral Programme: Melbourne, Geological Society of Australia, Abstract Series no. 22, p. 161-166.

McKee, E.H., 1989, Potassium argon and 40Ar/39Ar geochronology of selected plutons in the Buckingham area, in Theodore, T.G., Blake, D.W., Loucks, T.A., and Johnson, C.A., Geology of the Buckingham stockwork molybdenum deposit and surrounding area, Lander County, Nevada: U.S. Geological Survey Professional Paper 798-D (in press).

McKee, E.H., and Silberman, M.L., 1970, Geochronology of Tertiary igneous rocks in central Nevada: Geological Society of America Bulletin, v. 81, no. 8, p. 2317-2328.

Myers, G.L., and Meinert, L.D., 1988, Zonation of the Copper Canyon-Fortitude gold skarn system [abs.]: Geological Society of America Abstracts with Programs, v. 20, no. 7, p. A93.

Nash, J.T., and Theodore, T.G., 1971, Ore fluids in the porphyry copper deposit at Copper Canyon, Nevada: Economic Geology, v. 66, no. 3, p. 385-399.

Nilsen, T.H., and Stewart, J.H., 1980, Penrose Conference Report; The Antler orogeny, mid-Paleozoic tectonism in western North America: Geology, v. 8, no. 6, p. 298-302.

Noble, J.A., 1970, Metal provinces of the western United States: Geological Society of America Bulletin, v. 71, no. 6, p. 1607-1624.

Oldow, J.S., 1983, Tectonic implications of a late Mesozoic fold and thrust belt in northwestern Nevada: Geology, v. 11, no. 9, p. 542-546.

Orris, G.J., Bliss, J.D., Hammarstrom, J.M., and Theodore, T.G., 1987, Descriptions and grades and tonnages for gold-bearing skarns: U.S. Geological Survey Open-file Report 87-273, 50 p.

Parratt, R.L., Bloomstein, E.I., and Tapper, C.J., 1989, Discovery, geology, and mineralization of the Rabbitt Creek gold deposit, Humboldt County, Nevada: Program with Abstracts, Annual Meeting, American Institute Mining Engineers, March, 1989, Las Vegas, Nevada, p.

Percival, T.J., Bagby, W.C., and Radtke, A.S., 1988, Physical and chemical featrues of precious metal deposits hosted by sedimentary rocks in the western United States, in Schafer, R.W., Cooper, J.J., and Vikre, P.G., eds., Bulk minable

precious metal deposits of the western United States: Reno, Nevada, Geological Society of Nevada Symposium Proceedings, April 6-8, 1987, p. 11-34.

Plough, F.H., 1941, Occurrence of willemite: American Mineralogist, v. 26, p. 92-104.

Powers, S.L., 1978, Jasperoid and disseminated gold at the Ogee-Pinson mine, Humboldt County, Nevada: Reno, Nevada, University of Nevada, M.S. Thesis, 112 p.

Radtke, A.S., 1985, Geology of the Carlin gold deposit, Nevada: U.S. Geology Survey Professional Paper 1267, 124 p.

Ramdohr, Paul, 1969, The ore minerals and their intergrowths: London, Pergamon Press, 1174 p.

Roberts, R.J., 1964, Stratigraphy and structure of the Antler Peak quadrangle, Humboldt and Lander Counties, Nevada: U.S. Geological Survey Professional Paper 459-A, 93 p.

Roberts, R.J., 1966, Metallogenic provinces and mineral belts in Nevada: Nevada Bureau of Mines Report 13, part A, p. 47-72.

Roberts, R.J., and Arnold, D.C., 1965, Ore deposits of the Antler Peak quadrangle, Humboldt and Lander Counties, Nevada: U.S. Geological Survey Professional Paper 459-B, 94 p.

Roberts, R.J., and Hotz, P.E., Gilluly, James, and Ferguson, H.G., 1958, Paleozoic rocks in north-central Nevada: American Association Petroleum Geologists Bulletin, v. 42, no. 12, p. 2,813-2,857.

Romberg, S.B., 1986, Ore deposits #9. - Disseminated gold deposits: Geoscience Canada, v. 13, no. 1, p. 23-31.

Rose, A.W., and Kuehn, C.A., 1987, Ore deposition from acidic CO2-rich solutions at the Carlin gold deposit, Eureka County, Nevada [abs.]: Geological Society of America Abstracts with Programs, v. 19, no. 7, p. 824.

Rota, J.C., 1987, Geology of Newmont Gold Company's Gold Quarry deposit, Eureka County, Nevada, in Elliott, I.L., and Smee, B.W., eds., GEOEXPO/86 -- Exploration in the North American Cordillera: Calgary, Canada, Association of Exploration Geochemists, p. 42-50.

Roy, D.M., and Mumpton, F.A., 1956, Stability of minerals in the system ZnO-SiO_2-H_2O: Economic Geology, v. 51, no. 5, p. 432-443.

Sawkins, F.J., 1983, Metal deposits in relation to plate tectonics: Berlin, Springer-Verlag, 325 p.

Schmidt, K.W., Wotruba, P.R., and Johnson, S.D., 1988, Gold-copper skarn and related mineralization at Copper Basin, Nevada: Reno, NV, Geological Society of Nevada, Fall (1988) Field-trip Guidebook, 6 p.

Silberling, N.J., 1986, Pre-Tertiary stratified rocks of the Tonopah $1^{o} \times 2^{o}$ quadrangle [abs.] in, D.H. Whitebread, compiler, Abstracts of the symposium on the geology and mineral deposits of the Tonopah $1^{o} \times 2^{o}$ quadrangle, Nevada: U.S. Geological Survey Open-File Report 86-467, p. 2-3.

Silberling, N.J., and Roberts, R.J., 1962, Pre-Tertiary stratigraphy and structure of northwestern Nevada: Geological Society of America Special Paper 72, 58 p.

Silberman, M. L., Berger, B.R., and Koski, R.A., 1974, K-Ar age relations of granodiorite emplacement and tungsten and gold mineralization near Getchell Mine, Humboldt County Nevada: Economic Geology, V. 69, p. 646-656.

Silberman, M.L., and Berger, B.R., 1985, Relationship of trace-element patterns to alteration and morphology in epithermal precious-metal deposits, in Berger, B.R., and Bethke, P.M., eds., Geology and Geochemistry of epithermal systems: Society of Economic Geologists Reviews in Economic Geology, v. 2, p. 203-232.

Soulliere, S.J., Wilson, A.B., Moye, F.J., and Rhea, K.P., 1988, Analytical results and sample locality map of jasperoid samples from Mackay, Idaho: U.S. Geological Survey Open-file Report 88-589, 22p.

Speed, R.C., 1977, Island arc and other paleogeographic terranes of late Paleozoic age in the western Great Basin, in, Stewart, J.H., Stevens, C.H., and Fritsche, A.E., eds., Paleozoic paleogeography of the western United States: Pacific Coast Paleography Symposium 1, The Pacific Section; Los Angeles, Calif., Society of Economic Paleotologists and Mineralogists, p. 349-362.

Speed, R.C., Elison, M.W., and Heck, F.R., 1988, Phonerozoic tectonic evolution of the Great Basin, in Ernst, W.G., ed., Metamorphism and crustal evolution of the western United States, Rubey volume VII: Englewood Cliffs, New Jersey, Prentice-Hall, p. 572-605.

Speed, R.C., and Sleep, N.H., 1982, Antler orogeny and foreland basin: A model: Geologic Society of America Bulletin, v. 93, p. 815-828.

Spurr, J.E., 1898, Geology of the Aspen mining district, Colorado, with atlas: U.S. Geological Survey Monograph 31, 260 p., and atlas of 30 sheets folio.

Stewart, J.H., 1980, Geology of Nevada-A discussion to accompany the Geologic Map of Nevada: Nevada Bureau of Mines and Geology, Special Publication 4, 136 p.

Stewart, J.H., and Poole, F.G., 1974, Lower Paleozoic and upermost Precambrian Cordilleran miogeocline, Great Basin, Western United States, in Dickinson, W.R., ed., Tectonics and Sedimentation: Society of Economic Paleontologists and Mineralogists Special Publication 22, p. 28-57.

Stewart, J.H., and McKee, E.H., 1977, Geology, Part I, in Geology and mineral deposits of Lander County, Nevada: Nevada Bureau of Mines and Geology Bulletin 88, p. 1-59.

Sugaki, A., Kitakaze,A., and Shima, H., 1986, Synthesis of cosalite and its phase relations in the Cu-Pb-Bi-S quaternary system, in Bonev, I., Kamenov, B. K., Stefanov, D., Todorova, T., eds., Crystal chemistry of minerals, Proceedings of the 13th General Meeting of the International Mineralogical Association, Varna, Bulgaria, September, 1982, p. 291-298.

Theodore, T.G., 1982, Preliminary geologic map of the Buckingham-Copper Basin area, Lander County, Nevada: U. S. Geological Survey Open-file Report 82-54. scale 1:4,800, 1 sheet.

Theodore, T.G., and Blake, D.W., 1975, Geology and geochemistry of the Copper Canyon poryphyry copper deposit and surrounding area, Lander County, Nevada: U.S. Geological Survey Professional Paper 798-B, 86 p.

---- 1978, Geology and geochemistry of the west ore body and associated skarns, Copper Canyon porphyry copper deposits, Lander County, Nevada, with a section on Electron microprobe analyses of andradite and diopside by N.G. Banks: U.S. Geological Survey Professional Paper 798-C, p. C1-C85.

Theodore, T.G., Blake, D.W., Loucks, T.A., and Johnson, C.A., 1989, Geology of the Buckingham stockwork molybdenum deposit and surrounding area, Lander County, Nevada: U.S. Geological Survey Professional Paper 798-D (in press).

Theodore, T.G., and Hammarstrom, J.M., 1989, Petrochemistry and fluid-inclusion study of skarns from the northern Battle Mountain mining district, Nevada, in Augustithis, S.S., ed., Skarns -- their genesis and metallogeny: Athens, Greece, Theophrastus Publications, S.A., (in press).

Theodore, T.G., Howe, S.S., Blake, D.W., and Wotruba, P.R., 1986, Geochemical and fluid zonation in the skarn environment at the Tomboy-Minnie gold deposits, Lander County, Nevada: Journal of Geochemical Exploration, v. 25, p. 99-128.

Theodore, T.G., and McKee, E.H., 1983, Geochronology and tectonics of the Buckingham porphyry molybdenum deposit, Lander County, Nevada [abs.]: Geological Society of America Abstracts with Programs, May 2-4, 1983, Salt Lake City, Utah, v. 15, no. 5, p. 275.

Theodore, T.G., and Roberts, R.J., 1971, Geochemistry and geology of deep drill holes at Iron Canyon, Lander County, Nevada, with a section on Geophysical logs of drill hole DDH-2 by C.J., Zablocki: U.S. Geological Survey Bulletin 1318, 32 p.

Theodore, T.G., Silberman, M.L., and Blake, D.W., 1973, Geochemistry and K-Ar ages of plutonic rocks in the Battle Mountain mining district, Lander County, Nevada: U.S. Geological Survey Professional Paper 798-A, 24 p.

Turekian, K.K., 1972, Chemistry of the earth: New York, Holt, Rinehart, and Winston, Inc., 131 p.

Turekian, K.K., and Wedepohl, K.H., 1961, Distribution of the elements in some major units of the earth's crust: Geological Society of America Bulletin, v. 72, p. 175-192.

Turner, R.J.W., Madrid, R.J., and Miller, E.L., 1989, Roberts Mountains allochthon: Stratigraphic comparison with lower Paleozoic outer continental margin strata of the northern Canadian Cordillera: Geology, v. 17, no. 4, p. 341-344.

Wells, J.D., Stoiser, L.R., and Elliot, J.E., 1969, Geology and geochemistry of the Cortez gold deposit, Nevada: Economic Geology, v. 64, no. 5, p. 526-537.

White, D.E., 1955, Thermal springs and epithermal ore deposits, in Bateman, A.M., ed., Economic Geology, Fiftieth Anniversary Volume, p. 99-154.

Wilden, Ronald, 1979, Ruby orogeny--a major early Paleozoic tectonic event, in Newman, G.W., and Goode, H.D., eds., Basin and Range Symposium and Great Basin Field Conference: Denver, Colo., Rocky Mountain Association of Geologists, p. 55-73.

Williams, S.A., 1966, The significance of habit and morphology of wulfenite: American Mineralogist, v. 51, no. 7, p. 1212-1217.

Wilson, A.B., Souillere, S.J., Skipp, Betty, Worl, R.G., and Rhea, K.P., 1988, Geology and geochemistry of jasperoid near Mackay, Idaho, in Link, P.K., and Hackett, W.R., eds., Guidebook to the geology of central and southern Idaho: Idaho Geological Survey Bulletin 27, p. 183-192.

Wolfenden, E.B., 1965, Bau mining district, west Sarawak, Malaysia, part I, Bau: Geological Survey of Malaysia (Borneo Region) Bulletin 7, pt. 1, 147 p.

Wotruba, P.R., Benson, R.G., and Schmidt, K.W., 1986, Battle Mountain describes the geology of its Fortitude gold-silver deposit at Copper Canyon: Mining Engineering, July 1986, v. 38, no. 7, p. 495-499.

Table 1.--Description of rocks analyzed from the Elephant Head area. Sample numbers same as analysis numbers on table 2 and location numbers on plate 1.

[--, not available]

Sample Nos.	Rock Type	Color	Comments
1	micrite, incipient jaspero	- -	outcrop; some quartz replacement
2	limestone breccia	light brown	outcrop; some quartz replacement
3	limestone. porous	moderate brown	outcrop; some quartz replacement
4	limestone	light brown	open cut; partially silicified
5	limestone	light brown	outcrop; partially silicified
6	micrite, porous	gray	- -
7	sandy pelmicrite	- -	partly altered to jasperoid
8	sparite	- -	contains iron oxides
9	conglomerate	- -	outcrop
10	jasperoid, fractured	moderate brown	outcrop; probable micrite protolith
11	jasperoid, fractured	moderate brown	float
12	jasperoid	- -	outcrop shows steeply-dipping quartz vein
13	jasperoid, bedded	- -	small discontinuous outcrops
14	jasperoid	moderate brown	prospect dump; secondary copper minerals
15	jasperoid, fault gouge	orange	open cut; porous
16	jasperoid	dark brown	outcrop; chalcedony-filled vugs
17	jasperoid	- -	close to fault trace
18	jasperoid	reddish brown	outcrop(?); open spaces filled by clear quartz
19	jasperoid, breccia(?)	brown	outcrop; recemented by late jasperoid
20	jasperoid	grayish orange	outcrop; fractures filled by chalcedony
21	jasperoid breccia	dark red	exposed in trench
22	jasperoid, brecciated	pale to medium brown	float
23	jasperoid	pale to moderate brow	outcrop(?)
24	jasperoid	moderate brown	outcrop; fault-controlled
25	jasperoid breccia	light brown	fault-controlled; chalcedony filled open spaces
26	jasperoid	moderate to dark brow	interbedded with partially silicified micrite
27	jasperoid	moderate brown	open spaces filled by dark quartz
28	jasperoid breccia	dark yellow orange	probable micrite-cemented-arenite protolith
29	jasperoid breccia	variegated	chalcedonic quartz-coated open spaces
30	jasperoid, fractured	dark red	probable micrite protolith
31	jasperoid, fractured	dark to dusky red	fault contact between Antler peak Ls. and Battle
32	jasperoid	black	locally porous
33	jasperoid breccia	gray orange to brown	outcrop
34	jasperoid breccia	gray orange to brown	outcrop; colloform quartz
35	jasperoid breccia	gray orange to brown	outcrop; quartz-filled fractures
36	jasperoid	- -	micrite protolith
37	jasperoid	medium gray	outcrop; probable shaly protolith
38	jasperoid	- -	adjacent to micrite
39	jasperoid	- -	adjacent to micrite
40	jasperoid breccia	yellow brown	outcrop; Mnox along fractures
41	jasperoid breccia	yellow brown	outcrop; some bedding preserved
42	jasperoid breccia	yellow brown	outcrop; surrounded by micrite
43	jasperoid breccia	yellow brown	outcrop; possibly localized by chert
44	jasperoid, fractured	yellow brown	outcrop; 3-m wide jasperoid zone
45	jasperoid, fractured	yellow brown	outcrop; contains quartz veins
46	jasperoid, fractured	yellow brown	outcrop; abundant small pods quartz
47	jasperoid, fractured, vugg	brown to olive gray	outcrop; secondary Cu mins + qtz
48	jasperoid, waxy	light brown	sparse quartz veinlets
49	jasperoid breccia	brown to olive gray	outcrop
50	jasperoid breccia	moderate brown	prospect dump
51	jasperoid, fractured	light brown	open cut
52	jasperoid, fractured	light olive gray	open cut
53	jasperoid	brown, local variegate	some pods of quartz vein
54	jasperoid	red, local variegated	some pods of quartz vein
55	jasperoid, fractured	dark yellow and orange	at Caetano Tuff contact
56	jasperoid breccia	dark gray, dusky brown	open cut, fault exposed
57	jasperoid	variegated	open cut, fault exposed
58	jasperoid, vuggy	brown	exposed in trench
59	jasperoid breccia	medium brown	exposed in trench
60	jasperoid	dusky red	open cut
61	jasperoid	- -	outcrop
62	jasperoid, fractured	moderate brown	open cut; contains late calcite
63	jasperoid breccia(?)	- -	possibly fault-related
64	jasperoid, bedded	- -	relict parting along bedding obvious
65	jasperoid	dusky red	float
66	jasperoid, bedded	- -	pelmicrite protolith

Table 1.--(cont'd)

Sample Nos.	Rock Type	Color	Comments
67	jasperoid	light brown	recognizable detrital quartz grains
68	jasperoid, bedded	yellowish brown	shaly beds replaced by jasperoid
69	jasperoid, massive	yellowish brown	float
70	jasperoid breccia	gray-purple-red	outcrop
71	jasperoid, bedded	brown	outcrop
72	jasperoid, bedded	- -	outcrop
73	jasperoid, massive	- -	outcrop also shows some bedded jasp
74	jasperoid, bedded	pale yellowish brown	outcrop
75	jasperoid breccia	- -	outcrop(?)
76	jasperoid microbreccia	variegated	outcrop(?)
77	jasperoid	brown	outcrop
78	jasperoid breccia	variegated	float
79	jasperoid breccia	black to dark brown	along fault
80	jasperoid, porous	black	locally abundant gray calcite veins
81	jasperoid breccia	variegated	outcrop
82	jasperoid breccia	dark yellow	outcrop
83	jasperoid breccia	variegated	outcrop
84	jasperoid fault gouge	reddish brown	open cut
85	jasperoid	dark red	outcrop
86	jasperoid. fractured	reddish brown	float
87	jasperoid	dark red	dump along road
88	baked contact zone	chalky light brown	at Caetano Tuff contact
89	sulfide-bearing quartz vei	- -	prospect dump, 8 cm-wide vein
90	sulfide-bearing quartz vei	- -	open cut, some secondary Cu mins
91	quartz vein	- -	prospect dump, some galena
92	altered granodiorite	- -	porphyritic, dike
93	altered granodiorite	- -	contains iron oxides after sulfides
94	altered granodiorite	weathers reddish	approximately 30 m wide
95	altered granodiorite	- -	highly altered; iron oxides replace pyrite
96	altered granodiorite	- -	outcrop along road cut; broken by fractures
97	gossan	- -	small prospect pit

Table 2.--Analytical data obtained from rocks cropping out in the Elephant Head area, northern Battle Mountain Mining District, Lander County, Nevada.

[Inductively coupled plasma-atomic emission spectroscopy (ICP-AES) analyses using the 0.2-digestion methods of Lichte and others (1987); routine precision of any single reported concentration is 3- to to 5-percent relative standard deviation; looked for but not found at part-per-million detection levels shown in parentheses: Eu(2), Ho(4), Ta(40), and U (100); P.H. Briggs, L. Bradley, analysts. Quatitative ICP-AES analyses using 2.5 g-digestion methods by GSI, Torrance, CA. Quantitative direct-current arc emission spectrography analyses using the methods of Golightly and others(1987); C. Heropoulos, analyst; --, not determined]

Analysis No.	1	2	3	4	5	6	7	8	9	10	11	12	13	14	15	16	17	18
#Field No. (84GJ...)	21A	110B	111A	114A	115B	221	284	298	215	149B	6B	21B	88	111B	139	147B	175	182A
			Antler Peak Limestone					Battle Fm.						Jasperoid				
		Inductively coupled plasma-atomic emission spectrometry analyses (ICP-AES) (parts per million)																
As	<10.0	10	160	50	40	30	<10.0	40	50	160	<10.0	<10.0	<10.0	110	40	110	100	10
Ba	240	300	46	290	58	340	340	190	950	330	260	230	1600	61	320	720	680	420
Be	<1.	<1.	<1.	<1.	<1.	<1.	1	<1.	<1.	<1.	<1.	<1.	<1.	<1.	1	<1.	<1.	<1.
Bi	<10.	<10.	<10.	<10.	<10.	<10.	<10.	<10.	<10.	<10.	<10.	<10.	<10.	<10.	<10	<10.	20	<10.
Cd	<2.	2	80	11	3	<2.	<2.	11	2	<2.	<2.	<2.	<2.	79	<2.	7	3	<2.
Ce	<4.	27	<4.	18	17	7	33	12	28	9	4	<4.	<4.	<4.	59	9	30	17
Co	2	9	3	6	4	3	2	2	20	3	3	2	2	13	7	<1.	4	1
Cr	29	60	9	92	52	490	160	30	180	23	68	31	34	19	140	10	350	74
Cu	10	80	1600	370	75	10	21	5	91	15	23	16	53	1500	70	34	50	8
Ga	<4.	15	44	9	7	<4	8	<4	11	4	<4.	<4.	<4.	11	11	12	11	<4.
La	3	13	<2.	10	9	4	23	9	17	7	4	4	2	2	38	9	32	12
Li	9	220	20	20	73	8	14	5	4	9	11	11	5	17	11	6	12	8
Mn	30	1000	780	1900	1200	1000	120	1200	1600	3000	700	230	130	6100	250	23000	220	360
Mo	<2.	<2.	4	<2.	2	3	<2.	<2.	<2.	<2.	<2.	<2.	<2.	8	<2.	7	10	<2.
Nd	<4.	17	<4.	9	9	6	22	7	17	5	<4.	<4.	<4.	<4.	41	6	38	12
Ni	8	74	24	70	95	13	41	2	69	15	23	8	8	40	78	4	45	5
Pb	8	62	5300	970	130	8	7	540	77	52	17	<4.	5	10000	150	400	5800	74
Sc	<2.	8	<2.	5	4	<2.	6	<2.	10	<2.	<2.	<2.	<2.	<2.	7	<2.	5	2
Sn	<20.	<20.	80	<20	<20.	<20.	<20.	<20.	<20.	<20.	<20.	<20.	<20.	<20.	<20.	<20.	<20.	<20.
Sr	100	78	18	280	220	34	33	190	65	95	39	56	140	110	36	100	88	32
Th	<4.	5	<4.	<4	<4.	<4.	5	<4.	<4.	<4.	<4.	<4.	<4.	<4.	8	7	<4.	<4.
Ti	200	1700	70	800	800	200	1700	400	2200	100	300	200	200	200	2200	60	700	600
V	7	160	18	170	96	38	73	25	160	43	13	8	24	67	86	110	290	30
Y	4	19	<2.	13	13	8	25	12	17	10	4	5	<2.	7	45	4	47	17
Yb	<1.	2	<1.	1	1	<1.	2	<1.	1	<1	<1.	<1.	<1.	<1.	5	<1.	4	1
Zn	16	760	16000	460	760	12	130	120	490	1100	75	34	130	4200	110	870	2400	78

Table 2.--(con'td)

Analysis No.	1	2	3	4	5	6	7	8	9	10	11	12	13	14	15	16	17	18
#Field No. (84GJ...)	21A	110B	111A	114A	115B	221	284	298	215	149B	6B	21B	88	111B	139	147B	175	182A
		Quantitative ICP-AES analyses (parts per million)*																
Ag	0.12	3.06	89.3	6.41	0.613	0.717	–	–	7.46	5.69	1.48	<0.045	1.27	‡374.	1.34	35.7	–	0.27
As	4.39	18.7	36.4	94.7	27.1	35.2	–	–	40.5	172	9.42	<.915	5.71	595	113	135	–	8.1
Au (ppb)	<1.	11.7	7	2.6	<1.	74.8	–	–	12	170	1.4	<1.	<1.	15.7	39.5	57.6	–	1.6
Cu	15	88.1	462	542	55.1	52.7	–	–	78.2	13.3	34.1	27.4	46.3	‡5260	37.7	24.3	–	14.3
Hg	0.558	2.55	132	5.99	0.476	0.545	–	–	0.53	<.464	0.83	<.457	<.473	121	0.927	0.648	–	<.446
Mo	2.48	3.31	34.6	3.41	1.45	9.09	–	–	3	1.53	6.77	7.88	7.44	33.3	1.29	11.4	–	4.7
Pb	13.1	89.2	‡2550	‡2090	96	15.9	–	–	56.4	19.6	102	1.75	5.57	‡1920	62.5	54.6	–	10.6
Sb	2.34	22.8	257	429	58.8	4.31	–	–	6.5	6.43	10	<.915	1.48	‡756	12.9	8.49	–	1.9
Tl	<.896	<.936	<.943	<.936	<.912	<.9	–	–	<.976	<.929	<.965	<.915	<.946	<.874	<.954	<.957	–	<.892
Zn	54.5	760	‡5590	589	724	55.9	–	–	330	1040	82.9	19.8	86.8	1977	97.9	760	–	29.3
		Quantitative dc-arc emission spectrography analyses (parts per million)																
As	–	–	–	–	–	–	–	–	250	–	–	–	–	–	–	–	–	–
Au	–	–	–	–	–	–	–	–	<0.2	–	–	–	–	–	–	–	–	–
Sb	–	–	–	–	–	–	–	–	28	–	–	–	–	–	–	–	–	–
Tl	–	–	–	–	–	–	–	–	<2.	–	–	–	–	–	–	–	–	–
Hg	–	–	–	–	–	–	–	–	<1.	–	–	–	–	–	–	–	–	–

Rock types shown on table 1.

* Except gold which is shown in parts per billion (ppb).

‡ Value above high standard and probably not accurate (see text).

Table 2.--(con'td)

Analysis No.	19	20	21	22	23	24	25	26	27	28	29	30	31	32	33	34	35	36	37
#Field No. (84GJ..)	183A1	183A2	191B	203A1	207	252A	252B	269B	285	287A	287C	294	306	309	42A	42B	42C	43B	44
												Jasperoid							
As	10	40	320	20	80	30	<10.0	20	20	20	30	580	130	30	10	30	<10.0	20	<10.0
Ba	970	1100	500	770	240	170	120	320	270	630	690	390	1900	130	300	220	230	250	71
Be	<1.	<1.	<1.	<1.	1	<1	<1.	<1.	1	<1.	<1.	2	<1.	<1.	<1.	<1.	<1.	<1.	<1.
Bi	<10.	<10.	<10.	<10.	<10.	<10.	<10.	<10.	<10	<10.	<10.	<10.	<10.	<10.	<10	<10.	<10.	<10.	<10.
Cd	4	7	<2.	<2.	<2.	<2.	<2.	<2.	2	<2.	3	3	19	<2.	<2.	<2.	<2.	<2.	<2.
Ce	11	28	4	9	28	9	5	<4.	24	25	13	7	10	11	16	9	12	8	<4.
Co	50	12	<1.	3	3	3	2	<1.	4	7	7	2	2	2	2	2	1	2	2
Cr	38	120	25	14	360	38	14	22	170	25	32	38	6	88	220	47	110	74	35
Cu	33	56	17	9	34	10	35	6	31	9	51	40	43	32	6	6	2	5	4
Ga	<4.	9	<4.	<4.	9	<4.	<4.	<4.	9	5	4	<4.	<4.	4	4	<4	<4.	<4.	<4.
La	6	19	3	5	29	6	3	<2.	14	12	5	8	5	10	14	7	8	7	3
Li	4	9	17	4	7	7	5	8	22	9	5	14	2	4	11	6	11	10	6
Mn	5300	8000	760	2000	140	440	130	1500	120	1500	2400	970	3700	1800	1300	530	770	370	240
Mo	4	4	<2.	<2.	2	<2.	<2.	<2.	<2.	<2.	<2.	2	2	<2.	<2.	<2.	<2.	<2.	<2.
Nd	4	14	<4.	<4.	21	5	<4.	<4.	15	11	7	8	<4.	8	11	6	10	6	<4.
Ni	70	63	3	18	71	21	6	5	42	33	49	11	13	18	19	13	12	13	18
Pb	35	24	560	29	29	9	12	26	19	6	89	1400	300	7	7	6	<4.	4	<4.
Sc	<2.	2	<2.	<2.	7	<2.	<2.	<2.	6	4	3	<2.	<2.	<2.	<2.	<2.	<2.	<2.	<2.
Sn	<20.	<20.	<20.	<20.	<20.	<20.	<20.	<20.	<20.	<20.	<20.	<20.	<20.	<20.	<20	<20.	<20.	<20.	<20.
Sr	32	52	15	45	18	30	8	22	35	26	34	43	100	62	31	32	18	17	75
Th	<4.	5	<4.	<4.	5	<4.	<4.	<4.	5	<4.	<4.	<4.	<4.	<4.	<4.	<4.	<4.	<4.	<4.
Ti	100	600	100	200	1300	400	200	200	1400	900	600	1200	60	800	500	400	500	400	200
V	8	54	43	24	140	23	11	11	87	67	180	60	8	44	38	36	26	34	10
Y	12	18	2	3	18	6	2	8	10	11	5	15	3	9	11	9	8	9	5
Yb	<1.	1	<1.	<1.	2	<1.	<1.	<1.	1	<1.	<1.	1	<1.	<1.	<1.	<1.	<1.	<1.	<1.
Zn	240	310	340	66	430	100	43	64	300	58	300	1400	2000	73	30	30	20	48	25

Table 2.--(con'td)

Analysis No.	19	20	21	22	23	24	25	26	27	28	29	30	31	32	33	34	35	36	37
#Field No. (84GJ..)	*183A1*	*183A2*	*191B*	*203A1*	*207*	*252A*	*252B*	*269B*	*285*	*287A*	*287C*	*294*	*306*	*309*	*42A*	*42B*	*42C*	*43B*	*44*
Ag	0.246	0.4	31.1	–	1.21	–	–	–	–	0.22	0.12	–	9.42	0.5	–	0.18	–	0.05	0.05
As	11.4	30.7	314	–	141	–	–	–	–	10.1	28.7	–	270	16.3	–	26.8	–	16.2	1.61
Au (ppb)	2.4	1.5	11000	–	221	–	–	–	–	26.6	92.6	–	39.9	10	–	8.5	–	4	<1.
Cu	37.8	27.6	22.9	–	55.4	–	–	–	–	25.7	68.1	–	65.7	11.5	–	19.6	–	23	22.8
Hg	0.563	<.434	1.59	–	<.48	–	–	–	–	<.438	<.475	–	<.473	<0.432	–	<.449	–	<.466	<.466
Mo	5.89	4.87	4.3	–	4.82	–	–	–	–	3.8	4.31	–	8.57	4.75	–	6.83	–	6.63	4.76
Pb	9.23	26.3	433	–	65.8	–	–	–	–	8.03	83.9	–	56.6	8.82	–	4.64	–	5.34	3.8
Sb	2.03	4.73	73	–	18.7	–	–	–	–	3.54	20.8	–	22.8	3.42	–	2.09	–	2.68	1.41
Tl	<.929	<.87	<.905	–	<.961	–	–	–	–	<.88	1.68	–	<.946	1.99	–	1.31	–	1.35	1.25
Zn	181	226	201	–	636	–	–	–	–	41.5	264	–	1960	92.7	–	20.8	–	39.7	38.2
As	–	–	–	–	--	–	–	–	–	–	--	--	--	–	4	19	5	–	4
Au	–	–	–	–	--	–	–	–	–	–	--	--	--	–	<0.2	<0.2	<0.2	–	<0.2
Sb	–	–	–	–	--	–	–	–	–	–	--	--	--	–	<2.	<2.	<2.	–	<2.
Tl	–	–	–	–	--	–	–	–	–	–	--	--	--	–	<2.	<2.	<2.	–	<2.
Hg	–	–	–	–	--	–	–	–	–	–	--	--	--	–	<2.	<2.	<2.	–	<2.

Table 2.--(con'td)

Analysis No.	38	39	40	41	42	43	44	45	46	47	48	49	50	51	52	53	54	55
#Field No. (84GJ..)	50B	50C	76A	*76B*	*76E*	*76F*	*77B*	*77C*	*77E*	*92A*	*92D*	*93A*	*112C*	*113C*	*123B*	*148A1*	*148A2*	*148B*
															Jasperiod			
As	50	10	<10.0	<10.0	<10.0	<10.0	20	30	10	20	20	10	50	20	40	200	130	190
Ba	410	360	120	120	88	160	260	340	240	290	530	240	420	310	1000	1400	1200	1500
Be	<1.	<1.	<1.	<1.	<1.	<1.	<1.	<1.	<1.	<1.	<1.	<1.	<1.	<1.	2	4	1	4
Bi	<10.	<10.	<10.	<10.	<10.	<10.	<10.	<10.	<10.	<10.	<10.	<10.	<10.	<10.	<10	<10.	<10.	10
Cd	<2.	<2.	<2.	<2.	<2.	<2.	<2.	<2.	<2.	<2.	3	<2.	15	<2.	3	32	47	27
Ce	9	11	5	6	<4.	<4.	8	8	<4.	21	26	6	15	20	54	29	8	40
Co	3	2	1	1	<1.	<1.	2	3	1	4	7	3	6	10	24	5	2	6
Cr	72	69	37	49	15	13	34	50	41	130	240	95	43	120	160	59	21	110
Cu	6	4	3	2	<1.	2	<1.	2	2	5	9	7	31	160	66	36	15	18
Ga	<4.	<4.	<4.	<4.	<4.	<4.	<4.	<4.	<4.	<4.	5	<4	8	13	18	9	5	11
La	9	11	3	4	<2.	2	4	4	2	23	22	8	8	11	31	12	9	28
Li	7	6	4	8	3	9	4	7	4	6	13	5	21	150	71	3	<2.	5
Mn	2100	2000	280	180	140	930	630	2100	960	720	950	1100	3700	970	400	12000	12000	11000
Mo	10	5	<2.	<2.	<2.	<2.	<2.	<2.	<2.	<2.	<2.	<2.	4	<2.	<2.	7	8	7
Nd	10	10	4	<4.	<4.	<4.	5	6	<4.	14	19	5	9	13	29	11	9	23
Ni	24	24	8	8	4	8	10	18	8	30	94	19	55	85	84	57	36	55
Pb	10	23	6	6	<4.	5	6	7	5	17	11	38	140	19	39	1100	53	180
Sc	<2.	<2.	<2.	<2.	<2.	<2.	<2.	<2.	<2.	2	3	<2.	4	11	15	<2.	<2.	4
Sn	<20.	<20.	<20.	<20.	<20.	<20.	<20.	<20.	<20.	<20.	<20.	<20.	<20.	<20	<20	<20.	<20.	<20
Sr	51	28	13	15	13	9	29	38	26	27	50	24	360	66	160	140	100	97
Th	<4.	<4.	<4.	<4.	<4.	<4.	<4.	<4.	<4.	<4.	5	<4.	5	6	8	5	4	9
Ti	300	400	200	300	100	90	200	300	200	500	1100	200	700	1600	3600	200	60	400
V	59	43	11	11	5	3	15	18	11	46	51	10	180	200	210	210	66	250
Y	10	11	4	6	3	2	3	6	4	14	16	9	16	18	19	10	16	19
Yb	<1.	<1.	<1.	<1.	<1.	<1.	<1.	<1.	<1.	<1.	1	<1.	2	2	2	1	1	2
Zn	63	30	45	59	13	28	34	12	9	120	160	120	900	500	1800	2100	1400	1500

Table 2.--(con'td)

Analysis No.																		
#Field No. (84GJ..)	38	39	40	41	42	43	44	45	46	47	48	49	50	51	52	53	54	55
	50B	50C	76A	76B	76E	76F	77B	77C	77E	92A	92D	93A	112C	113C	123B	148A1	148A2	148B
Ag	–	–	0.19	–	–	–	0.255	0.179	0.337	0.33	0.35	0.081	1.37	1.52	0.906	4.79	3.71	3.95
As	–	–	3.63	–	–	–	19	20.8	9.71	17.3	17.8	12	49.8	20.1	34.3	213	151	190
Au (ppb)	–	–	9.3	–	–	–	<1.	10.3	6.7	<1.	<1.	<1.	<1.	<1.	4.2	34.6	4.9	9.2
Cu	–	–	18.8	–	–	–	23.7	13.4	16	22.9	19.3	16.5	34.5	116	69	66.4	39.1	22.3
Hg	–	–	2.04	–	–	–	<.466	<.451	<.473	<.475	<.451	<.446	<.478	1.07	0.809	0.57	<.443	<.482
Mo	–	–	5.79	–	–	–	7.89	7.95	6.67	6.27	4.95	6.53	6.56	2.36	2.38	8.48	10.2	7.95
Pb	–	–	5.72	–	–	–	8.31	6.83	5.54	17.2	12.7	29.7	110	14.3	32.5	927	52.4	141
Sb	–	–	2.2	–	–	–	2.57	3.61	1.87	3.69	4.45	1.75	13.1	7.01	5.28	96.7	70.5	33
Tl	–	–	<.936	–	–	–	1.03	1.6	<.946	<.95	<.9	1.5	1.01	1.9	0.962	3.77	1.21	1.93
Zn	–	–	38.6	–	–	–	33.9	10.9	7.25	101	128	88.2	720	427	1570	1910	1220	1280
As	43	5	2	2	<2.0	<2.0	14	19	5	21	13	10	235	16	124	210	140	360
Au	<0.2	<0.2	<0.2	<0.2	<0.2	<0.2	<0.2	<0.2	<0.2	<0.2	<0.2	<0.2	<0.2	<0.2	<0.2	<0.2	<0.2	<0.2
Sb	4	<2.	<2.	<2.	<2.	<2.	3	4	3	5	7	3	42	9	32	120	93	42
Tl	<2.	<2.	<2.	<2.	<2.	<2.	<2.	<2.	<2.	<2.	<2.	<2.	<2.	<2.	<2.	<2.	<2.	<2.
Hg	<2.	<2.	11	<2.	<2.	<2.	<2.	<2.	<2.	<2.	<2.	<2.	<1.	<2.	<1.	<2.	<2.	<2.

Table 2.--(con'td)

Analysis No.	56	57	58	59	60	61	62	63	64	65	66	67	68	69	70	71
#Field No. (84GJ..)	159B	159C	163A	163B	166A	166C	166D	169A	169B	171A	171B	195	176A	176B	212	222A
As	2100	23000	80	920	1100	740	1000	30	40	70	50	50	60	20	30	320
Ba	170	170	420	240	380	370	670	440	240	680	360	440	360	270	250	500
Be	<1.	<1.	<1.	<1.	<1.	<1.	<1.	<1.	<1.	<1.	<1.	<1.	1	<1.	<1.	<1.
Bi	<10.	10	<10.	10	<10.	<10.	<10.	<10.	<10.	<10.	<10.	<10.	<10.	<10.	<10.	<10.
Cd	53	490	<2.	8	30	9	20	2	<2.	2	<2.	4	<2.	<2.	<2.	3
Ce	41	16	34	9	7	4	17	22	7	23	5	44	19	22	<4.	17
Co	2	3	14	4	1	2	3	3	2	3	2	1	3	3	<1.	1
Cr	48	130	110	66	43	47	35	4	43	220	120	66	870	220	47	22
Cu	180	930	8	19	38	22	27	7	7	6	3	34	64	16	6	7
Ga	4	11	14	<4.	4	<4.	5	<4.	<4.	4	<4.	8	8	6	<4.	<4.
La	38	17	18	13	7	4	13	11	5	26	6	27	18	20	3	13
Li	50	4	50	4	17	23	13	5	4	9	6	10	24	10	9	4
Mn	7100	4600	940	920	5000	570	3600	2100	90	1200	940	45	70	480	880	3000
Mo	3	<2.	<2.	17	<2.	<2.	4	4	2	3	<2.	<2.	3	<2.	<2.	<2.
Nd	27	13	18	15	<4.	<4.	8	9	4	15	4	23	21	18	<4.	12
Ni	11	18	69	87	11	8	9	19	10	26	12	18	120	53	3	12
Pb	20000	>100000	350	400	5900	1600	5400	36	36	150	31	140	44	15	490	230
Sc	<2.	3	10	<2.	<2.	<2.	<2.	<2.	<2.	<2.	<2.	5	6	5	<2.	<2.
Sn	<20.	<20	<20.	<20.	<20.	<20.	<20.	<20.	<20.	<20.	<20.	<20.	<20.	<20.	<20.	<20.
Sr	18	48	140	28	32	38	98	45	37	57	25	18	58	35	24	41
Th	<4.	<4	5	<4.	<4.	<4.	<4.	<4.	<4.	<4.	<4.	<5.	<4.	4	<4.	<4.
Ti	200	700	1800	300	200	200	300	200	90	400	300	1700	1200	1000	90	200
V	44	280	170	50	57	82	82	35	13	110	34	130	220	78	27	59
Y	12	21	19	12	8	5	11	10	6	13	4	8	24	22	2	15
Yb	1	1	2	<1.	<1.	<1.	<1.	<1.	<1.	<1.	<1.	<1.	3	2	<1.	1
Zn	15000	56000	370	2400	4800	1800	3400	200	77	280	140	250	540	150	96	900

Table 2.--(con'td)

Analysis No.	56	57	58	59	60	61	62	63	64	65	66	67	68	69	70	71
#Field No. (84GJ..)	*159B*	*159C*	*163A*	*163B*	*166A*	*166C*	*166D*	*169A*	*169B*	*171A*	*171B*	*195*	*176A*	*176B*	*212*	*222A*
Ag	2.14	70.9	0.38	6.07	12	10.5	10.2	0.28	0.33	0.51	0.674	0.57	0.412	0.249	3.24	0.434
As	215	2500	102	653	824	629	468	32.2	38.4	72.8	75.6	47.5	58.5	17.2	25.5	315
Au (ppb)	406	3250	18	15.5	3490	1190	458	34.1	17.7	5.7	11.3	1.5	<1.	9.8	38.2	18
Cu	62.3	2880	33.2	40.4	145	47.7	101	68.8	28.1	25.5	14.3	41.1	68.3	24.2	32.1	64.2
Hg	0.078	2.69	<.477	0.959	15	4.7	8.62	<.456	0.78	<.466	<.484	<.468	0.702	<.477	0.994	0.488
Mo	0.973	8.3	3.39	20.6	5.04	4.76	5.75	8.17	6.83	5.29	4.14	2.84	5.89	2.04	4.01	6.32
Pb	285	‡2050.	408	326	‡2560.	1060	‡2590.	99.2	28.4	92.2	58.1	138	31.3	13.6	425	174
Sb	50.3	‡799.	11.7	74.8	188	58.4	143	4.25	2.33	10.8	7.58	6.23	4.15	3.12	9.25	9.11
Tl	<.11	<.972	<.954	25.7	4.23	<.909	2	<.912	<.954	<.932	<.968	1.13	2.99	<.954	<.896	1.9
Zn	536	‡4700.	384	2060	‡4730.	1140	2790	235	65.1	276	252	239	517	137	77.1	786
As	>500	>500	15	>500	>500	>500	>500	39	77	410	193	280	120	17	29	245
Au	3.2	2.8	<0.2	<0.2	3.4	0.9	0.3	<0.2	<0.2	<0.2	<0.2	<0.2	<0.2	<0.2	<0.2	<0.2
Sb	>500	>500	12	88	260	60	230	8	<2.	29	25	28	12	<2.	13	10
Tl	<2.	<2.	<2.	41	<2.	<2.	<2.	<2.	<2.	<2.	<2.	<2.	<2.	<2.	<2.	<2.
Hg	<2.	<2.	<2.	<2.	36	16	36	<2.	<2.	<1.	<1.	<1.	<2.	<2.	<2.	<2.

Table 2.--(con'td)															
Analysis No.	72	73	74	75	76	77	78	79	80	81	82	83	84	85	86
#Field No. (84GJ..)	235A	235B	238	245	247	248	249C	225	226A	288A	288B	289	295	299D	302B
										Jasperoid Baked zone					
As	10	20	10	90	20	230	<10.0	40	80	10	20	20	130	1500	20
Ba	88	360	62	280	740	280	200	150	190	340	420	650	980	210	560
Be	<1.	<1.	<1.	<1.	1	<1.	<1.	<1.	<1.	<1.	<1.	1	2	<1.	1
Bi	<10.	<10.	<10.	<10.	<10.	<10.	<10.	<10.	<10.	<10.	<10.	<10.	<10.	<10.	<10.
Cd	<2.	<2.	<2.	<2.	2	2	<2.	3	2	<2.	<2.	<2.	3	120	2
Ce	5	11	<4.	17	15	17	<4.	7	<4.	14	14	17	30	12	34
Co	2	3	1	3	6	2	<1.	2	2	4	6	5	6	3	3
Cr	50	82	26	150	290	35	12	66	31	31	33	78	180	30	170
Cu	5	9	3	29	11	6	2	5	5	39	24	13	16	410	14
Ga	<4.	<4.	<4.	5	5	<4.	<4.	<4.	<4.	<4.	5	6	10	5	5
La	6	11	<2.	12	16	11	<2.	9	4	6	6	12	24	11	54
Li	7	8	<2.	6	7	8	<2.	<2.	6	10	17	10	21	7	6
Mn	150	1700	200	970	1800	1100	620	3500	2900	1000	1100	1600	990	2100	230
Mo	<2.	<2.	<2.	<2.	<2.	<2.	<2.	<2.	<2.	<2.	<2.	<2.	<2.	6	<2.
Nd	5	9	<4.	10	12	12	<4.	6	<4.	6	6	13	23	10	49
Ni	8	17	4	100	32	16	<2.	21	11	27	43	33	21	5	35
Pb	7	18	46	16	22	38	4	20	54	9	15	32	570	46000	31
Sc	<2.	<2.	<2.	3	2	2	<2.	<2.	<2.	2	3	3	6	<2.	5
Sn	<20.	<20.	<20.	<20.	<20.	<20.	<20.	<20.	<20.	<20.	<20.	<20.	<20.	<20.	<20.
Sr	17	29	15	27	38	110	11	45	56	73	120	31	130	190	52
Th	<4.	<4.	<4.	<4.	<4.	<4.	<4.	<4.	<4.	<4.	<4.	6	6	<4.	6
Ti	200	300	50	900	500	800	80	200	90	700	800	900	1900	60	1600
V	18	33	32	59	74	45	5	29	21	48	61	52	190	840	53
Y	6	12	<2.	7	13	10	2	9	3	10	10	12	20	12	46
Yb	<1.	<1.	<1.	<1.	1	1	<1.	<1.	<1.	<1.	1	1	2	1	4
Zn	63	140	160	190	190	190	57	250	250	120	90	150	990	27000	100

Table 2.--(con'td)															
Analysis No.	72	73	74	75	76	77	78	79	80	81	82	83	84	85	86
#Field No. (84GJ..)	235A	235B	238	245	247	248	249C	225	226A	288A	288B	289	295	299D	302B
Ag	–	–	–	–	–	–	–	0.349	16.2	1.82	1.79	0.047	0.684	38.5	0.239
As	–	–	–	–	–	–	–	28.4	75.1	10.7	16.4	15.1	126	‡2420.	107
Au (ppb)	–	–	–	–	–	–	–	15.1	28.1	9.4	8.1	20.2	1070	95.2	1.6
Cu	–	–	–	–	–	–	–	21.3	67.1	49.5	30.1	27.2	49.2	888	208
Hg	–	–	–	–	–	–	–	<.444	<.437	3.16	1.14	<.478	<.446	0.732	<.466
Mo	–	–	–	–	–	–	–	5.71	4.79	4.03	3.27	3.17	2.08	5.91	1.95
Pb	–	–	–	–	–	–	–	20.7	42.1	12	15.3	31.1	559	‡2420	268
Sb	–	–	–	–	–	–	–	19.3	9.62	4.35	3.07	5.51	50.8	‡930	7.15
Tl	–	–	–	–	–	–	–	<.889	1.06	<.95	<.98	<.957	<.892	3.7	<.932
Zn	–	–	–	–	–	–	–	163	236	98.9	77.6	125	817	‡5030.	305
As	10	12	9	110	10	300	5	200	690	32	98	67	940	>1000.0	144
Au	<0.2	<0.2	<0.2	<0.2	<0.2	<0.2	<0.2	<0.2	<0.2	<0.2	<0.2	<0.2	<0.2	<0.2	<0.2
Sb	<2.	5	<2.	25	3	6	<2.	63	18	18	17	20	117	>1000.	<2.
Tl	<2.	<2.	<2.	<2.	<2.	<2.	<2.	<2.	<.2	<2.	<2.	<2.	<2.	<2.	<2.
Hg	<2.	<2.	<2.	<2.	<2.	<2.	<2.	<1.	<1.	<1.	<1.	<1.	<1.	<1.	<1.

Table 2.--(con'td)											
Analysis No.	87	88	89	90	91	92	93	94	95	96	97
#Field No. (84GJ..)	*307A*	*125*	*111C*	*114B*	*115C*	*206A*	*210*	*204*	*167*	*153B*	*229*
		Baked zone			Quartz vein		Altered granodiorite				Gossan
As	7000	60	50	100	1000	30	20	20	70	30	440
Ba	130	260	48	1600	540	970	480	1400	1300	900	480
Be	<1.	1	<1.	<1.	<1.	1	2	2	2	2	<1.
Bi	130	<10.	<10.	<10.	<10.	<10.	<10.	<10.	<10.	<10.	10
Cd	12	3	30	7	510	6	<2.	2	3	<2.	3
Ce	21	48	<4.	<4.	<4.	71	69	78	52	69	18
Co	41	13	2	2	2	9	4	8	2	8	6
Cr	91	300	43	43	13	7	13	8	9	7	99
Cu	24000	110	1400	1400	49000	42	6	20	11	11	41
Ga	9	19	<4.	<4.	23	25	21	24	23	22	14
La	15	36	<2.	<2.	<2.	37	45	40	29	40	11
Li	11	70	30	30	14	51	15	10	170	130	39
Mn	160	320	630	630	140	980	170	690	33	410	88
Mo	56	<2.	370	370	3	<2.	<2.	<2.	3	<2.	8
Nd	9	33	<4.	<4.	6	31	35	32	23	31	7
Ni	100	150	12	17	28	10	3	4	10	6	37
Pb	110	230	4300	4300	>10000.	34	8	190	92	36	17
Sc	<2.	12	<2.	<2.	<2.	8	8	7	6	7	6
Sn	40	<20.	<20.	<20.	<20.	<20.	<20.	<20.	<20.	<20.	<20.
Sr	100	26	58	58	190	130	60	55	39	61	51
Th	6	10	<4.	<4.	<4.	11	11	13	12	11	8
Ti	300	3100	100	100	<50.	3200	1800	2600	3200	3100	2200
V	72	200	67	67	15	81	90	100	92	77	230
Y	4	27	<2.	<2.	3	16	15	15	14	14	6
Yb	<1.	3	<1.	<1.	<1.	2	1	2	2	1	<1.
Zn	1800	310	260	260	5600	450	110	210	640	140	190

Table 2.--(con'td)											
Analysis No.	87	88	89	90	91	92	93	94	95	96	97
#Field No. (84GJ..)	*307A*	*125*	*111C*	*114B*	*115C*	*206A*	*210*	*204*	*167*	*153B*	*229*
Ag	29.6	3.28	32.9	52.4	180	–	–	–	–	–	–
As	‡2710.	48.9	22.9	84.4	106	–	–	–	–	–	–
Au (ppb)	20.3	5.6	2.6	16.4	27.6	–	–	–	–	–	–
Cu	‡5420.	63.5	268	559	984	–	–	–	–	–	–
Hg	1.11	0.859	75.5	21.5	53.4	–	–	–	–	–	–
Mo	62.8	2.96	5.26	5.76	16.8	–	–	–	–	–	–
Pb	107	113	1340	‡2520.	‡2530.	–	–	–	–	–	–
Sb	83.5	19.7	140	215	‡896.	–	–	–	–	–	–
Tl	<.957	<.965	<.892	<.943	<.954	–	–	–	–	–	–
Zn	1450	240	‡5260.	227	1020	–	–	–	–	–	–
As	>1000.0	–	–	–	–	–	28	–	–	–	–
Au	<0.2	–	–	–	–	–	<0.2	–	–	–	–
Sb	200	–	–	–	–	–	12	–	–	–	–
Tl	<2.	–	–	–	–	–	<2.	–	–	–	–
Hg	<1.	–	–	–	–	–	<2.	–	–	–	–

Table 3.--Composite chemical analyses for silver, arsenic, gold, barium, copper, molybdenum, manganese, lead, antimony, strontium, and zinc for 78 samples of jasperoid from the Elephant Head area, Lander County, Nevada, used in statistical calculations.

[in parts per million; modified from table 2 (see text); n.d., not determined or qualified "less than" concentration with a sensitivity less than that available for other samples; analysis nos., same as table 2]

Analysis Nos.	Ag	As	Au	Ba	Cu	Mo	Mn	Pb	Sb	Sr	Zn
10	5.69	172	0.017	330	13.3	1.53	3000	19.6	6.43	95	1040
11	1.477	9.42	0.0014	260	34.1	6.765	700	102.4	10.02	39	82.91
12	0.023	0.45	0.0005	230	27.42	7.875	230	1.752	0.45	56	19.8
13	1.272	5.711	0.0005	1600	46.33	7.438	130	5.565	1.482	140	86.84
14	374	595	0.0157	61	5000	33.31	6100	10000	750	110	1976
15	1.339	112.6	0.0395	320	37.73	1.287	250	62.48	12.9	36	97.86
16	35.71	134.7	0.0576	720	24.26	11.42	23000	54.64	8.494	100	760.3
17	1.5	100	n.d.	680	50	10	220	5800	n.d.	88	2400
18	0.2696	8.102	0.0016	420	14.26	4.696	360	10.56	1.899	32	29.3
19	0.2459	11.3	0.0024	970	37.79	5.888	5300	9.225	2.025	32	180.6
20	0.4	30.66	0.0015	1100	27.63	4.865	8000	26.33	4.276	52	225.9
21	31.09	314.4	11.03	500	22.85	4.302	760	433	72.98	15	200.6
22	n.d.	20	n.d.	770	9	1	2000	29	n.d.	45	66
23	1.213	140.8	0.2208	240	55.43	4.816	140	65.83	18.69	18	636.4
24	0.5	30	n.d.	170	10	1	490	9	n.d.	30	100
25	n.d.	n.d.	n.d.	120	35	1	130	12	n.d.	8	43
26	n.d.	20	n.d.	320	6	1	1500	26	n.d.	22	64
27	0.7	20	n.d.	270	31	1	120	19	n.d.	35	300
28	0.2207	10.09	0.0266	630	25.7	3.795	1500	8.032	3.538	26	41.46
29	0.1224	28.71	0.0926	690	68.1	4.314	2400	83.88	20.83	34	264.4
30	5	580	n.d.	390	40	2	970	1400	n.d.	43	1400
31	9.418	270.2	0.0399	1900	65.74	8.571	3700	56.62	22.76	100	1956
32	0.4992	16.32	0.01	130	11.51	4.75	1800	8.821	3.417	62	92.69
33	3	10	n.d.	300	6	1	1300	7	n.d.	31	30
34	0.1792	26.8	0.0085	220	19.6	6.83	530	4.64	2.09	32	20.8
35	n.d.	5	n.d.	230	2	1	770	2	n.d.	18	20
36	0.0539	16.2	0.004	250	23.02	6.626	390	5.34	2.679	17	39.66
37	0.0541	1.614	0.0005	71	22.83	4.762	240	3.798	1.4	75	38.2
38	3	43	n.d.	410	6	10	2100	10	4	51	63
39	n.d.	10	n.d.	360	4	5	2000	23	n.d.	28	30
40	0.1941	3.63	0.0093	120	18.8	5.794	280	5.717	2.2	13	38.56
41	n.d.	2	n.d.	120	2	1	180	8	n.d.	15	59
42	n.d.	n.d.	n.d.	88	0.5	1	140	n.d.	n.d.	13	13
43	n.d.	n.d.	n.d.	160	2	1	930	5	n.d.	9	28
44	0.2548	19	0.0005	260	23.7	7.89	630	8.31	2.571	29	33.9
45	0.1785	20.8	0.0103	340	13.4	7.95	2100	6.83	3.608	38	10.9
46	0.3372	9.71	0.0067	240	16	6.67	960	5.54	1.871	26	7.25
47	0.3277	17.3	0.0005	290	22.9	6.27	720	17.2	3.69	27	101
48	0.3507	17.8	0.0005	530	19.3	4.95	950	12.7	4.45	50	128
49	0.081	12	0.0005	240	16.5	6.53	1100	29.7	1.75	24	88.2

Table 3.--(con'td)

Analysis Nos.	Ag	As	Au	Ba	Cu	Mo	Mn	Pb	Sb	Sr	Zn
50	1.37	49.8	0.0005	420	34.5	6.56	3700	125	28	360	810
51	1.52	20.1	0.0005	310	116	2.36	970	14.3	7.01	66	427
52	0.9059	34.3	0.0042	1000	69	2.38	400	32.5	5.28	160	1570
53	4.791	213	0.0346	1400	66.4	8.48	12000	927	96.7	140	1910
54	3.711	151	0.0049	1200	39.11	10.2	12000	52.4	70.5	100	1220
55	3.95	190	0.0092	1500	22.25	7.85	11000	141	33	97	1280
56	2.14	215	0.406	170	62.27	0.973	7100	285	50.3	18	536
57	70.92	2500	3.25	170	2881	8.3	4600	100000	1600	48	56000
58	0.3802	102	0.018	420	33.22	3.39	940	408	11.7	140	384
59	6.07	653	0.0155	240	40.42	20.6	920	326	74.8	28	2060
60	12	824	3.49	380	144.9	5.04	5000	5900	188	32	4800
61	10.5	629	1.19	370	47.65	4.76	570	1060	58.4	38	1140
62	10.2	468	0.458	670	100.6	5.75	3600	5400	143	98	2790
63	0.2811	32.2	0.0341	440	68.77	8.17	2100	99.2	4.25	45	235
64	0.3286	38.4	0.0177	240	28.08	6.83	90	28.4	2.33	37	65.1
65	0.5052	72.8	0.0057	680	25.5	5.29	1200	92.2	10.8	57	276
66	0.674	75.6	0.0113	360	14.3	4.14	940	58.1	7.58	25	252
67	0.5661	47.5	0.0015	440	41.1	2.84	45	138	6.23	18	239
68	0.412	58.5	0.0005	360	68.34	5.89	70	31.3	4.15	58	517
69	0.2487	17.2	0.0098	270	24.23	2.04	480	13.6	3.12	35	137
70	3.24	25.5	0.0382	250	32.12	4.01	880	425	9.25	24	77.1
71	0.4336	315.2	0.018	500	64.21	6.318	3000	174	9.11	41	786
72	n.d.	10	n.d.	88	5	1	150	7	n.d.	17	63
73	n.d.	20	n.d.	360	9	1	1700	18	5	29	140
74	n.d.	10	n.d.	62	3	1	200	46	n.d.	15	160
75	n.d.	90	n.d.	280	29	1	970	16	25	27	190
76	n.d.	20	n.d.	740	11	1	1800	22	3	38	190
77	n.d.	230	n.d.	280	6	1	1100	38	6	110	190
78	n.d.	5	n.d.	200	2	1	620	4	n.d.	11	57
79	0.3494	28.4	0.0151	150	21.3	5.711	3500	20.7	19.3	45	163
80	16.2	75.1	0.0281	190	67.1	4.79	2900	42.1	9.62	56	236
81	1.82	10.7	0.0094	340	49.48	4.03	1000	12	4.35	73	98.9
82	1.79	16.4	0.0081	420	30.1	3.27	1100	15.3	3.07	120	77.6
83	0.4066	15.1	0.0202	650	27.15	3.17	1600	31.1	5.51	31	125
84	0.684	126	1.067	980	49.2	2.08	990	559	50.8	130	817
85	38.52	15000	0.0952	210	888	5.91	2100	46000	1000	190	27000
86	0.2388	107	0.0016	560	208	1.95	230	268	7.15	52	305
87	29.6	7000	0.0203	130	24000	62.8	160	107	83.52	100	1450

Table 4. -- Summary statistics for 11 elements in 78 samples of jasperoid from the Elephant Head area, Lander County, Nevada.

[from table 3]

	Number of valid determinations	Median (ppm)	Mean	Valid determinations (parts per million) Standard deviation	Minimum	Maximum	Coefficient variation	Geometric mean	Log-transformed data Kurtosis	Skewness
Ag	63.	1/ 0.7	11.2	48.0	0.023	374.0	429.0	1.18	0.22	0.632
As	75	30.	431.	1907.	.45	15000.	442.	45.4	.924	.613
Au	57	1/ .01	.38	1.58	.0005	11.	410.	.013	.288	.711
Ba	78	325.	442.	369.	61.	1900.	84.	334.	- .115	.042
Cu	78	27.5	453.	2778.	.5	24000.	613.	28.7	4.681	1.292
Mo	78	4.8	5.77	8.	.97	62.8	139.	3.7	- .069	.104
Mn	78	970.	2178.	3500.	45.	23000.	161.	954.	- .4	- .015
Pb	77	29.	2355.	12500.	1.75	100000.	531.	50.3	1.57	1.293
Sb	63	1/ 6.7	74.5	252.	.45	1600.	339.	10.5	.92	1.059
Sr	78	38.	56.7	52.9	8.	360.	93.	41.8	- .241	.255
Zn	78	172.	1558.	6974.	7.25	56000.	447.	204.	.651	.693

1/ Median not including number of samples showing undetermined concentrations

Table 5. -- Array of Spearman correlation coefficients for 78 samples of jasperoid at Elephant Head.

	Log (Ag)	Log (As)	Log (Au)	Log (Ba)	Log (Cu)	Log (Mo)	Log (Mn)	Log (Pb)	Log (Sb)	Log (Sr)	Log (Zn)
Log (Ag)	1.0										
Log (As)	.706	1.0									
Log (Au)	.53	.65	1.0								
Log (Ba)	.071	.221	.015	1.0							
Log (Cu)	.42	.594	.35	.269	1.0						
Log (Mo)	.113	.257	-.082	.195	.415	1.0					
Log (Mn)	.364	.359	.338	.378	.145	.256	1.0				
Log (Pb)	.638	.815	.618	.303	.64	.223	.305	1.0			
Log (Sb)	.761	.852	.655	.084	.563	.065	.419	.865	1.0		
Log (Sr)	.366	.398	-.038	.45	.496	.425	.372	.35	.247	1.0	
Log (Zn)	.673	.842	.47	.365	.712	.266	.367	.833	.828	.538	1.0

Table 6. -- Array of orthogonal varimax loadings.

	Factor 1	Factor 2	Factor 3
Log (Ag)	.829	.155	.268
Log (As)	.909	.111	.16
Log (Au)	.794	.005	-.425
Log (Ba)	-.111	.838	-.193
Log (Cu)	.682	-.155	.558
Log (Mo)	.164	-.104	.785
Log (Mn)	.348	.616	-.006
Log (Pb)	.925	.125	.031
Log (Sb)	.948	.15	.135
Log (Sr)	.12	.631	.577
Log (Zn)	.832	.342	.203

Table 7. Results of Mann-Whitney test of geometric means of gold concentration with respect to jasperoid brecciation, fault association, variegated coloration, and host-facies. Where T is outside critical limits, means of two groups are different at 90 percent confidence. Number of samples in group, n and m. Au means are in log units of Au abundances, in ppm.

A.	Brecciated jasperoid:			Group n	
	Non-brecciated jasperoid:			Group m	
	n	m	T	Critical Limits	Significance
	18	47	469	340-626	No
Au means	-1.78	-2.99			
B.	Fault associated:			Group n	
	Not fault associated:			Group m	
	n	m	T	Critical Limits	Significance
	15	43	522	202-441	Yes
Au means	-0.81	-2.09			
C.	Variegated:			Group n	
	Other colors:			Group m	
	n	m	T	Critical Limits	Significance
	8	47	256	143-255	Yes
Au means	-1.14	-1.84			
D.	Carbonate-dominant facies:			Group n	
	Clastite-dominant facies:			Group m	
	n	m	T	Critical Limits	Significance
	48	16	-298		Yes
Au means	-1.66	-2.17			

Table 8. -- Analytical data obtained from jasperoid cropping out in the workings of the Empire Mine, Lander County, Nevada.

Emission spectrographic analyses by J. Harris and B. Spillane. The relative standard deviation of any single, reported concentration should be taken as plus 50 percent and minus 33 percent. Looked for but not found at part-per-million detection levels shown in parentheses: Cd (32), Dy (22), Er (10), Eu (2.2), Hf (15), Ho (6.8), In (6.8), Ir (15), Nd (32), Os (22), Pr (68), Pt (4.6), Re (10), Rh (2.2), Ru (2.2), Sm (10), Ta (460), Tb (32), Th (22), Tm (4.6), U (320). Au was determined by fire assay followed by flameless atomic absorption spectroscopy; Hg was determined by cold vapor atomic absorption spectroscopy; As and Sb were determined by flameless atomic absorption spectroscopy; analysts, R. Moore and W. D'Angelo. P was determined by specific-ion electrode; Tl was determined by flameless atomic absorption spectroscopy; W was determined colorimetrically; analysts, E. Campbell, M. Doughten, and J. Gillison; --, not detected; H, unresolved interference.

Field Number	1 82TT57	2 82TT58	3 82TT59	4 82TT60	5 82TT61	6 82TT62	7 82TT63	8 82TT64	9 82TT65	10 82TT66	11 82TT67	12 82TT68	13 82TT69	14 82TT70	15 82TT71	16 82TT72	17 82TT73	18 82TT74	19 82TT75	20 82TT76	21 82TT77	22 82TT78
Emission spectrographic analyses (parts per million)																						
Ag	3.1	6.7	8.8	5.6	6.2	6.5	3.8	2.1	0.75	5.9	4.9	2.4	0.48	0.97	5.7	8.3	0.16	0.6	5.6	0.96	4.3	3.5
As	720.	270.	200.	–	–	–	620.	–	330.	1100.	–	–	–	–	–	–	–	190.	270.	270.	180.	–
B	H	120.	H	H	110.	100.	79.	H	H	H	110.	–	31.	–	–	–	–	–	–	–	–	33.
Ba	1500.	1700.	650.	1600.	2400.	2400.	1300.	910.	890.	1300.	550.	390.	560.	86.	1200.	1100.	92.	190.	280.	370.	500.	210.
Be	2.2	3.	2.2	2.2	2.9	2.6	2.1	2.5	2.8	1.8	3.4	–	–	–	–	–	–	–	–	–	–	–
Bi	56.	32.	–	95.	120.	140.	27.	30.	79.	44.	210.	56.	–	–	56.	480.	–	46.	41.	77.	–	25.
Cb	230.	110.	–	–	160.	160.	140.	–	180.	–	–	–	–	–	130.	57.	–	140.	59.	–	–	84.
Co	20.	20.	18.	15.	19.	18.	20.	15.	20.	18.	20.	2.3	1.7	–	1.2	–	–	–	–	–	–	–
Cr	160.	150.	170.	120.	130.	130.	100.	88.	97.	120.	100.	12.	4.3	3.8	20.	26.	2.8	50.	6.4	100.	28.	6.4
Cu	43.	47.	87.	120.	86.	90.	190.	91.	68.	260.	51.	50.	11.	35.	50.	33.	37.	71.	32.	120.	55.	54.
Ga	34.	45.	40.	40.	39.	39.	26.	32.	32.	31.	24.	13.	–	3.8	7.5	7.3	–	15.	4.1	27.	18.	5.2
Gl	–	–	–	–	–	–	–	–	–	17.	–	–	–	–	–	–	–	–	–	–	–	–
Ge	3.6	4.1	–	2.3	2.9	2.1	2.4	4.8	3.1	–	5.3	2.2	–	–	–	–	–	–	–	–	–	2.8
La	26.	34.	39.	39.	53.	49.	31.	31.	18.	45.	24.	–	–	–	43.	37.	–	38.	14.	–	13.	–
Li	H	–	H	H	–	H	H	H	H	H	180.	H	–	–	–	–	–	H	–	H	H	–
Mn	600.	520.	500.	490.	490.	510.	520.	610.	610.	540.	490.	99.	67.	46.	70.	44.	20.	15.	31.	27.	22.	34.
Mo	–	1.7	9.6	–	–	–	6.4	–	–	–	–	–	–	–	–	1.	–	–	–	H	–	–
Nb	23.	32.	24.	38.	84.	84.	47.	26.	27.	39.	20.	11.	6.5	27.	24.	29.	6.	13.	4.4	17.	8.5	14.
Ni	38.	38.	34.	29.	38.	36.	39.	34.	33.	38.	40.	2.	2.7	–	2.1	1.6	–	2.5	–	4.7	–	2.6
Pb	190.	200.	130.	170.	150.	160.	160.	150.	90.	220.	42.	97.	8.7	21.	240.	160.	11.	190.	160.	250.	53.	14.
Pd	–	–	–	–	–	–	–	–	–	–	–	–	–	–	–	–	–	–	–	1.3	–	–
Sb	–	–	–	–	–	–	–	–	–	–	62.	–	–	–	–	–	–	–	–	–	–	–
Sc	16.	16.	16.	16.	22.	20.	17.	16.	18.	19.	14.	4.	1.5	2.7	3.4	5.	1.4	3.2	1.2	4.3	2.5	2.7
Sn	H	5.7	H	H	5.5	4.	6.4	–	H	H	1.7	–	3.2	–	37.	6.6	–	H	–	H	–	–
Sr	280.	320.	290.	310.	400.	390.	250.	290.	290.	210.	220.	35.	40.	9.1	130.	150.	6.1	28.	31.	110.	200.	23.
Ti	2300.	2400.	2600.	3700.	4900.	4500.	2600.	1800.	2000.	4100.	1600.	1500.	1100.	1600.	2000.	2100.	400.	1300.	430.	1500.	680.	1100.
V	94.	100.	110.	110.	110.	110.	120.	88.	79.	130.	94.	28.	9.2	9.6	12.	18.	3.1	110.	9.4	170.	51.	76.
Y	23.	17.	18.	16.	22.	20.	18.	17.	16.	25.	11.	5.7	2.2	6.8	6.3	11.	8.3	4.5	4.	7.9	6.1	8.2
Yb	2.5	2.4	1.	1.4	3.2	2.8	1.1	.92	1.1	2.6	1.9	–	.39	–	.26	1.2	–	–	–	H	.97	.89
Zn	130.	78.	120.	120.	110.	91.	110.	120.	130.	140.	73.	55.	17.	27.	–	20.	44.	88.	44.	150.	52.	30.
Zr	360.	440.	680.	390.	770.	690.	460.	450.	380.	450.	110.	74.	170.	300.	240.	160.	220.	61.	82.	57.	170.	370.
Chemical analyses (parts per million)																						
As	750.0	140.0	130.0	56.0	98.0	7.4	660.0	22.0	300.0	1300.0	5.6	130.0	9.6	8.3	4.5	7.3	1.6	190.0	300.0	280.0	140.0	120.0
Au	.2	.06	<.05	<.05	<.05	<.05	<.05	<.05	<.05	<.05	.06	<.05	<.05	<.05	<.05	<.05	<.05	<.05	<.05	<.05	<.05	<.05
P	200.	300.	100.	200.	100.	200.	100.	100.	100.	100.	100.	200.	100.	200.	200.	200.	100.	100.	200.	100.	–	–
Hg	.89	.96	.17	.31	.19	.42	.95	.26	.26	.34	1.	.82	.24	.02	.12	.96	.02	.28	.96	.84	.82	.89
Sb	5.1	2.7	2.6	5.7	14.	.5	4.2	6.8	11.	4.6	.5	6.8	7.5	3.8	1.7	3.2	<.3	22.	14.	7.1	6.	2.8
Tl	.32	1.1	.8	1.1	.55	.8	.2	.44	.59	.11	<.1	.84	<.1	<.1	.42	.63	<.1	.53	.75	.8	1.7	.35
W	83.	27.	16.	70.	130.	180.	73.	19.	50.	150.	11.	50.	28.	14.	120.	380.	5.6	110.	31.	86.	23.	89.

Table 9. -- **Summary statistics for 14 elements in 22 samples of jasperoid from the Empire open-pit gold-silver deposit.**

[from table 8; --, not determined]

	Number of undetermined concentrations	Quantitative determinations (parts per million)						
		Median	Mean	Standard deviation	Minimum	Maximum	Coefficient variation	Geometric mean
B	0.	3.8	4.	2.6	0.16	8.8	66.7	2.6
As	0.	120.	212.	316.	1.6	1,300.	149.	62.
Au	19.	--	--	--	.06	.2	--	--
Ba	0.	650.	917.	694.	86.	2,400.	75.7	640.
Cu	0.	54.	76.	57.	11.	260.	74.2	62.
Hg	0.	.34	.53	.37	.02	1.	68.5	.35
Mo	18.	--	--	--	1.	9.6	--	--
Mn	0.	99.	289.	254.	15.	610.	88.	140.
Pb	0.	150.	130.	77.	8.7	250.	58.8	92.
1/ Sb	1.	4.6	6.	5.2	.15	22.	87.	3.8
Sr	0.	200.	182.	131.	6.1	400.	71.9	110.
2/ Tl	4.	.53	.56	.42	.05	1.7	75.4	.36
W	0.	50.	79.	83.	5.6	380.	105.	49.6
Zn	0.	88.	83.	43.	17.	150.	51.6	70.

1/ Includes one "less-than" determination replaced by 50 percent of value at lower-determination limit for statistical calculations.

2/ Includes four "less-than" determinations replaced by 50 percent of value at lower-determination limit for statistical calculations.

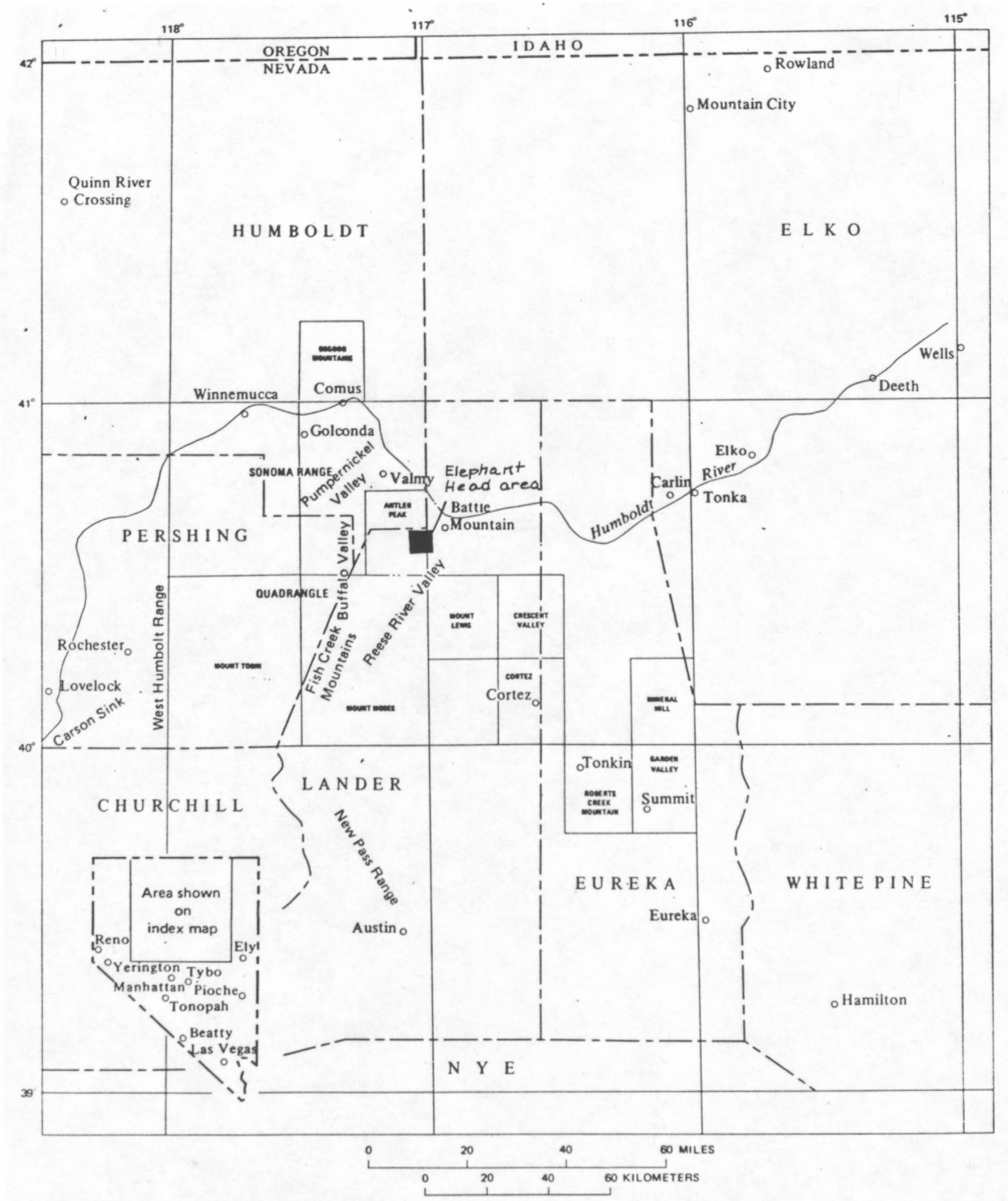

Figure 1. Location map of the Elephant Head area.

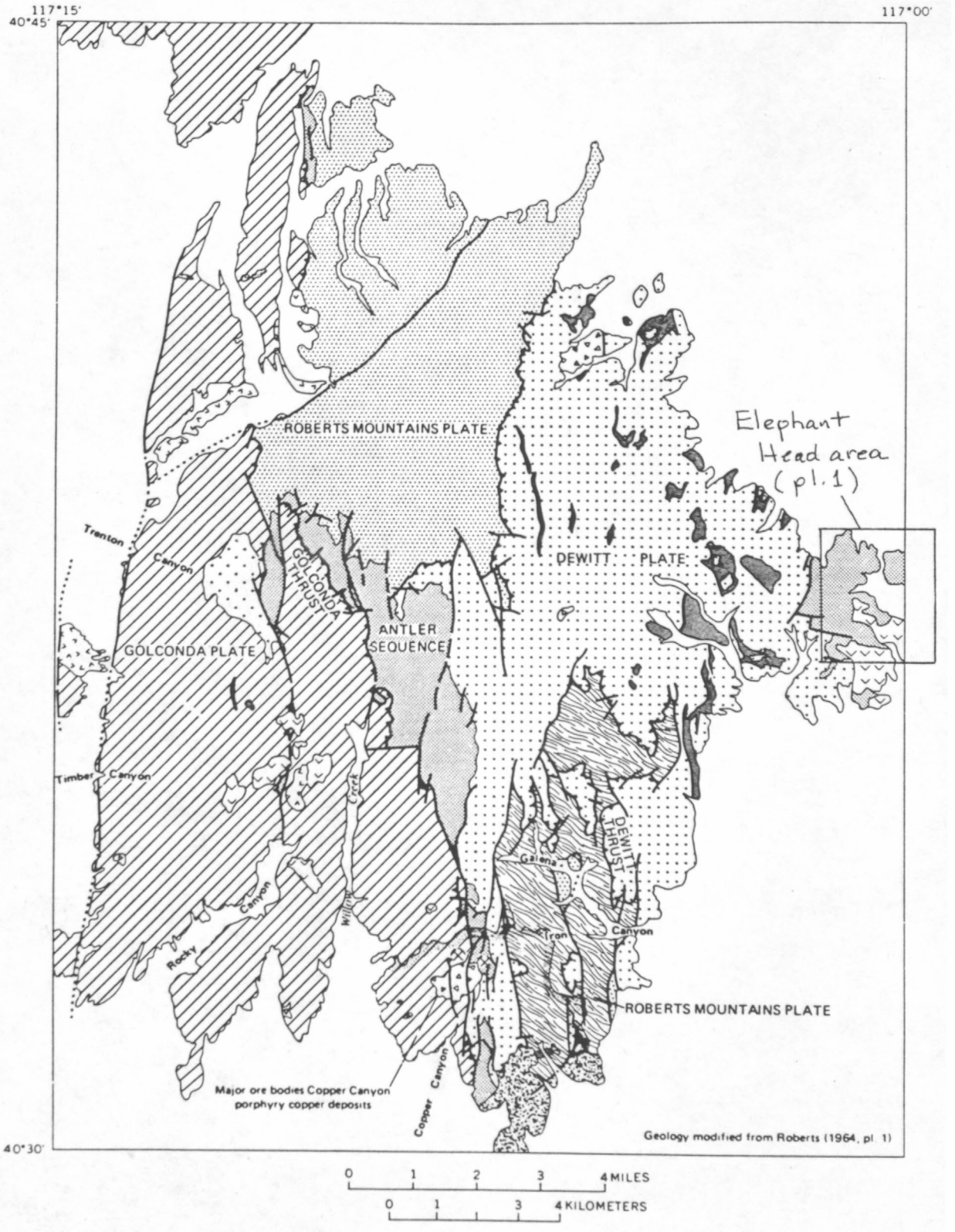

Figure 2. -- Generalized geology of the Battle Mountain Mining District, Nevada, showing location of the Elephant Head area. Geology modified from Roberts (1964, pl. 1). See figure 1 for location.

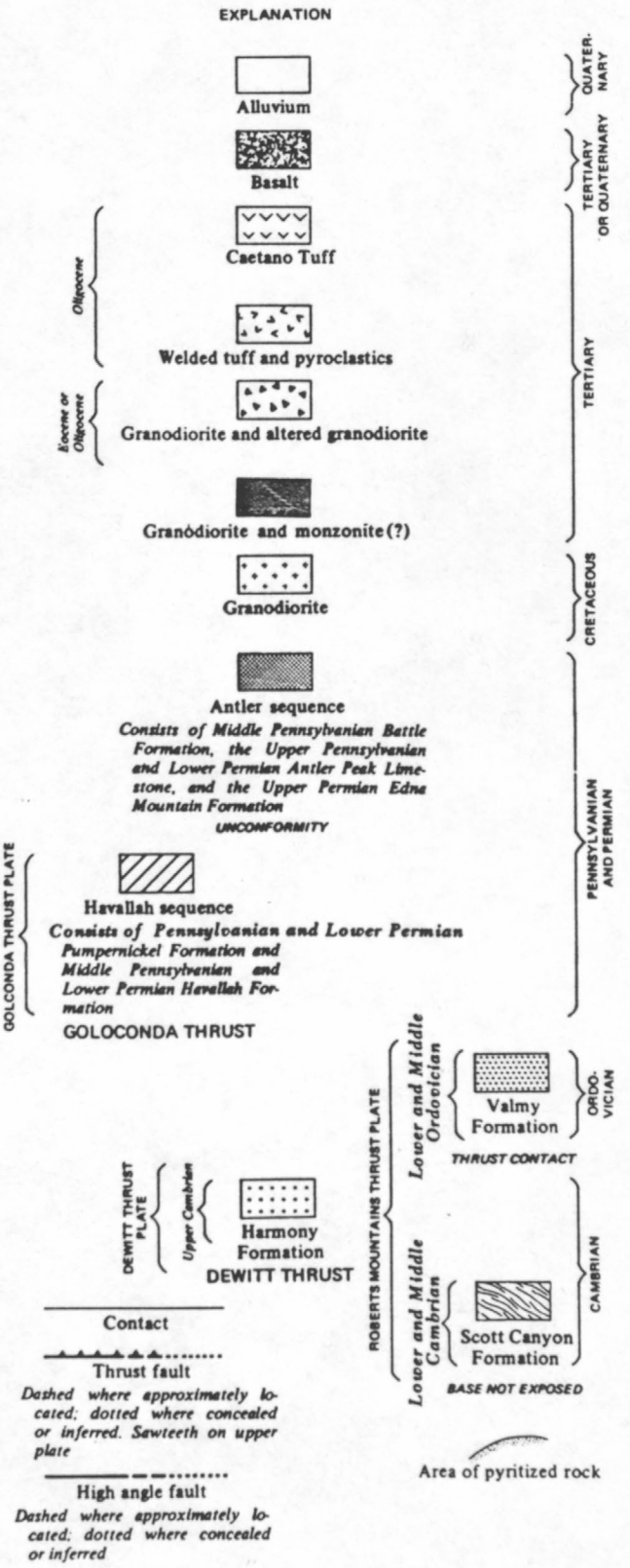
EXPLANATION
Alluvium
Basalt
Caetano Tuff
Welded tuff and pyroclastics
Granodiorite and altered granodiorite
Granodiorite and monzonite(?)
Granodiorite
Antler sequence
Consists of Middle Pennsylvanian Battle Formation, the Upper Pennsylvanian and Lower Permian Antler Peak Limestone, and the Upper Permian Edna Mountain Formation
UNCONFORMITY
Havallah sequence
Consists of Pennsylvanian and Lower Permian Pumpernickel Formation and Middle Pennsylvanian and Lower Permian Havallah Formation
GOLOCONDA THRUST
Valmy Formation
THRUST CONTACT
Harmony Formation
DEWITT THRUST
Scott Canyon Formation
BASE NOT EXPOSED
Contact
Thrust fault
Dashed where approximately located; dotted where concealed or inferred. Sawteeth on upper plate
High angle fault
Dashed where approximately located; dotted where concealed or inferred
Area of pyritized rock
Oligocene
Eocene or Oligocene
Lower and Middle Ordovician
Upper Cambrian
Lower and Middle Cambrian
GOLCONDA THRUST PLATE
DEWITT THRUST PLATE
ROBERTS MOUNTAINS THRUST PLATE
QUATERNARY
TERTIARY OR QUATERNARY
TERTIARY
CRETACEOUS
PENNSYLVANIAN AND PERMIAN
ORDOVICIAN
CAMBRIAN

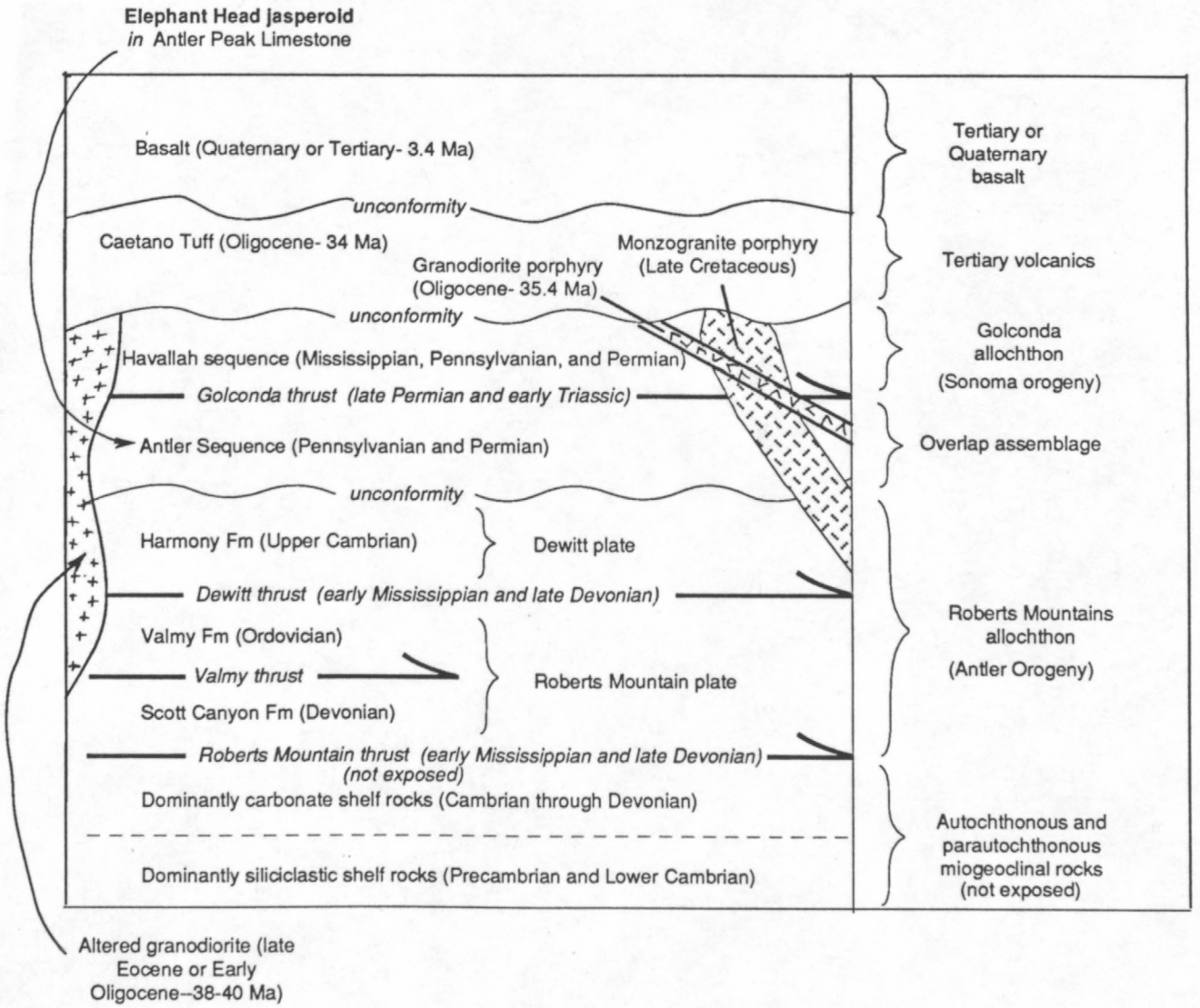

Figure 3.-- Schematic section showing tectonostratigraphic relations in the Battle Mountain Mining District. Modified from Roberts (1964).

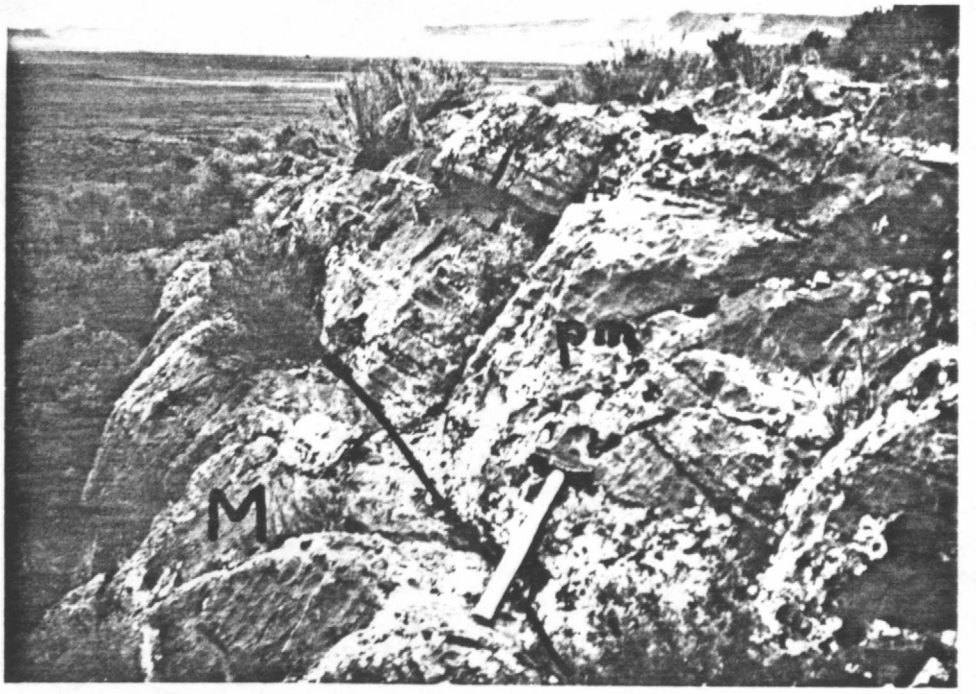

A

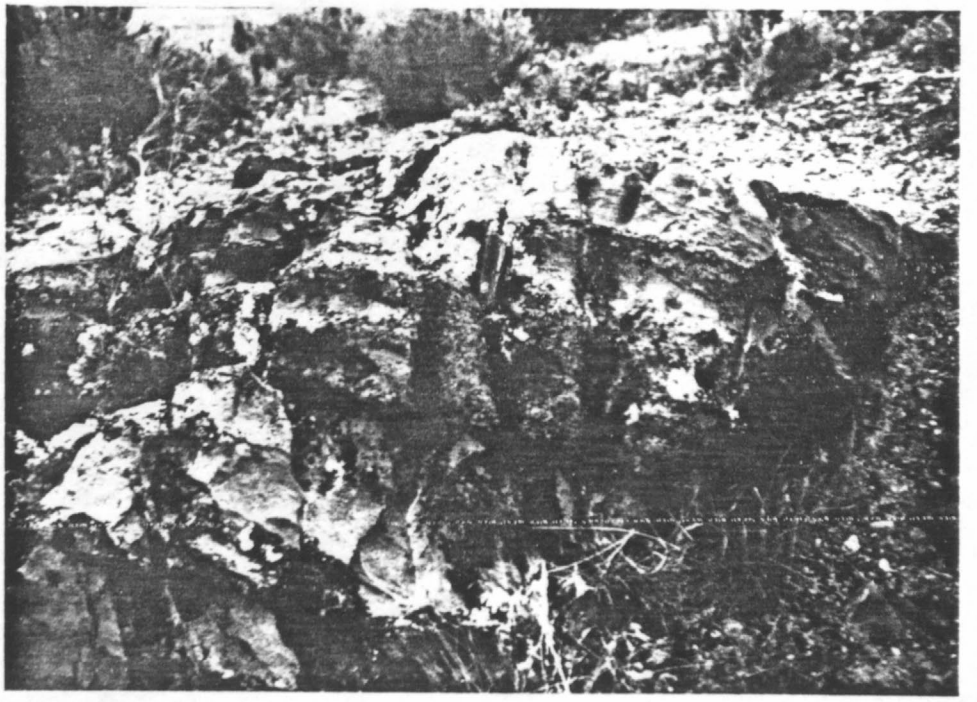

B

Figure 4. -- Photographs showing typical exposures of carbonate facies of Upper Pennsylvanian and Lower Permian Antler Peak Limestone. A, conformable contact between massive gray micrite (M), at base of hammer handle, and thinly-bedded, sandy pelmicrite (pm). Both rock types contain sparse concentrations of calcite veins. B, close-up view of gray pelmicrite containing resistant chert-pebble interbeds; bedding cut by calcite veins. Note pocket knife in center of photograph for scale.

A

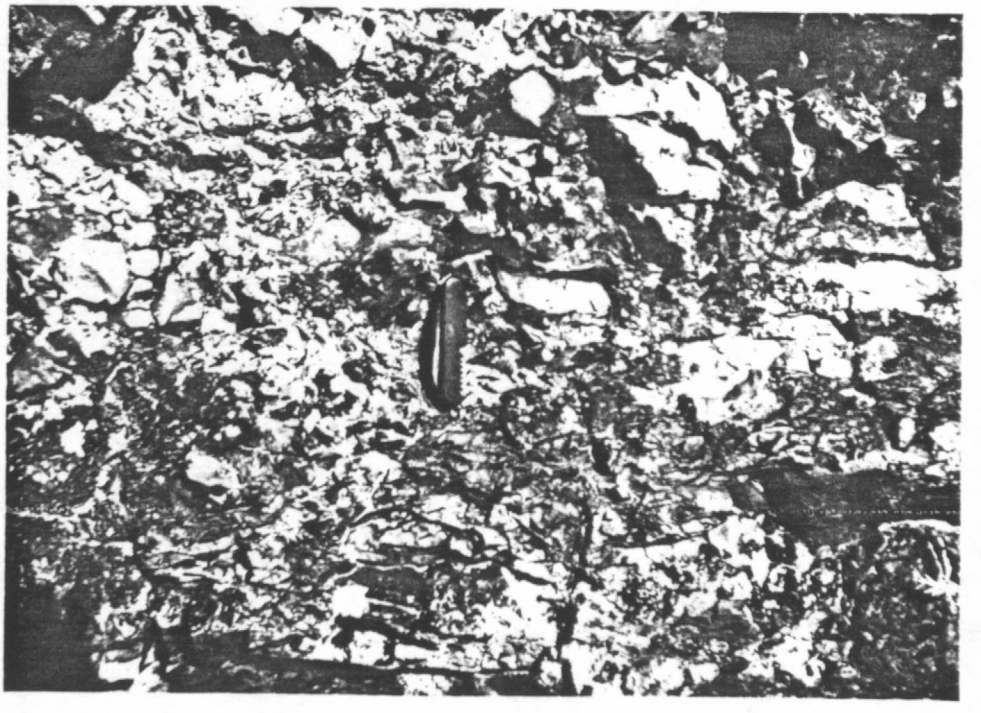

B

Figure 5. -- Photographs showing typical exposures of various types of jasperoid at Elephant Head. A, bedded jasperoid containing sparse amounts of vein quartz that is parallel to parting surfaces of bedding; B, Brecciated jasperoid subsequently recemented by introduced quartz.

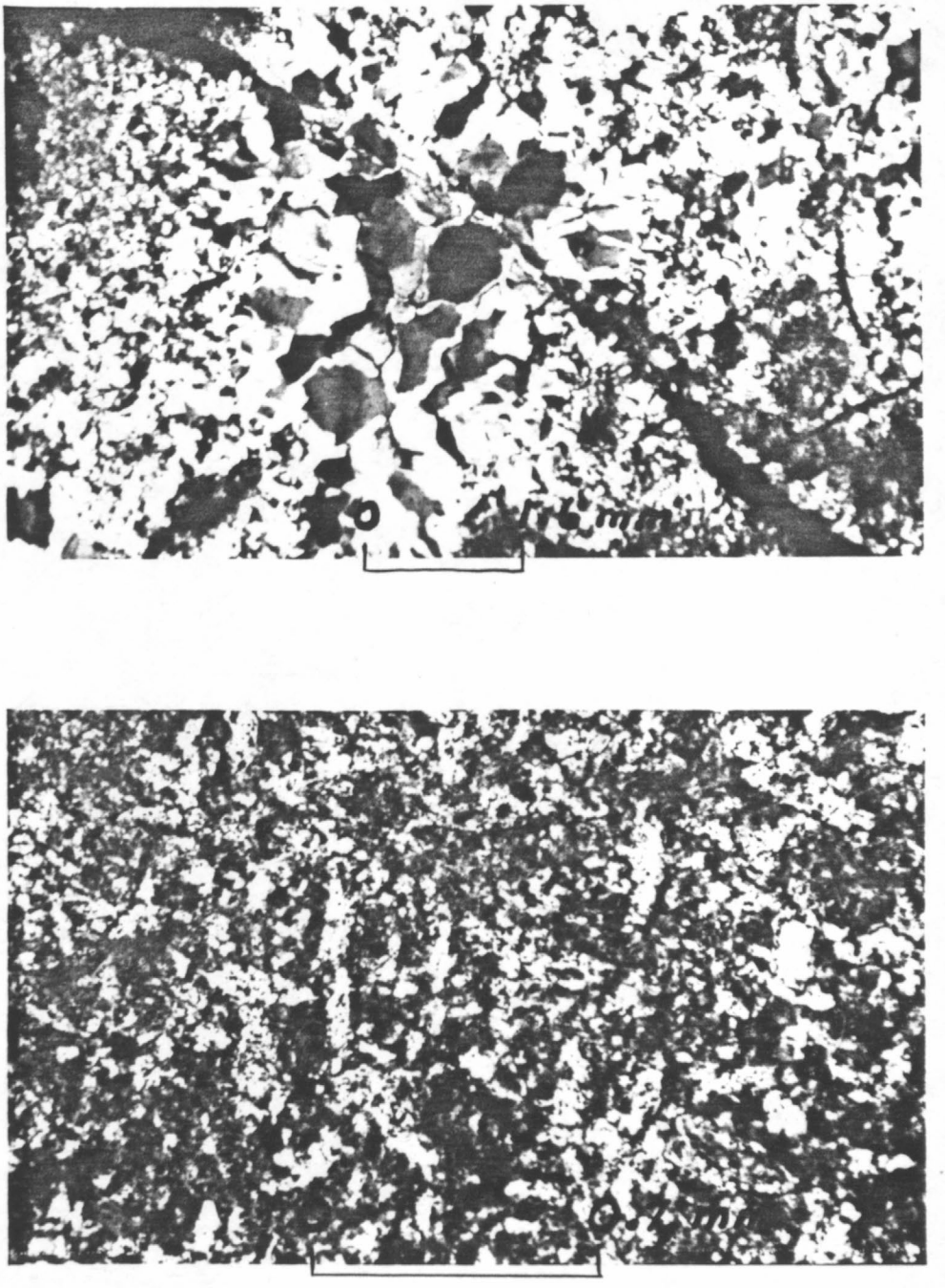

A

B

Figure 6. -- Photographs of jasperoid showing typical examples of granular- and feathery-textured jasperoid.

A, Granular-textured jasperoid concentrated in an ovoid-shaped area. Crossed nicols. Sample no. 84GJ226a;

B, Feathery-textured jasperoid. Plane polarized light. Sample no. 84GJ159b.

Figure 7. -- Photomicrographs showing textural relations in jasperoid. Q, quartz.

A, Relict rhombic-shaped crystals of dolomite (D), whose cores are replaced partly by jigsaw textured jasperoid (at head of arrow), residing in a mass of coloform-banded chalcedonic quartz. Partially crossed nicols. Sample no. 84GJ42b;

B, Crossed-fiber-textured chalcedonic quartz as final phase to crystallize in open spaces developed in silty pelmicrite (sp), partly silicified by opaline silica. Crossed nicols. Sample no. 84GJ42b;

C, Sheaf-like aggregates of hemimorphite (H), developed in open spaces formed in manganiferous, goethitic jasperoid (J) and subsequently infilled by granular-textured jasperoidal silica (gj). Partially crossed nicols. Sample no. 84GJ159b

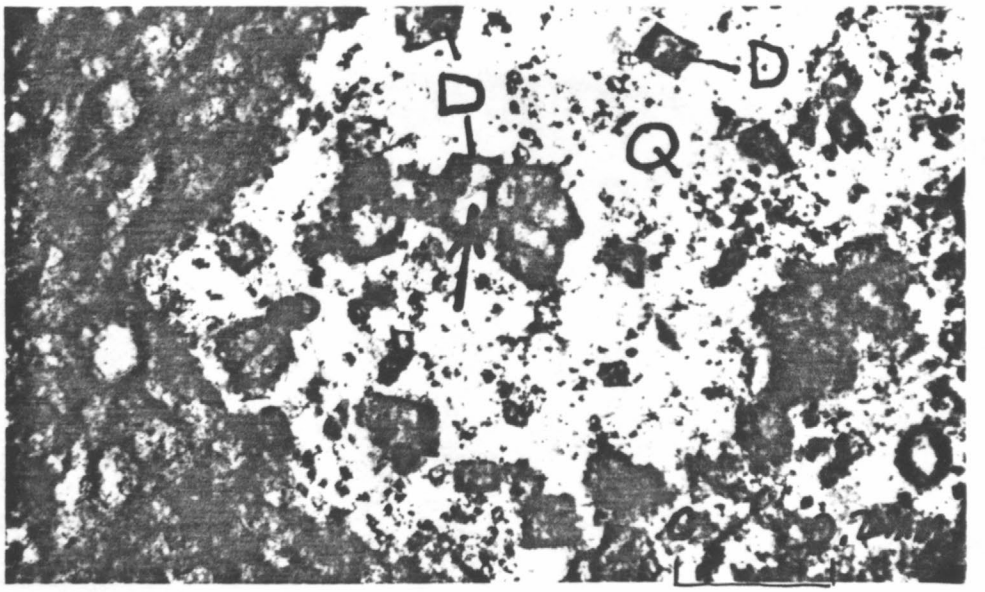

A

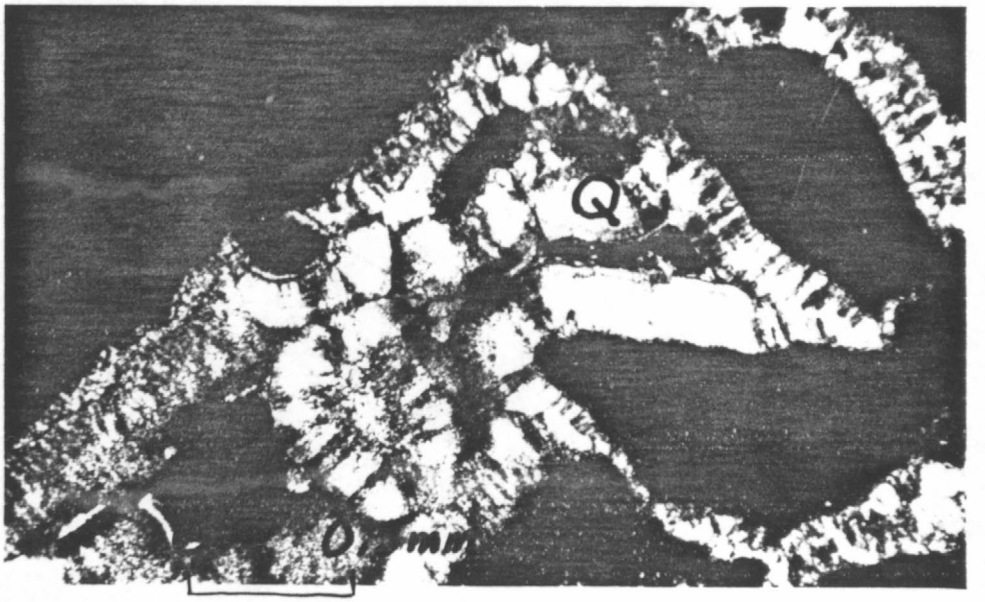

B

C

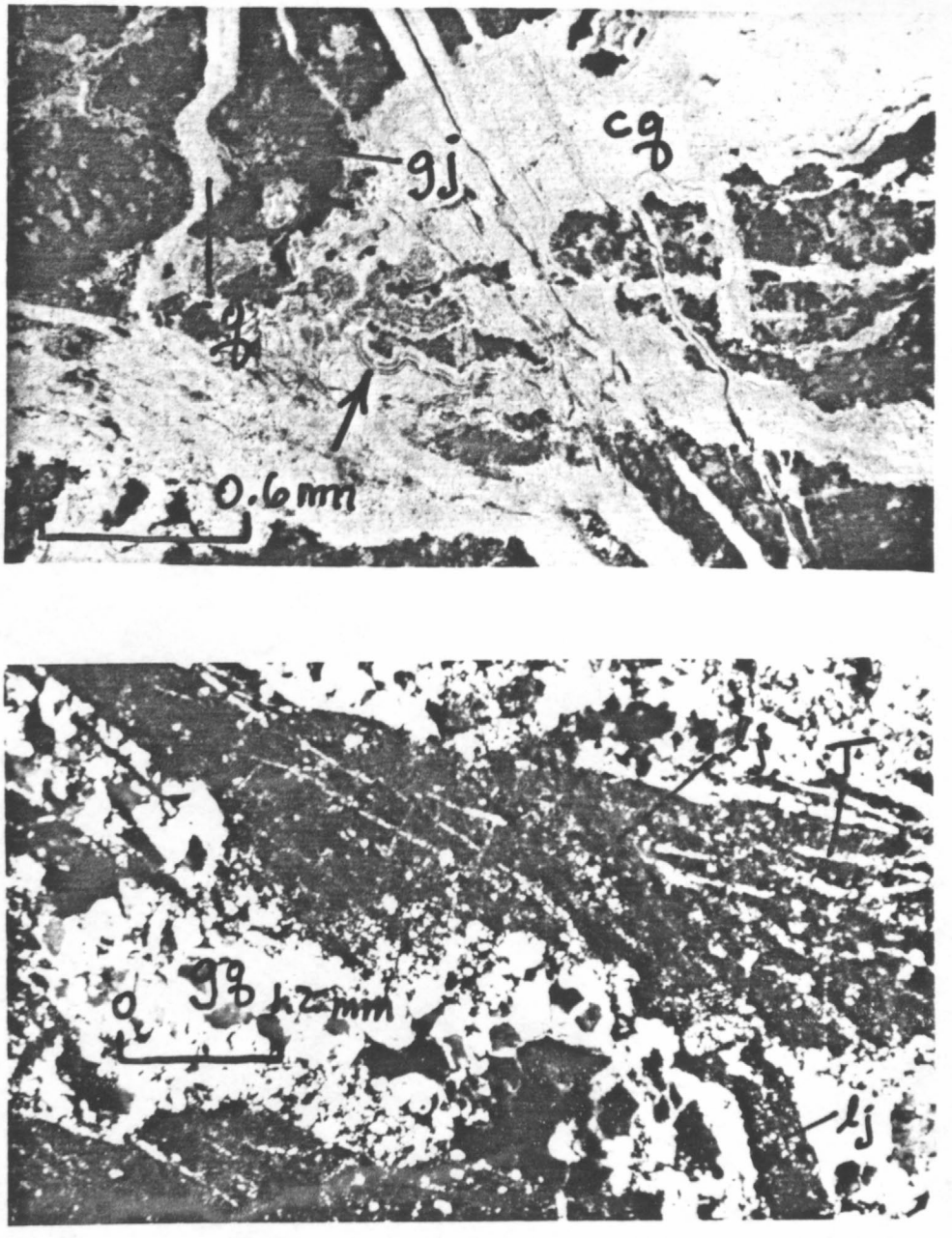

Figure 8. -- Photomicrographs of jasperoid showing sequential development of various types of silica-bearing phases.

A, Goethite-rich jasperoid (gj), fractured and then lined by opaline-rich silica (at head of arrow), and finally cut by cross-fiber-textured chalcedonic quartz (cq), in part along veins. Plane-polorized light. Sample no. 84GJ42B;

B, Jasperoid (J) veined by granulose-textured quartz (gq) that is veined subsequently by a later generation of jasperoid (lj). Crossed nicols. Sample no. 84GJ023.

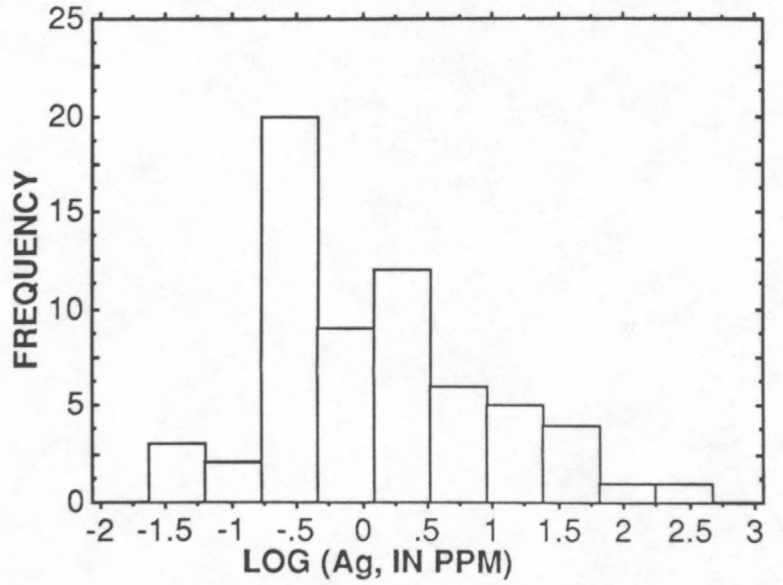

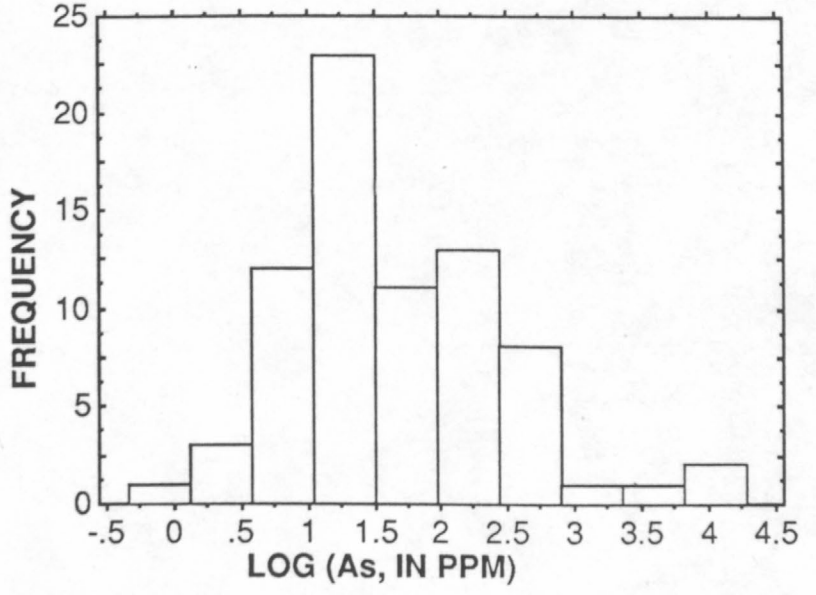

Figure 9. -- Frequency distribution of 11 elements in 78 samples of jasperoid from the Elephant Head area. Distributions are based on data of table 3 transformed by logarithms to the base ten.

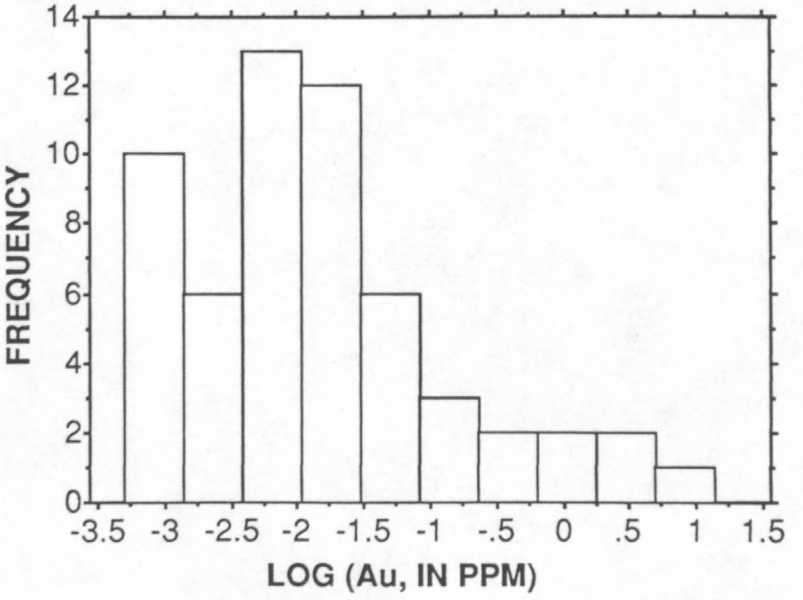
FREQUENCY
14
12
10
8
6
4
2
0
-3.5 -3 -2.5 -2 -1.5 -1 -.5 0 .5 1 1.5
LOG (Au, IN PPM)

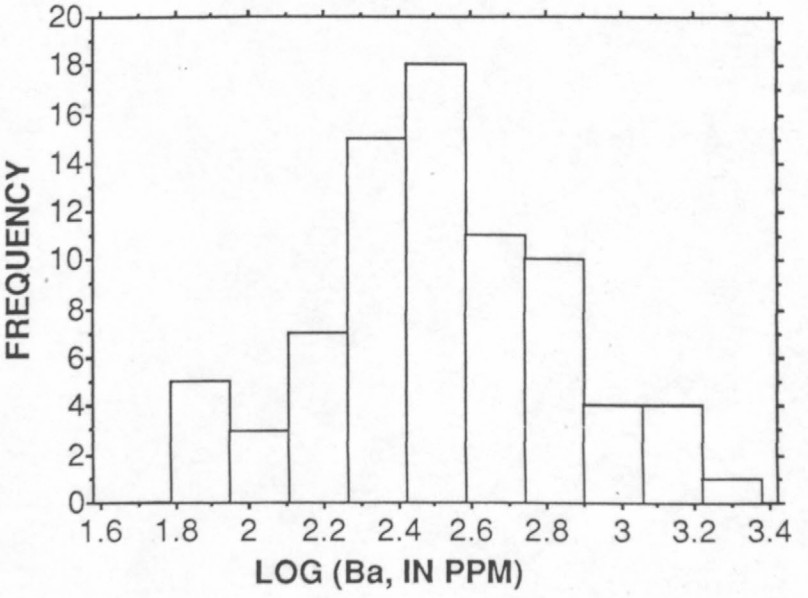
FREQUENCY
20
18
16
14
12
10
8
6
4
2
0
1.6 1.8 2 2.2 2.4 2.6 2.8 3 3.2 3.4
LOG (Ba, IN PPM)

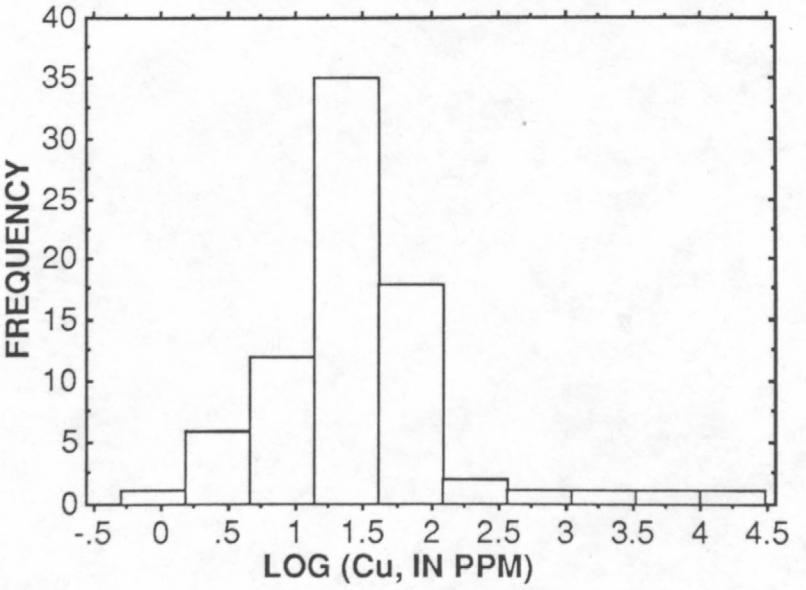
FREQUENCY
40
35
30
25
20
15
10
5
0
-.5 0 .5 1 1.5 2 2.5 3 3.5 4 4.5
LOG (Cu, IN PPM)

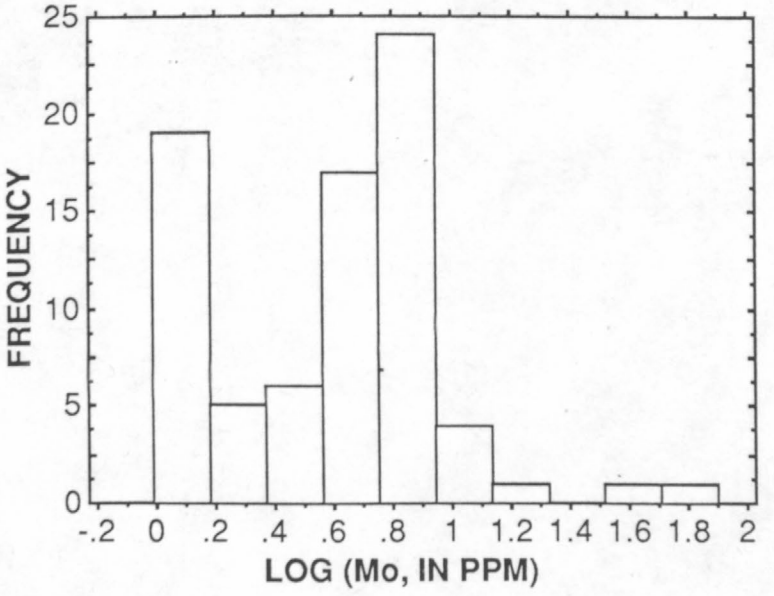
FREQUENCY
25
20
15
10
5
0
-.2 0 .2 .4 .6 .8 1 1.2 1.4 1.6 1.8 2
LOG (Mo, IN PPM)

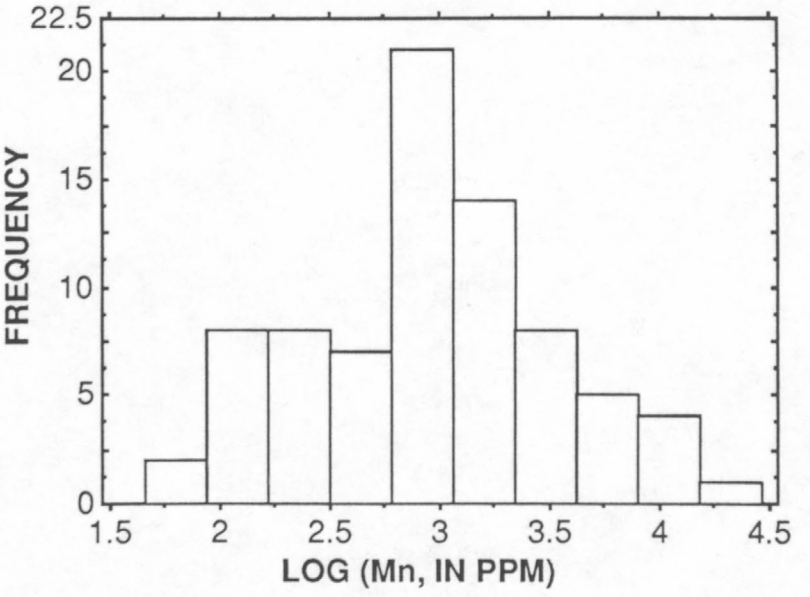
22.5
20
15
10
5
0
FREQUENCY
1.5
2
2.5
3
3.5
4
4.5
LOG (Mn, IN PPM)

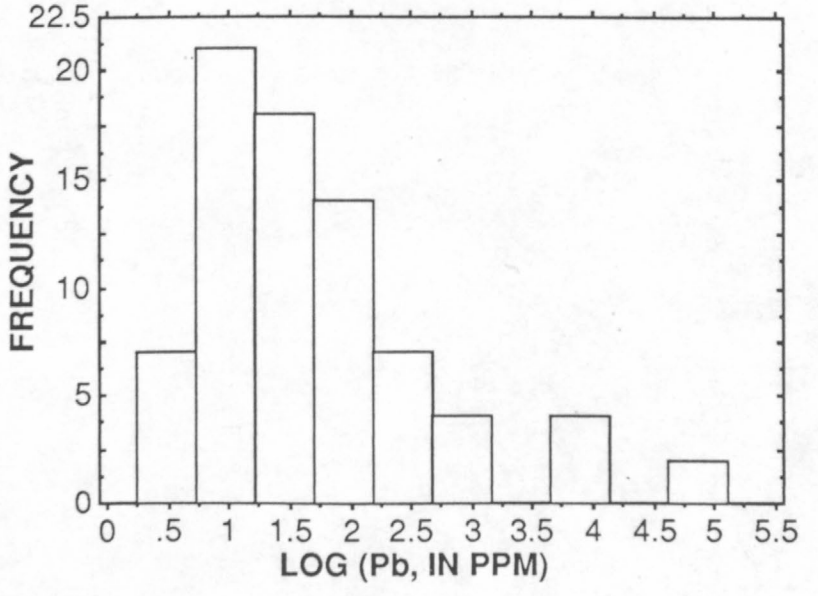
22.5
20
15
10
5
0
FREQUENCY
0
.5
1
1.5
2
2.5
3
3.5
4
4.5
5
5.5
LOG (Pb, IN PPM)

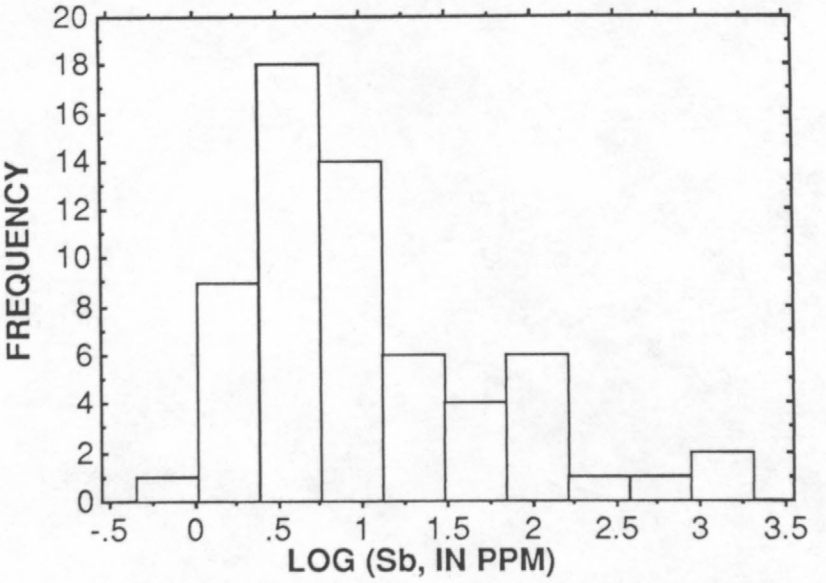
FREQUENCY
20
18
16
14
12
10
8
6
4
2
0
-.5
0
.5
1
1.5
2
2.5
3
3.5
LOG (Sb, IN PPM)

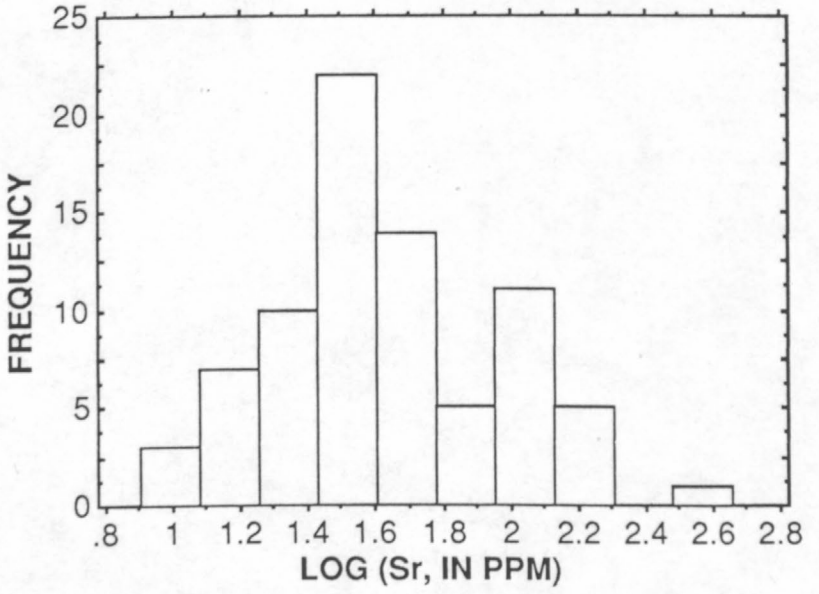
FREQUENCY
25
20
15
10
5
0
.8
1
1.2
1.4
1.6
1.8
2
2.2
2.4
2.6
2.8
LOG (Sr, IN PPM)

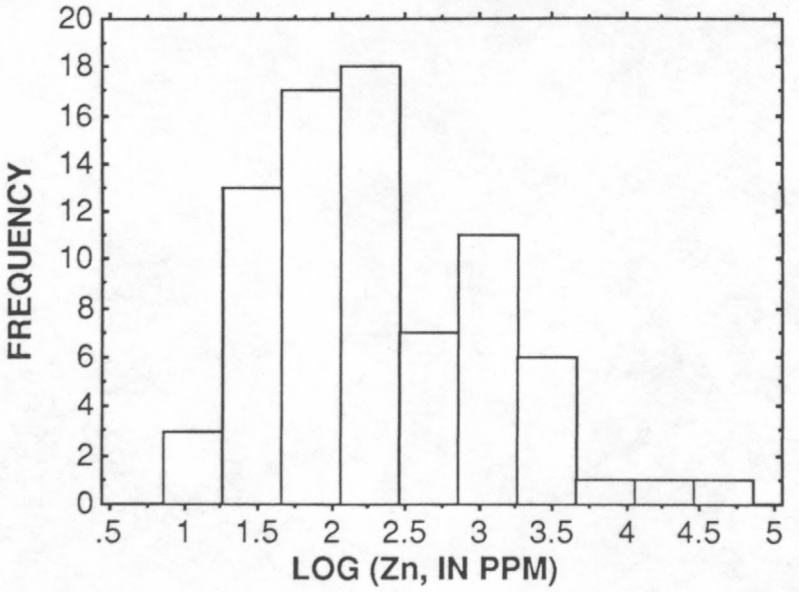
FREQUENCY
20
18
16
14
12
10
8
6
4
2
0
.5
1
1.5
2
2.5
3
3.5
4
4.5
5
LOG (Zn, IN PPM)

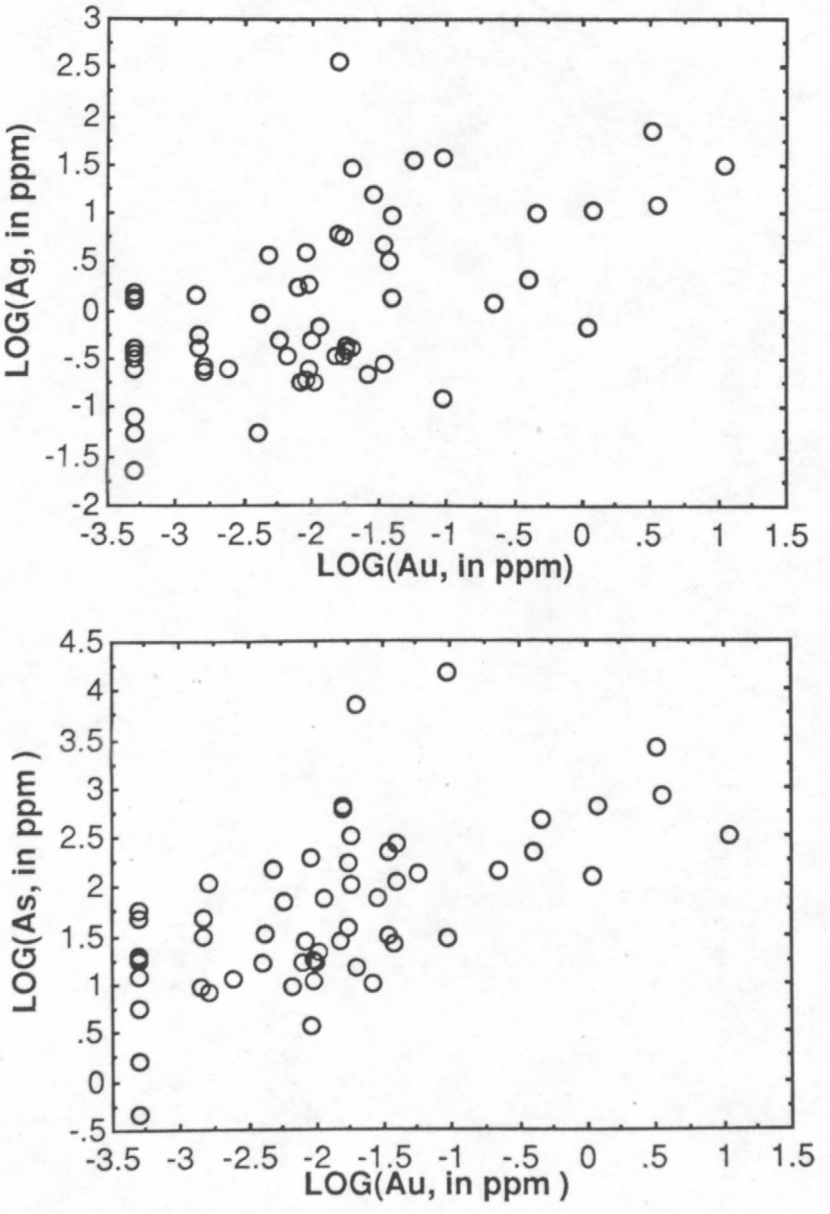

Figure 10. -- Plots of log (Au) compared with the logarithmic value of Ag (A), As (B), Ba (C), Cu (D), Mo (E), Mn (F), Pb (G), Sb (H), Sr (I), and Zn (J) in 78 samples of jasperoid at the Elephant Head area.

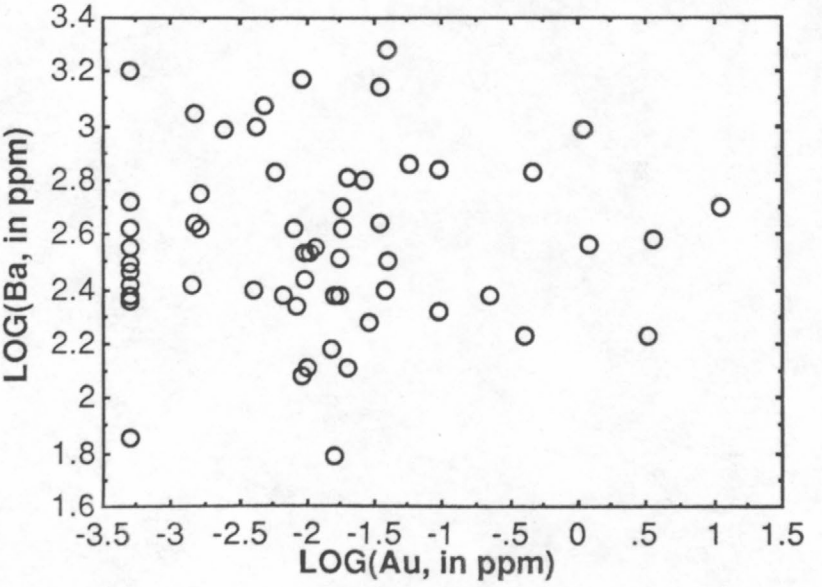
LOG(Ba, in ppm)
3.4
3.2
3
2.8
2.6
2.4
2.2
2
1.8
1.6
-3.5 -3 -2.5 -2 -1.5 -1 -.5 0 .5 1 1.5
LOG(Au, in ppm)

C

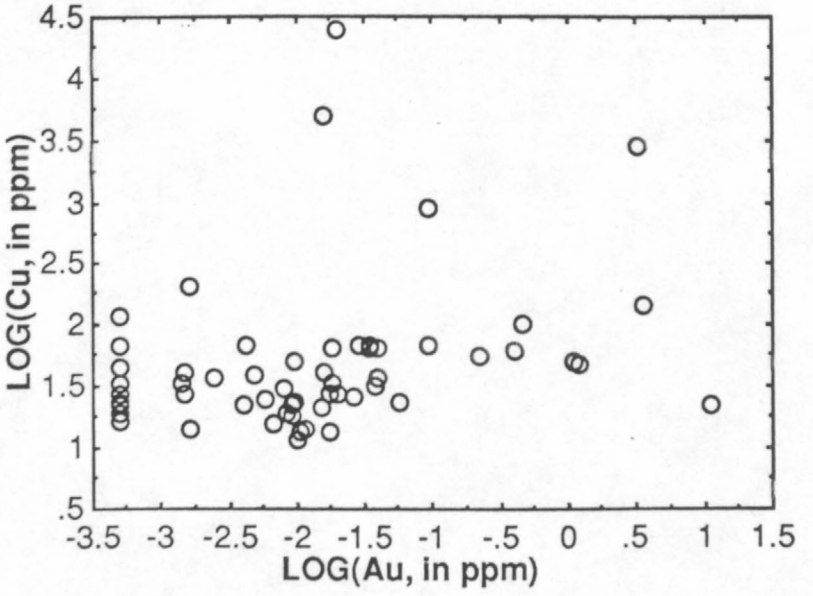
LOG(Cu, in ppm)
4.5
4
3.5
3
2.5
2
1.5
1
.5
-3.5 -3 -2.5 -2 -1.5 -1 -.5 0 .5 1 1.5
LOG(Au, in ppm)

D

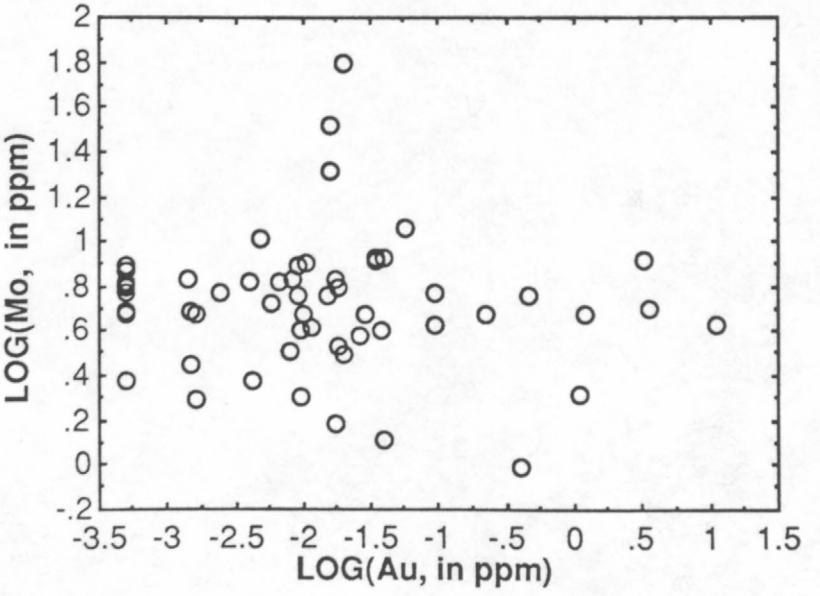
LOG(Mo, in ppm)
2
1.8
1.6
1.4
1.2
1
.8
.6
.4
.2
0
-.2
-3.5 -3 -2.5 -2 -1.5 -1 -.5 0 .5 1 1.5
LOG(Au, in ppm)

E

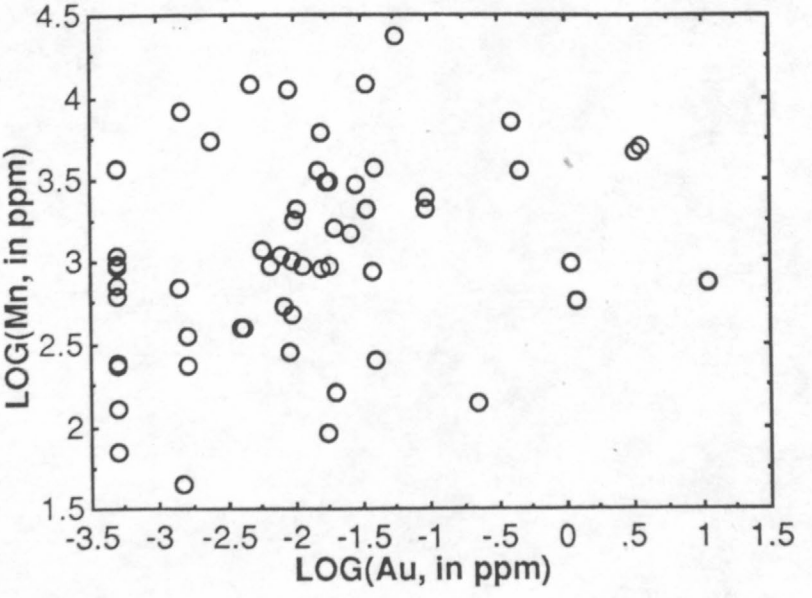
LOG(Mn, in ppm)
4.5
4
3.5
3
2.5
2
1.5
-3.5 -3 -2.5 -2 -1.5 -1 -.5 0 .5 1 1.5
LOG(Au, in ppm)

F

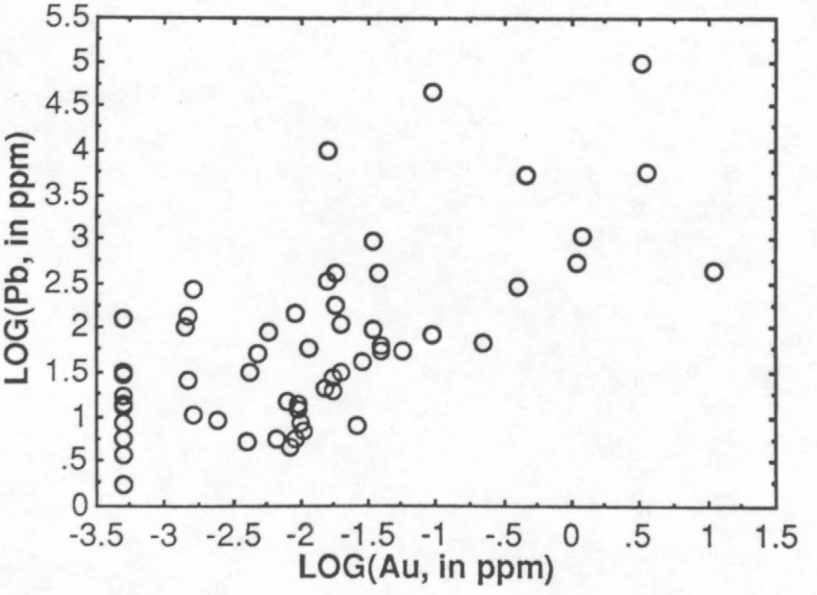
LOG(Pb, in ppm)
LOG(Au, in ppm)
5.5
5
4.5
4
3.5
3
2.5
2
1.5
1
.5
0
-3.5 -3 -2.5 -2 -1.5 -1 -.5 0 .5 1 1.5

5

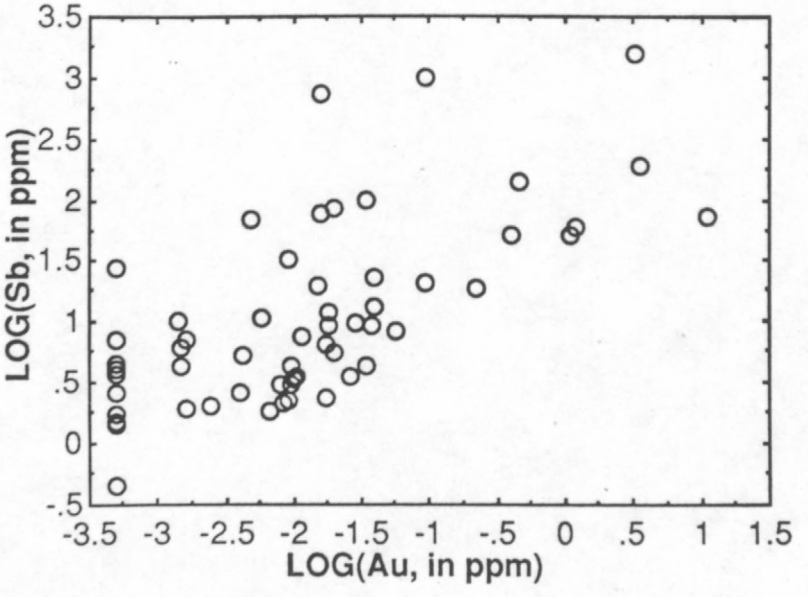
LOG(Sb, in ppm)
LOG(Au, in ppm)
3.5
3
2.5
2
1.5
1
.5
0
-.5
-3.5 -3 -2.5 -2 -1.5 -1 -.5 0 .5 1 1.5

H

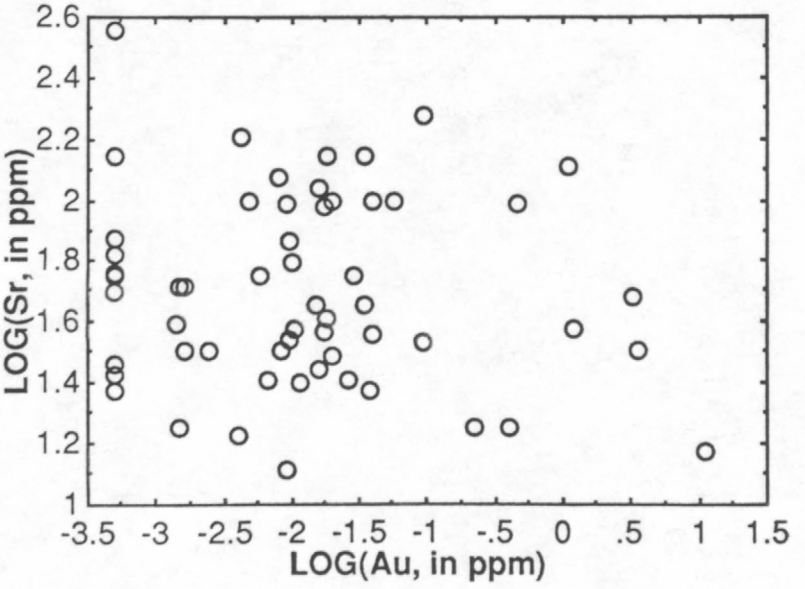
LOG(Sr, in ppm)
2.6
2.4
2.2
2
1.8
1.6
1.4
1.2
1
-3.5 -3 -2.5 -2 -1.5 -1 -.5 0 .5 1 1.5
LOG(Au, in ppm)

I

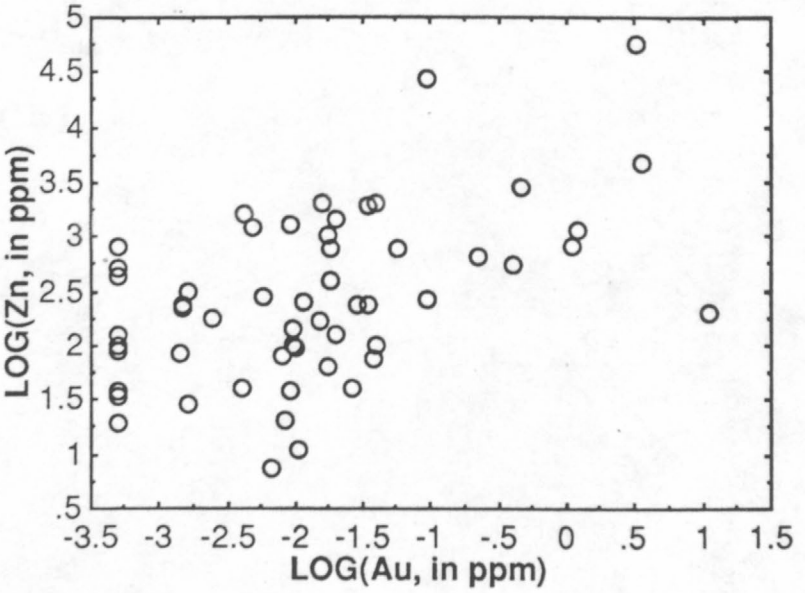
LOG(Zn, in ppm)
5
4.5
4
3.5
3
2.5
2
1.5
1
.5
-3.5 -3 -2.5 -2 -1.5 -1 -.5 0 .5 1 1.5
LOG(Au, in ppm)

J

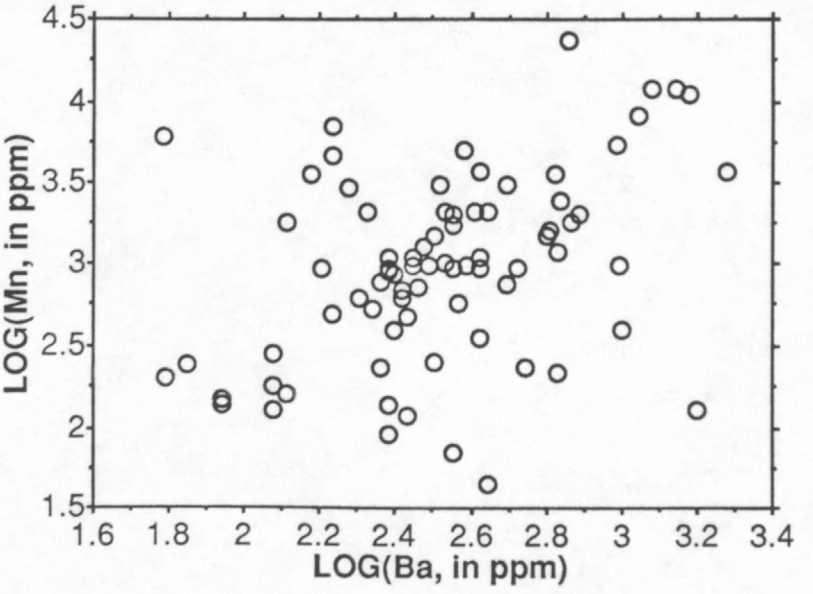

A

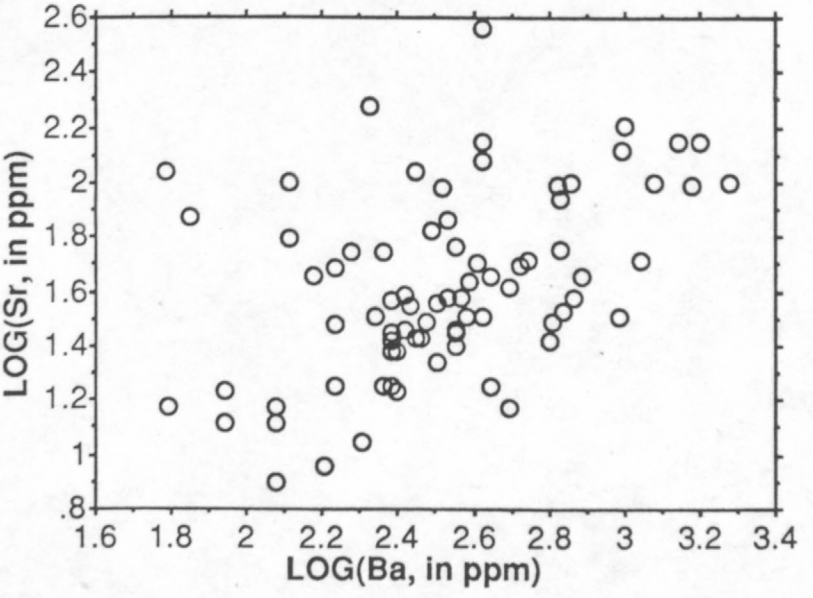

B

Figure 11. -- Graphs showing barium compared with manganese (A) and strontium (B) in jasperoid at Elephant Head.

Figure 12. -- Spider-graph plots of 11 elements in selected samples of jasperoids. Normalized to analysis no. 2 (table 3; see text).

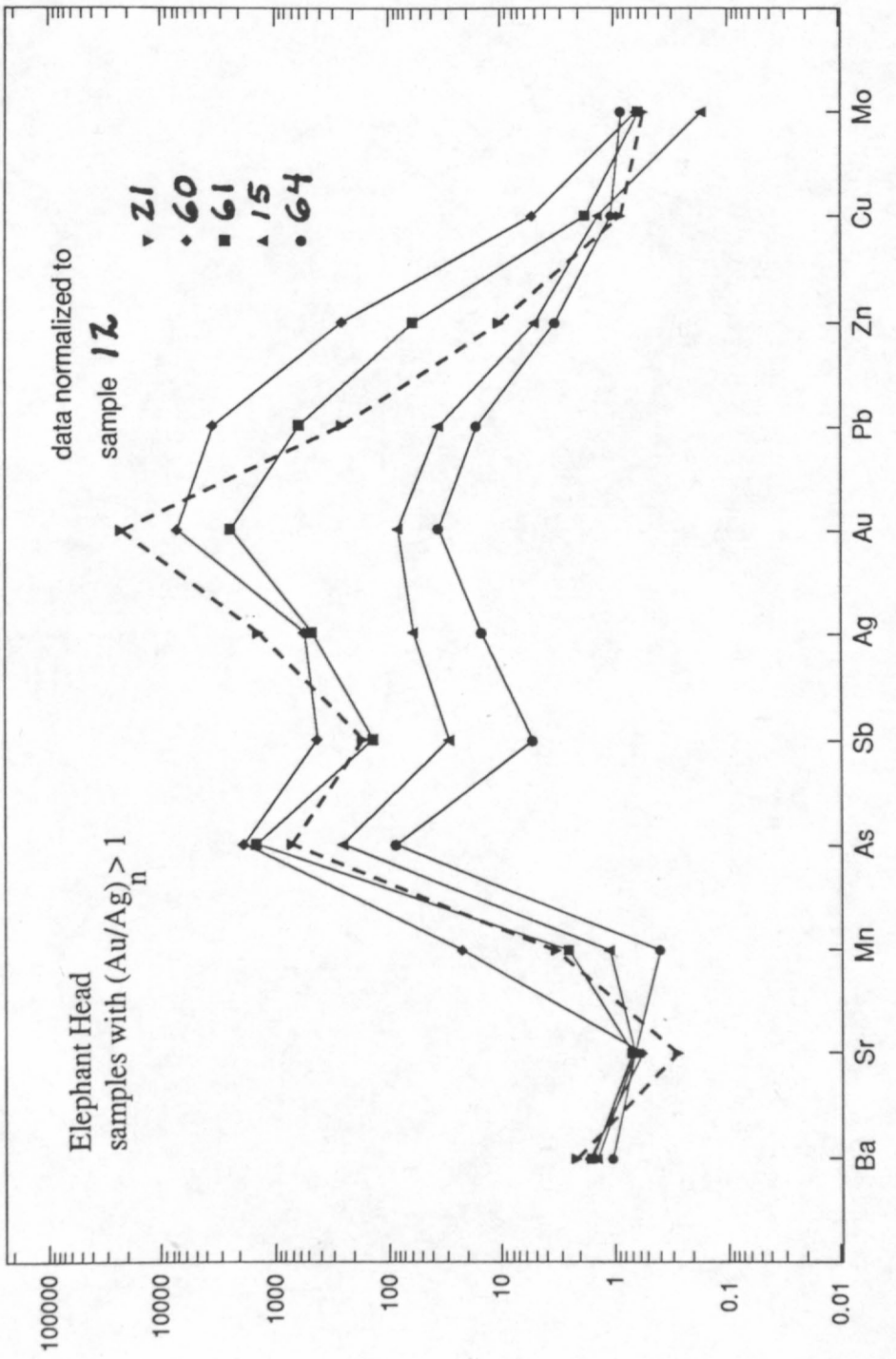

A

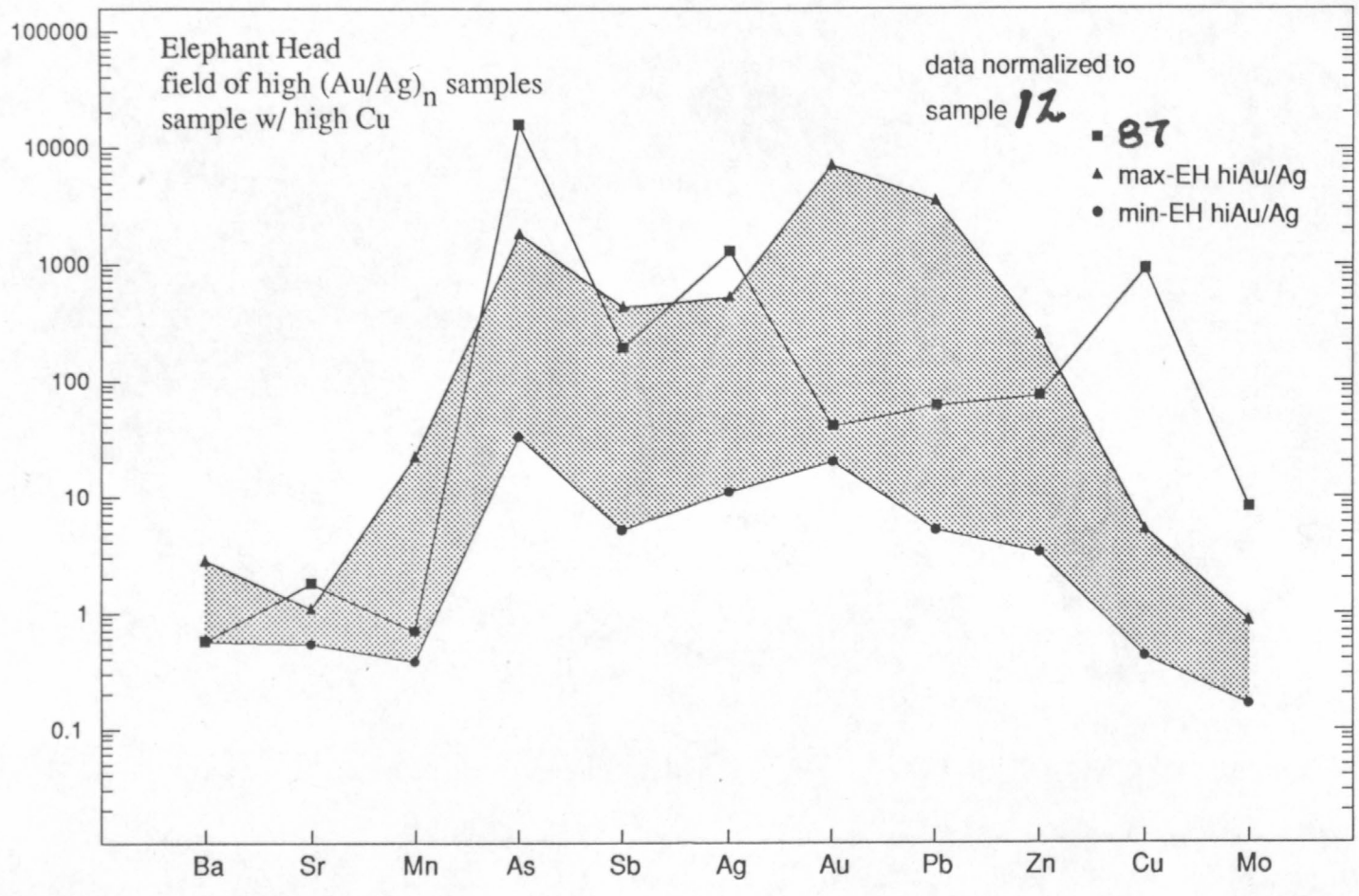
Elephant Head
field of high (Au/Ag)n samples
sample w/ high Cu
data normalized to
sample 12
87
max-EH hiAu/Ag
min-EH hiAu/Ag
100000
10000
1000
100
10
1
0.1
Ba
Sr
Mn
As
Sb
Ag
Au
Pb
Zn
Cu
Mo

B

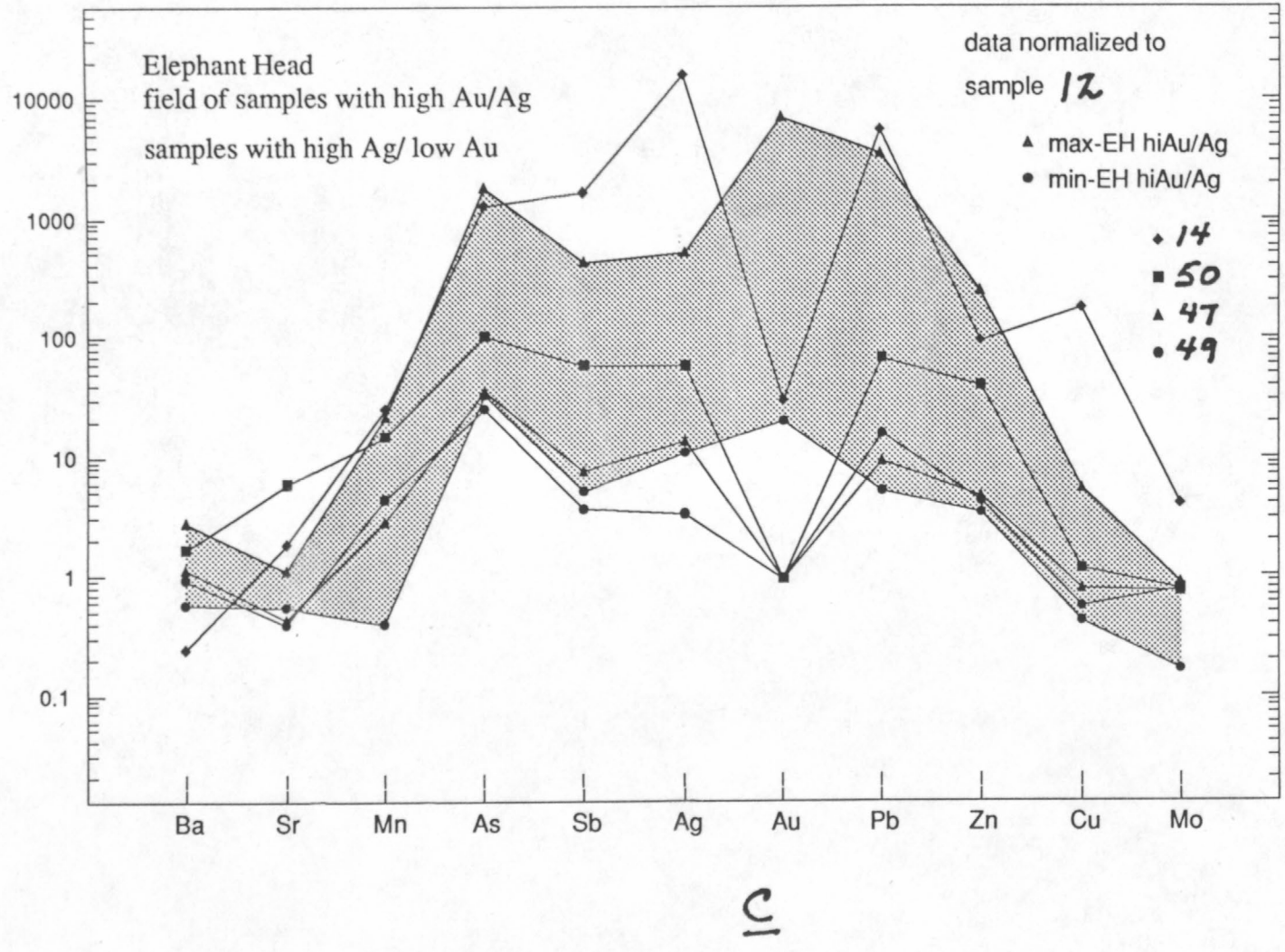
Elephant Head
field of samples with high Au/Ag
samples with high Ag/ low Au
data normalized to
sample 12
max-EH hiAu/Ag
min-EH hiAu/Ag
14
50
47
49
10000
1000
100
10
1
0.1
Ba
Sr
Mn
As
Sb
Ag
Au
Pb
Zn
Cu
Mo

C

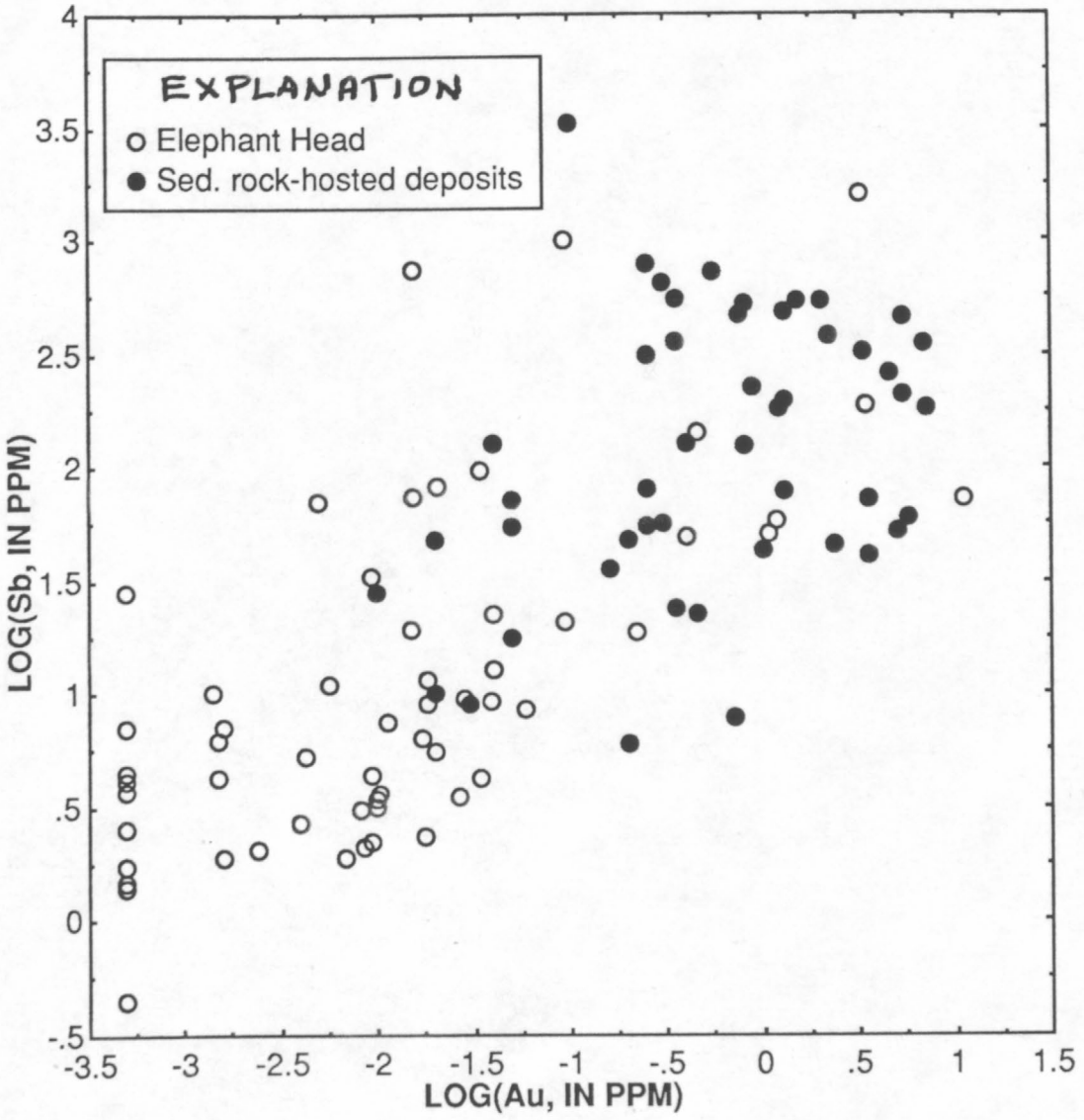

Figure 13. -- Graphs of gold compared with antimony (A), arsenic (B) and zinc (C) in jasperoid at Elephant Head and at 11 sedimentary rock-hosted disseminated gold deposits in the northern Great Basin. Data for 11 sedimentary rock-hosted deposits from Holland and others (1988), and Hill and others (1986).

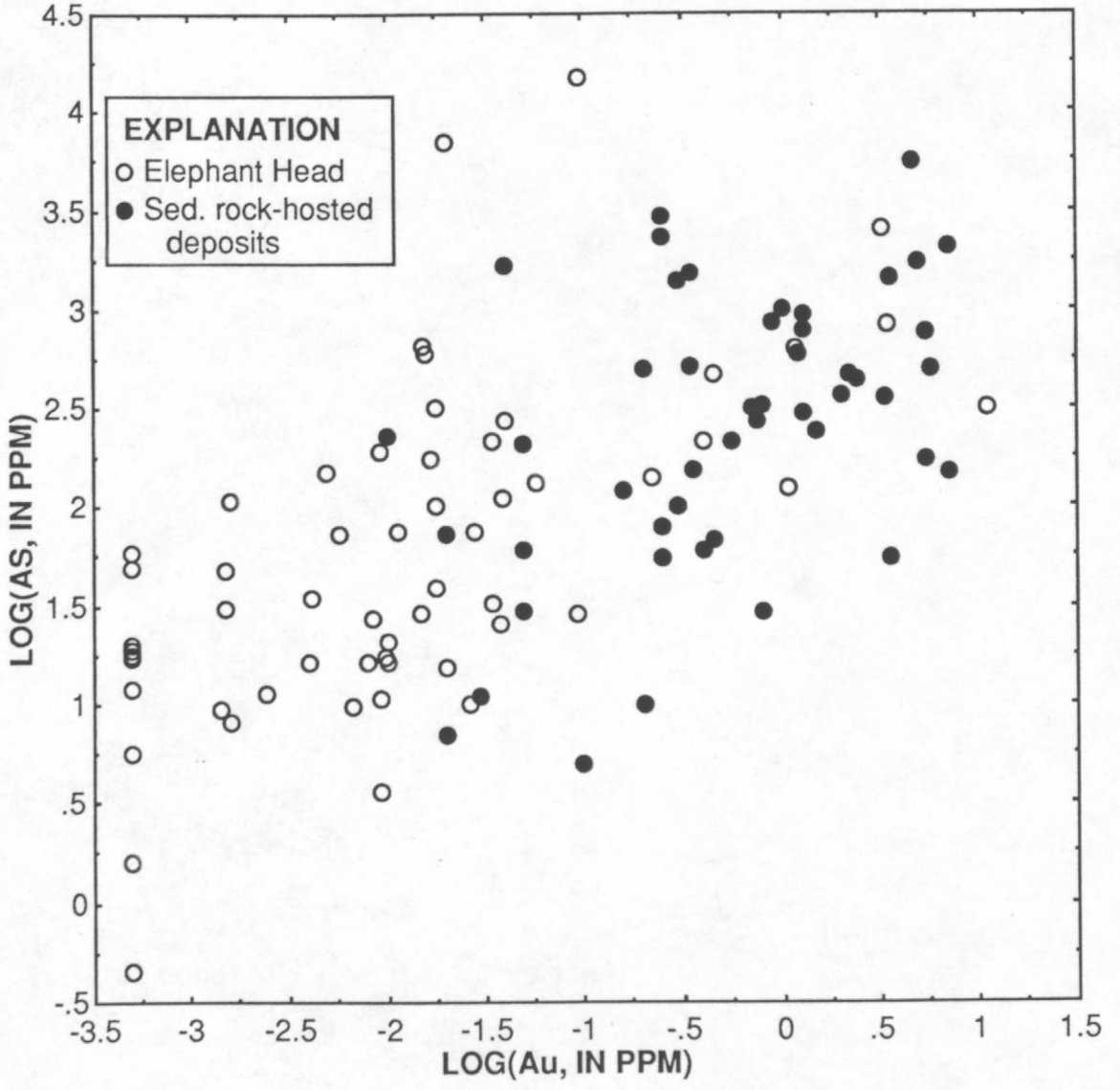
EXPLANATION
Elephant Head
Sed. rock-hosted deposits
LOG(AS, IN PPM)
LOG(Au, IN PPM)
4.5
4
3.5
3
2.5
2
1.5
1
.5
0
-.5
-3.5
-3
-2.5
-2
-1.5
-1
-.5
0
.5
1
1.5

B

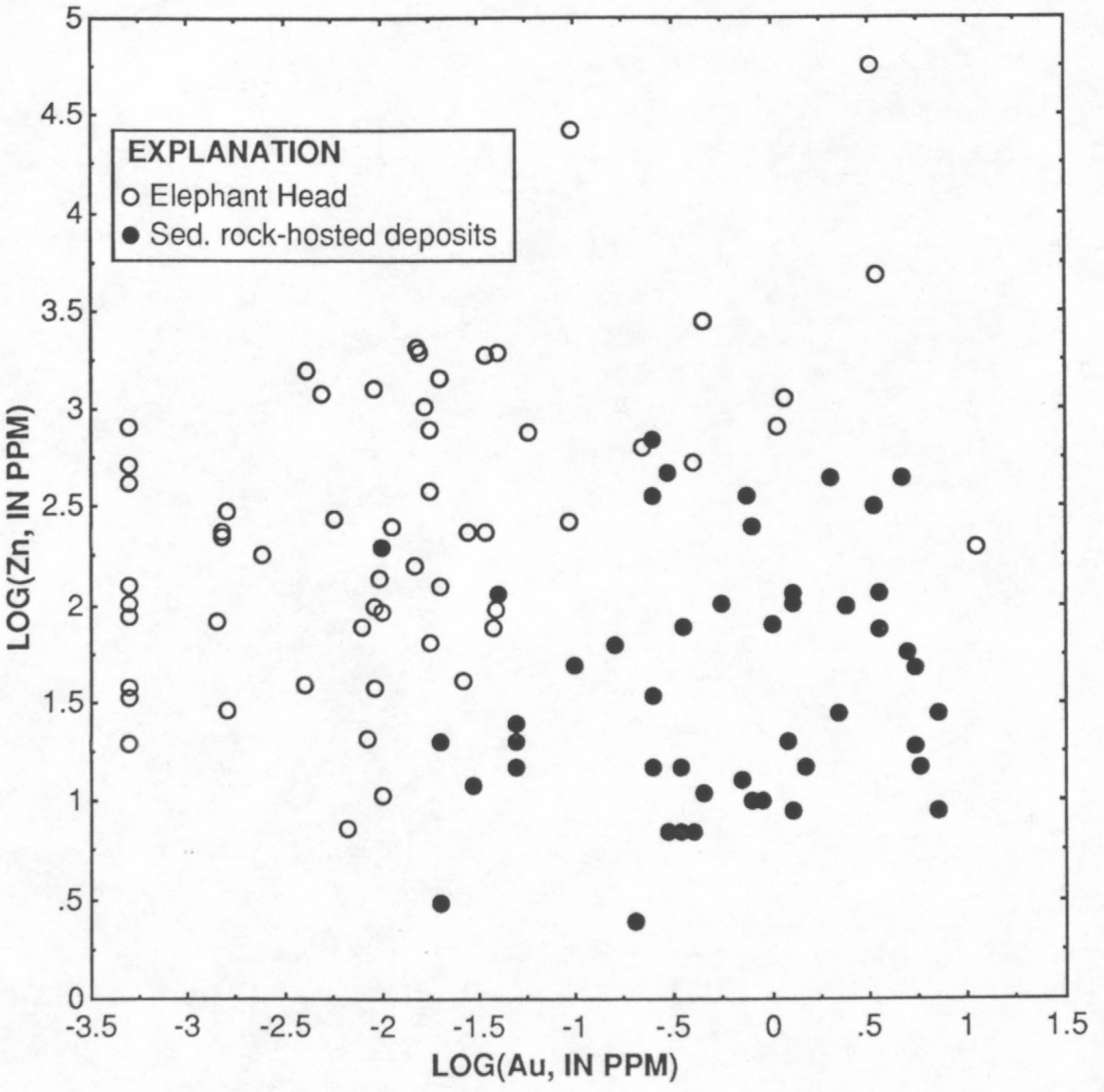
EXPLANATION
Elephant Head
Sed. rock-hosted deposits
LOG(Zn, IN PPM)
LOG(Au, IN PPM)
5
4.5
4
3.5
3
2.5
2
1.5
1
.5
0
-3.5
-3
-2.5
-2
-1.5
-1
-.5
0
.5
1
1.5

C

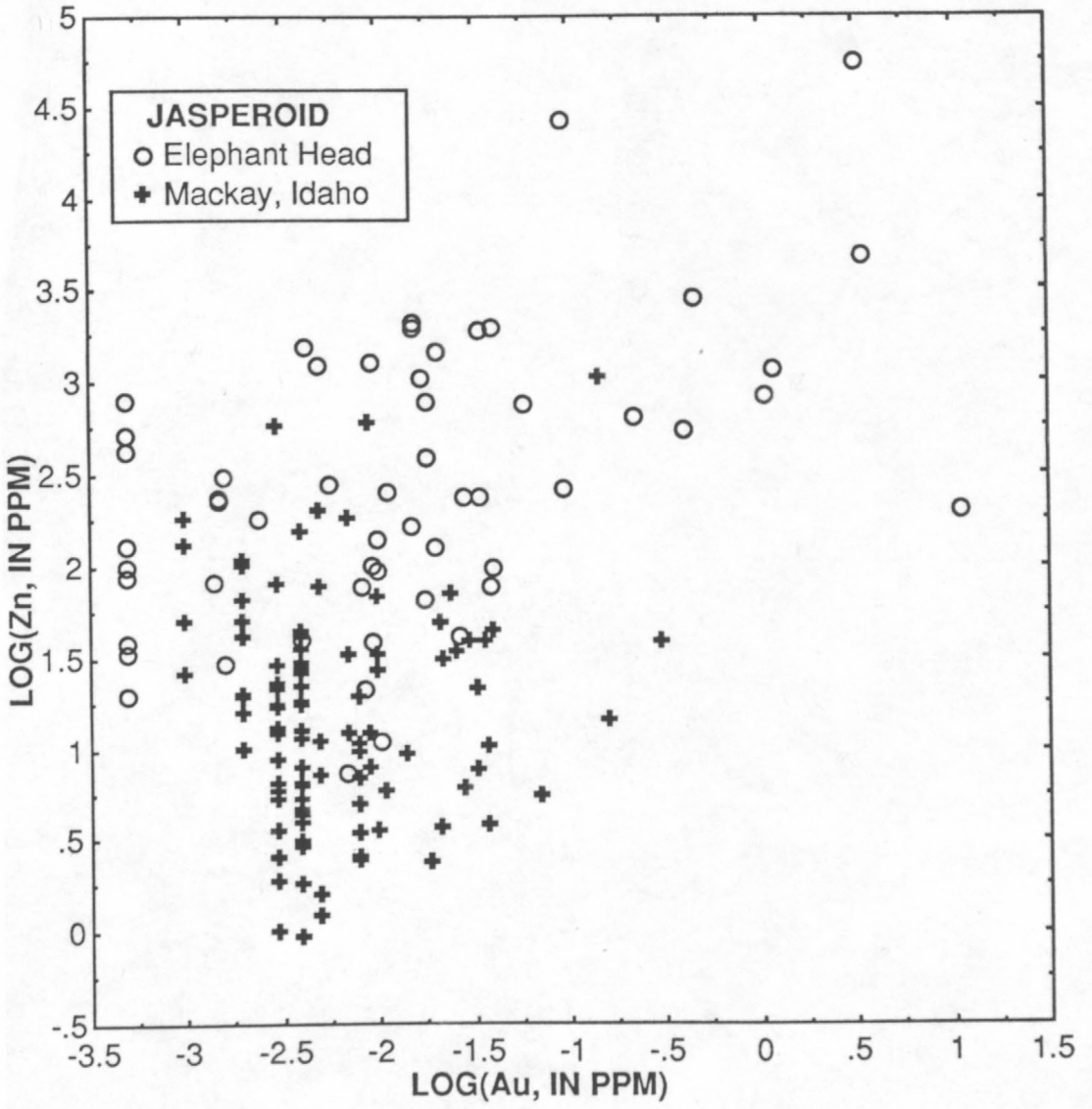

Figure 14. -- Graph showing log (Au) compared with log (Zn) for jasperoid at Elephant Head (table 3) and at Mackay, Idaho from Soulliere and others (1988).

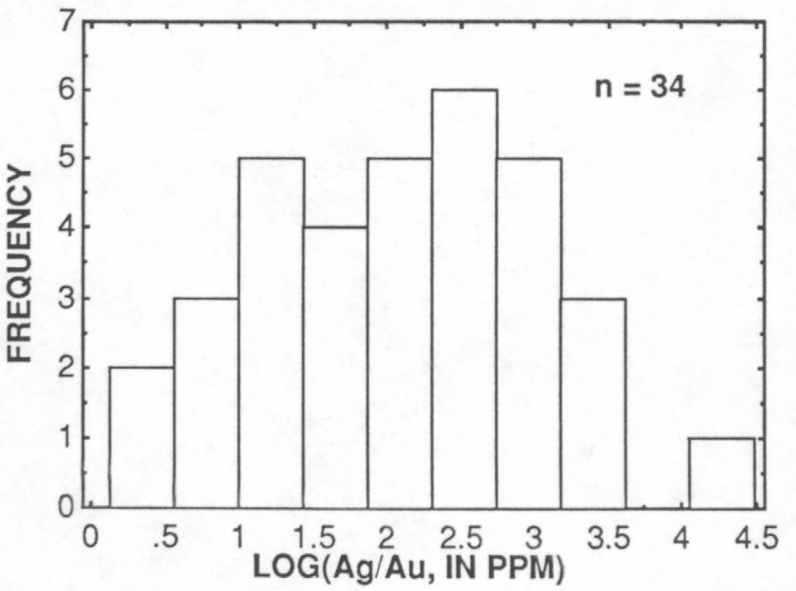

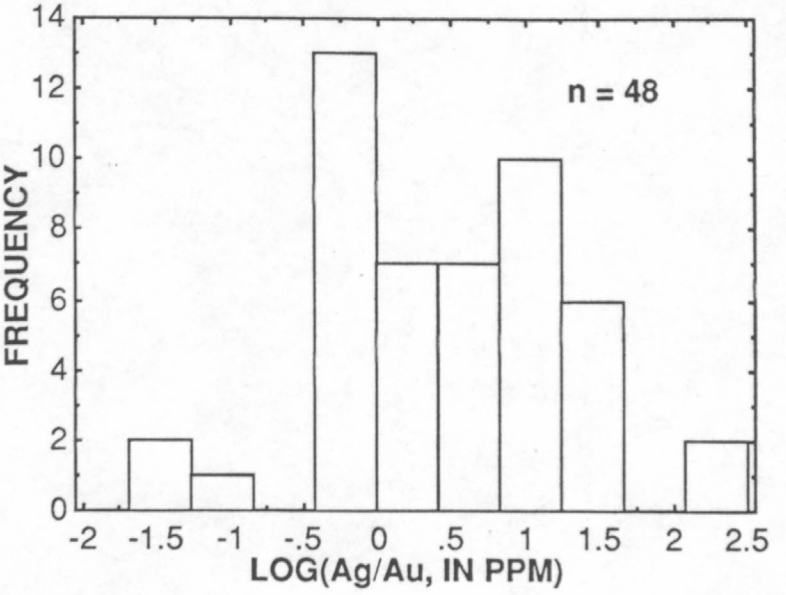

Figure 15. -- Histograms showing distributions of Ag:Au ratios in jasperoid; n, number of ratios. A, at Elephant Head (from table 3); B, from 11 sedimentary rock-hosted disseminated Au-Ag deposits in Holland and others (1988) and Hill and others (1986).

Figure 16. -- Back-scattered electron micrographs of native bismuth, galena, and free gold at the northern edge of the Fortitude gold skarn deposit, Battle Mountain Mining District. Bi, native bismuth; gn, galena; Au, free gold. Scale shown is in micrometers (1 um = 10^{-6} m).

A, Eutectoid-type intergrowth of native bismuth, and sparse gold set in galena. Sample no. 85TT99;

B, Close-up view of textural relations of gold shown in A;

C, Textural relations of gold mantled by a narrow rim of electrum (E) that shows a very high Ag:Au ratio; px, hedenbergitic clinopyroxene. Sample no. 85TT95.

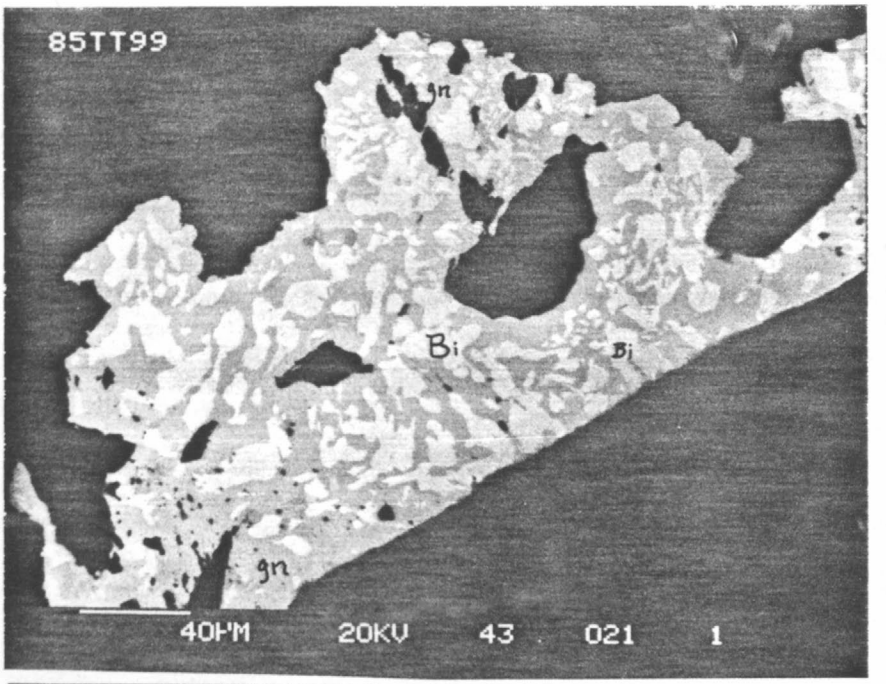
85TT99
gn
Bi
Bi
gn
40UM 20KV 43 021 1

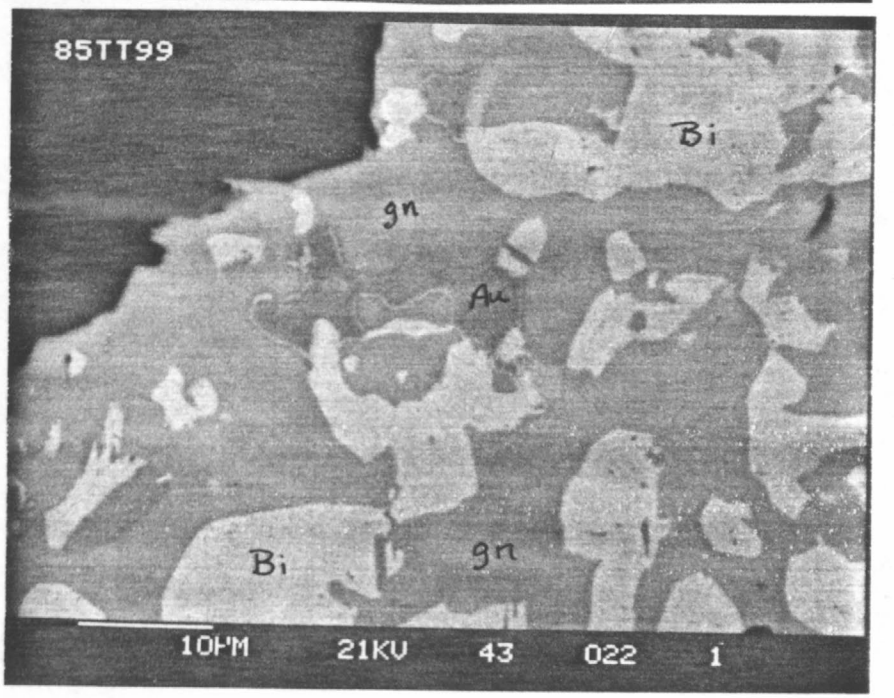
85TT99
Bi
gn
Au
Bi
gn
10UM 21KV 43 022 1

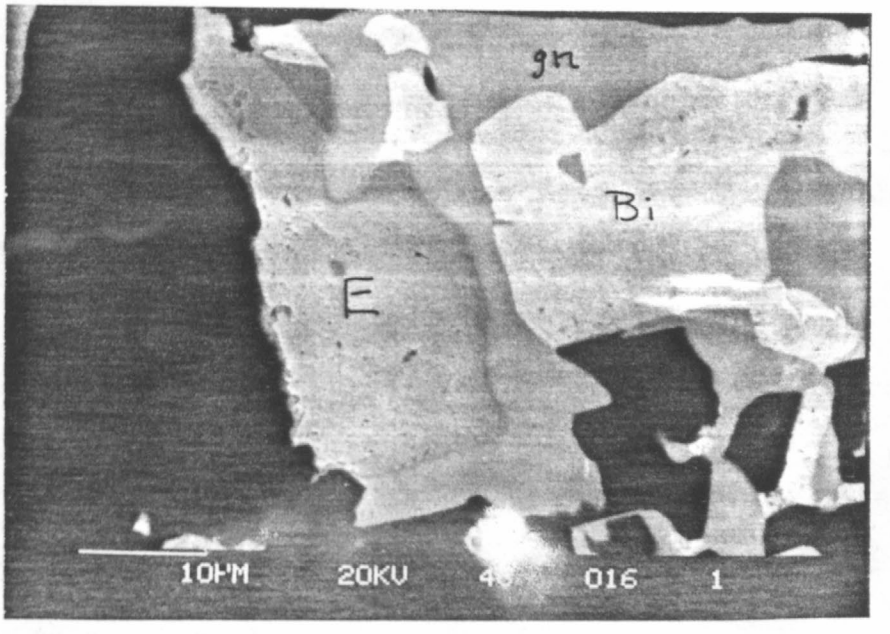
gn
Bi
E
10UM 20KV 4 016 1

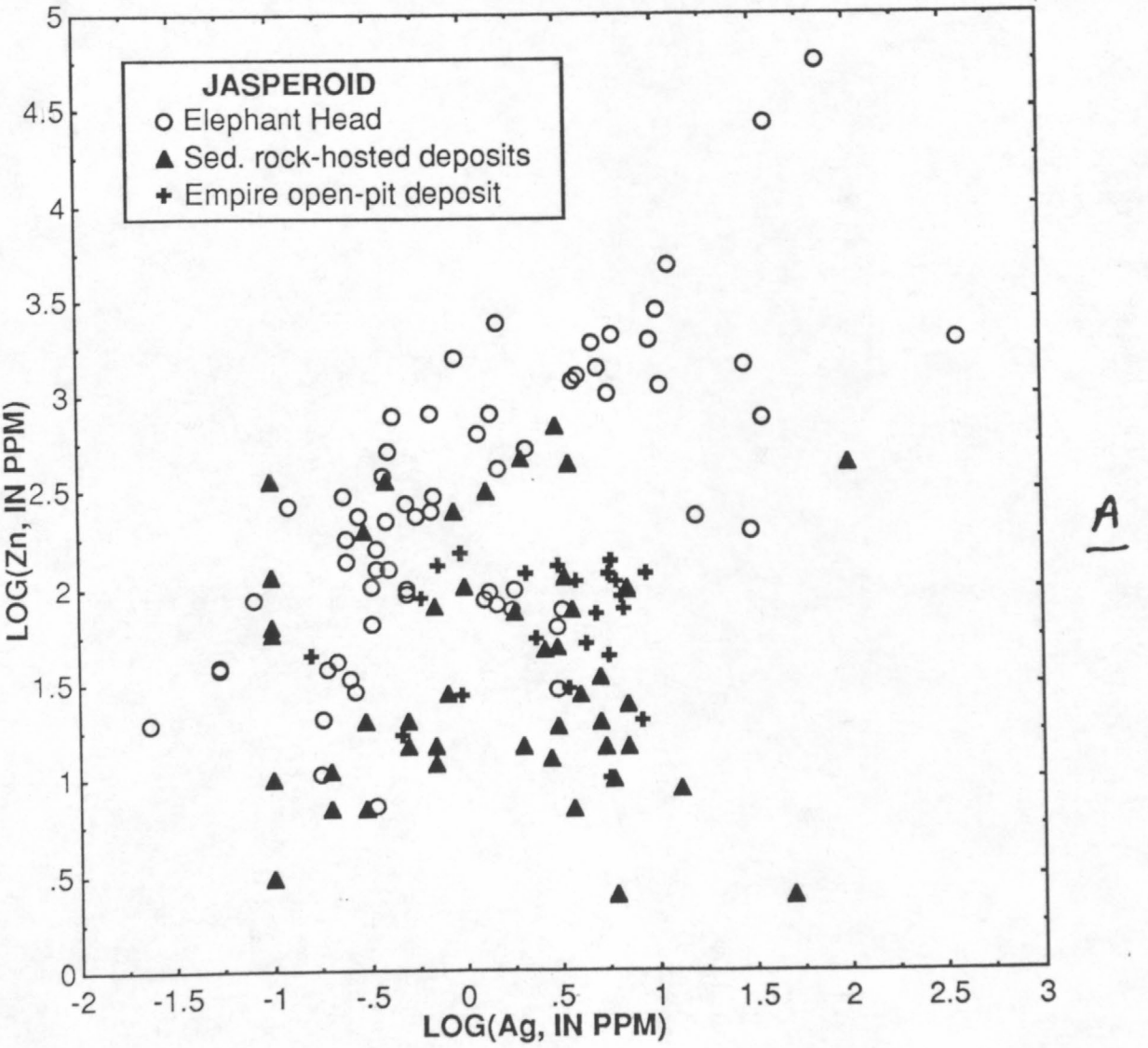

Figure 17. -- Plots of log (Ag, in ppm) compared with log (Zn, in ppm) (A), log (As, in ppm) (B) and log (Sb, in ppm) (C) for samples of jasperoid analyzed from Elephant Head (table 3), selected sedimentary rock-hosted Au-Ag deposits (Hill and others, 1986; Holland and others, 1988), and the Empire open-pit deposit (table 8).

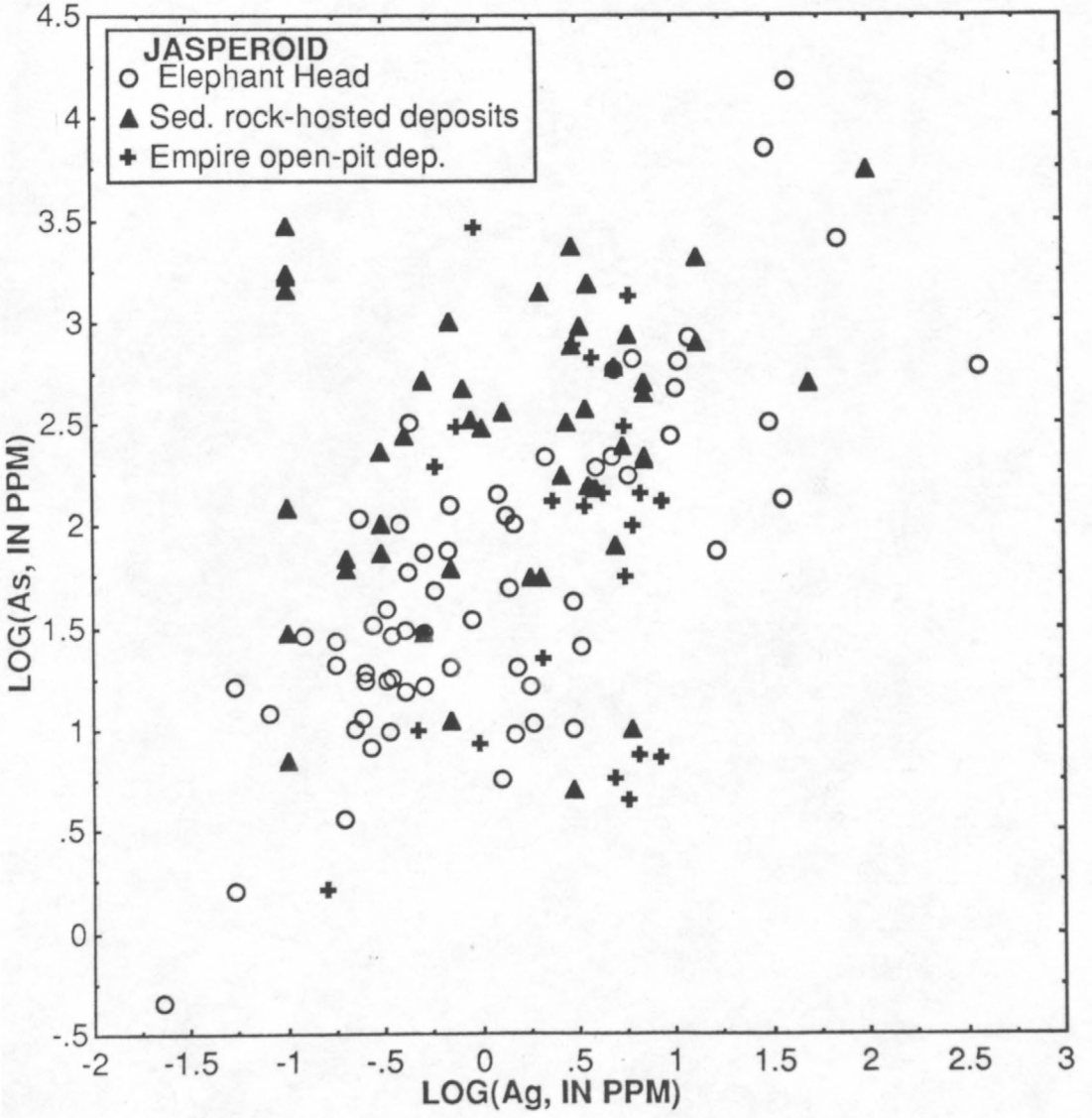
JASPEROID
Elephant Head
Sed. rock-hosted deposits
Empire open-pit dep.
LOG(As, IN PPM)
LOG(Ag, IN PPM)
4.5
4
3.5
3
2.5
2
1.5
1
.5
0
-.5
-2
-1.5
-1
-.5
0
.5
1
1.5
2
2.5
3

B

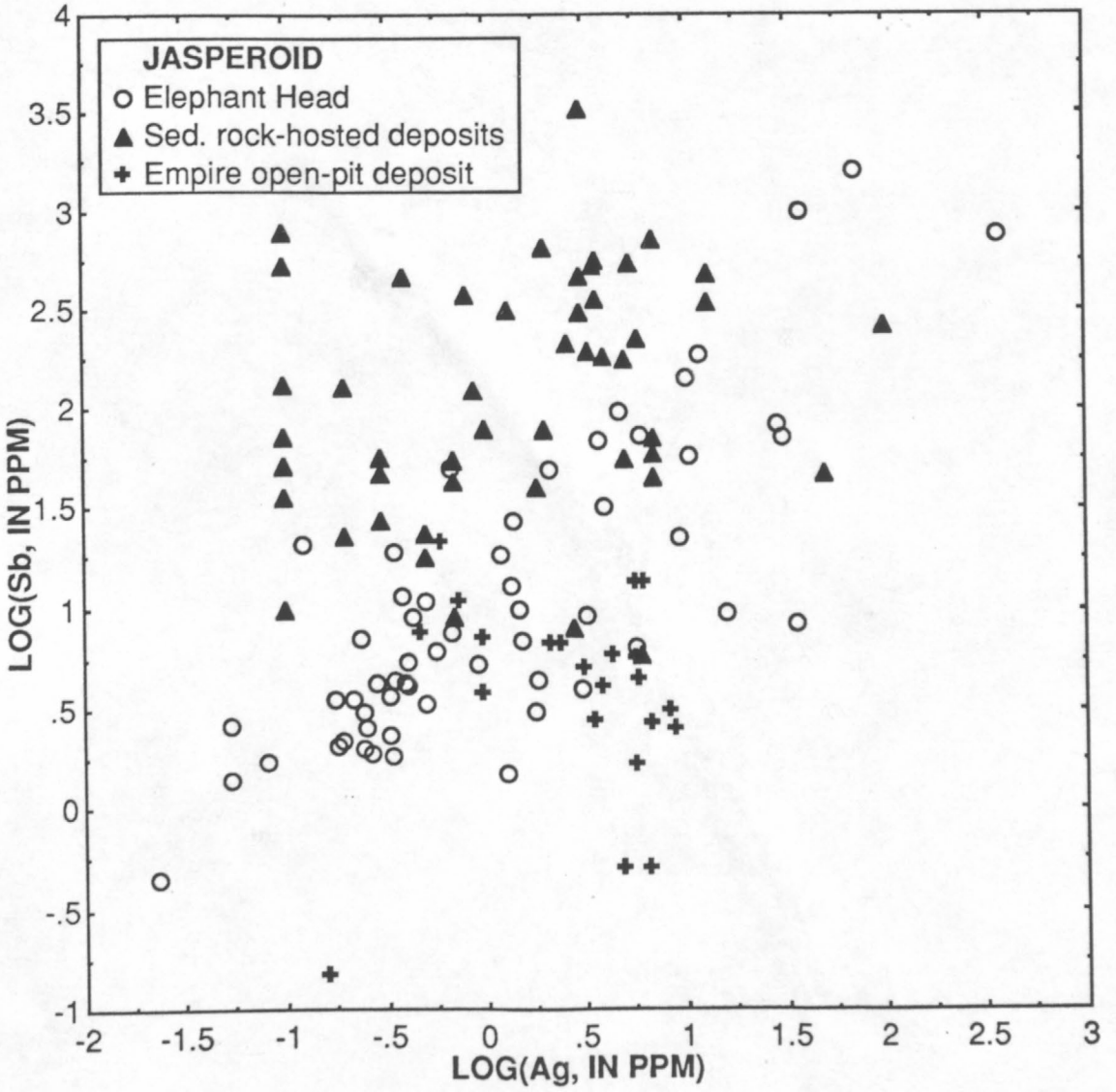
JASPEROID
Elephant Head
Sed. rock-hosted deposits
Empire open-pit deposit
LOG(Sb, IN PPM)
LOG(Ag, IN PPM)
4
3.5
3
2.5
2
1.5
1
.5
0
-.5
-1
-2
-1.5
-1
-.5
0
.5
1
1.5
2
2.5
3

C1

POCKET CONTAINS:
1 ITEMS
PM